Particulate emissions from a steel works a quantitative ecological assessment

Rachael Heather Turton

Particulate emissions from a steel works: A quantitative ecological assessment.

Rachael Heather Turton
BSc

Department of Biological and Biomedical Sciences,
University of Durham.
2008

A thesis submitted for the degree of

Master of Philosophy

Declaration

The material contained within this thesis has not previously been submitted for a degree at the University of Durham or any other university. The research reported within this thesis has been conducted by the author unless indicated otherwise.

Abstract

Particulate emissions from a steel works: A quantitative ecological assessment.

Rachael Heather Turton

The research presented here was the response to an improvement condition issued by the Environment Agency. The aim of the present study was to examine the potential effects of the particulate emissions from an integrated iron and steel works, to an adjacent sand dune ecosystem, identified as a Site of Special Scientific Importance (SSSI) for its flora, fauna and bird life. A monitoring and assessment of the deposition and flux of particulates was undertaken from April 2006 to September 2007 at monitoring sites located on the iron and steel works and in the surrounding area.

A passive particulate deposition and flux monitoring study was undertaken at six sites on and surrounding the integrated iron and steel works using Frisbee deposit gauges and sticky pads. The deposition and flux of particulates was significantly higher at the monitoring sites located on or close to the works, and decreased up to 3 km from the works. The particles found on and near the works were predominately iron-rich, and most likely to be a result of emissions from the works. The chemical characteristics of the particles identified further away from the works were more diverse, and a combination of marine, soil, combustion or industrially derived particles.

A desk-top review and development of the model scenario was undertaken, to assess the relevance of the modelled scenarios of PM_{10} emissions, to the total dust deposited to the passive deposition gauges. The model scenario was found to be an important qualitative tool, but could not be used to predict quantitative measurements of particulate deposition due to the limitations and uncertainty of modelling.

The deposition of particulates to the SSSI was significantly higher at sites located closer to the works, and increased significantly with exposure time. The iron concentration of the soil was found to be significantly higher on the SSSI than at a sand dune ecosystem 3.5 km away. Cleaned leaves of *Leymus arenarius* and *Plantago lanceolata* had a significantly higher rate of photosynthesis compared to untreated leaves growing on the SSSI. Therefore at sites where the rate of particulate deposition was relatively higher, and increased soil iron concentration was enhanced in comparison to similar sites, the rate of photosynthesis was significantly reduced in leaves of *Leymus* and *Plantago* on the SSSI.

Acknowledgements

I would like to express my gratitude here to those people whose guidance, assistance, support and friendship were of great importance to me in the completion of this thesis. Firstly I'd like to thank my supervisors, Dr. Bob Baxter and Dr. Sarah Wilbourn for their advice, encouragement and opportunity to undertake this project. I'd also like to thank Corus for the funding of this project, in particular Pete Boydell, but also Neil Haines for running the model scenarios, Victor Chao for conducting the SEM-EDX analyses, and Alasdair Ross and Gareth Williams for their kind help and assistance in data collection.

Thanks to all those kind people who assisted me on various field campaigns Andy Lloyd, Dave Sayer, Jon Bennie and Michael Bone. I'd also like to thank the department technician staff in Biology and Geography, in particular Judith Chambers, John Summerill and Karen Smith and Martin West. I'd also like to mention the rest of my co-workers in Biology to whom I'm grateful for their continued support and encouragement, in particular Judy Allen, Natalie Doswald, Jillian Lynn and Georgie Palmer.

Finally I'd like to thank my friends and most of all my family for their love and kind words of support and encouragement.

Glossary of Acronyms

AAC	Absolute Area Coverage (%)
AAS	Atomic Absorption Spectrometry
ADMS	Atmospheric Dispersion Modelling System
BOS	Basic Oxygen Steel-making plant
CCSEM	Computer Controlled Scanning Electron Microscopy
CFD	Computational Fluid Dynamic (model)
EAC	Effective Area Coverage (%)
EEL	Evans Electroselenium (Smokestain Reflectometer)
EPAQS	Expert Panel on Air Quality Standards
GPS	Global Positioning System
IPPC	Integrated Pollution Prevention and Control
IRGA	Infra-Red Gas Analyser
PM_{10}	Particulate matter of the aerodynamic diameter 2.5 to 10 μm
SEI	Stockholm Environment Institute, York
SEM	Scanning Electron Microscopy
SEM-EDX	Scanning Electron Microscopy coupled with energy dispersive x-ray detection
SEM-EDS	Scanning Electron Microscopy coupled with energy dispersive x-ray spectrometry
SEM-WDX	Scanning Electron Microscopy coupled with wavelength dispersive x-ray detection
SSSI	Site of Special Scientific Importance

Notes on nomenclature used in this thesis

Grasses and other species follow Stace (1997)

Contents Page

Chapter 1 - Introduction

1.1 Introduction

The present study investigated the potential ecological effects of particulate matter emissions from an integrated iron and steel works to a Site of Special Scientific Interest (SSSI). The steel works (subsequently referred to as the "Corus works") was located in the North-East of England, 7 miles to the north-east of Middlesbrough, 3 miles to the north-west of Redcar, and on the southern bank of the river Tees. The site of the Corus works has been involved in iron and steel manufacture since 1875. The Corus works has undergone several important stages of development and was integrated into one site in 1988. The Corus works are now a major producer of liquid steel and tap-hole iron, producing over 3 million tonnes annually, and are an important employer in the local area. The Corus works are located adjacent to Coatham Sands and South Gare SSSI (subsequently referred to as "the SSSI"). The SSSI is primarily a sand dune ecosystem. The main dune system runs from the Tees estuary for approximately 5 km in a south-easterly direction towards the town of Redcar. The sand dunes were designated as a SSSI as they support a rich diversity of invertebrate fauna, flora and bird life including an internationally important community of *Calidris alba* (Sanderlings).

The present study was initiated by an improvement condition set by the Environment Agency as part of the Integrated Pollution Prevention and Control (IPPC) permit application. A model scenario produced by Corus had highlighted the expected environmental concentration of particulate matter in the size range 2.5 to 10 micrometers or PM_{10} was expected to exceeded the human health standard set by the Expert Panel on Air Quality Standards (EPAQS) of 50 $\mu g\ m^{-3}\ s^{-1}$ as a 24 hour running average (EPAQS, 1995; QUARG, 1996). Therefore, two key areas were identified for further research; firstly to determine the relevance of the modelled PM_{10} scenarios to particulate matter deposition on the SSSI, and secondly, to determine the potential ecological effects of particulate matter deposition to the flora and fauna of the SSSI.

Particulate matter is an extremely diverse material, which although predominately classified by size fraction, can also be classified by shape, phase, physical behaviour, biological activity or chemical species (Environment Agency, 2004; Grantz *et al.*, 2003; QUARG, 1996). Fugitive emissions of particulates are known to be emitted from the loading, unloading, transport, storage and handling of dry stock including iron ore and

coal (Gupta *et al.*, 2005), alongside other potential particulate generating processes which occur on the Corus works. The particulates of concern in the present study are the coarse or PM_{10} fraction, which is typically deposited quickly, due to their large size. Previous studies on the emissions from steel works have found the particulates are mainly deposited near to the plant works (Mukherjee & Nuorteva, 1994; Pilegaard, 1979; Turkan *et al.*, 1995; Vestergaard *et al.*, 1986), and more specifically iron-rich particles are associated with emissions from the works (DeBock *et al.*, 1994; Katrinak *et al.*, 1995; Kemppainen *et al.*, 2003; Michaud *et al.*, 1993; Polizzi *et al.*, 2007; Post & Buseck, 1984; Van Malderen *et al.*, 1996a; Xhoffer *et al.*, 1991). Therefore, there is a high potential for iron-rich particulate matter emissions to be deposited to the SSSI.

There is a wealth of literature on the potential effects of particulate matter emissions on human health. Particulate matter emissions are thought to exacerbate conditions including asthma, emphysema, bronchitis, silicosis and lung cancer (Anderson *et al.*, 1992; Aunan, 1996; Chillrud *et al.*, 2004; Dockery *et al.*, 1993; Dockery & Pope, 1994), hence the EPAQS human health standard of 50 $\mu g\ m^{-3}\ s^{-1}$ as a 24 hour running average. A recent study on emissions from the Corus works found evidence for acute lung inflammation in rats instilled with PM_{10} collected on the works during normal working conditions, in comparison to samples taken from a period of closure (Hutchison *et al.*, 2005). However, there is not a set environmental standard of PM_{10} or total particulate matter for the environment, and in comparison relatively few studies have examined the impacts of particulate emissions on vegetation.

In a review by Farmer (1993) on the effects of particulate matter deposition to vegetation, the varied physiological response of vegetation are hypothesized to be dependant on localised conditions. Hence the findings from the published literature cannot be easily extrapolated to other sites as the impacts of particulate deposition require greater attention (Farmer, 1993).

The effects of particulate matter deposition to soil, flora and fauna have been reported as highly variable in the current literature. The effects of particulate matter deposition can be from the physical or chemical nature of the particulates, or a combination of both factors. Symptoms include leaf shading, stomatal blocking, leaf injury (necrosis), increased diffusion resistance, increased leaf temperature, inhibit of transpiration, reduced photosynthesis, increased water loss, reduced vegetative growth and reduced reproductive output and reduced fruit set which are exacerbated by chemically active dusts (Czaja, 1961; Eller, 1977; Eveling, 1969; Farmer, 1993; Grantz *et al.*, 2003; Hirano *et al.*, 1995; Sharifi *et al.*, 1997; Talley *et al.*, 2006). Dust deposition

can also alter community structure within ecosystems by causing extinctions, invasive species to spread or altering the balance of dominant species within the community (Brandt & Rhoades, 1972; Brandt & Rhoades, 1973; Gilbert, 1976). Dust can also significantly effect plants indirectly through secondary stresses such as drought or pathogens, as they alter the competitive balance between species, alter the soil chemistry and soil microbial communities (Farmer, 1993).

The terminology particulate, particulate matter and dust are used interchangeably in the present thesis and refer to the all fractions of particulate matter, unless otherwise stated.

1.3 Aims

The main aims of the present study were identified as the following:

1. To quantify the total particulate matter deposition to South Gare and Coatham Sands SSSI.
2. To quantify the total particulate matter flux to South Gare and Coatham Sands SSSI.
3. To characterise the flux and deposited particulate matter to identify potential sources of particulate emissions.
4. To identify the limitations of the IPPC model scenario produced by Corus and to undertake development to assess the relevance of the model scenario for predicting the particulate matter deposition onto South Gare and Coatham Sands SSSI.
5. To assess the potential impact of deposited particulate matter to the flora of South Gare and Coatham Sands SSSI.

1.3 Thesis Outline

The present thesis outline is as follows;

Chapter 2 covers the background to the project and site; particulate matter, specifically its deposition, monitoring, characterisation, and modelling; the steel production process, further details on the site including potential sources of particulate emissions, the effects of particulate matter on vegetation and lastly the research hypotheses for the project.

In chapter 3 the monitoring programme for the flux and deposition of particulate matter on and surrounding the Corus works are discussed. It examines the annual deposition and flux of particulate matter to six dry foam Frisbee dust deposit gauges and sticky pads.

Chapter 4 examines the characteristics of the particulate matter measured on the Corus works, in relation to reference samples taken on the Corus works.

In chapter 5 the modelling of particulate matter emissions from the Corus works to the surrounding area will be discussed. Assessing the most recent model scenario and developing the scenario to compare the expected rate of deposition with measured particulate matter deposition.

Chapter 6 examines the ecological impacts of particulate matter by quantifying the deposition to Coatham Sands and South Gare SSSI, examining the iron concentration of the soil in comparison to another sand dune ecosystem, and determining the effects of particulate matter deposition on the gas exchange of plants growing on the SSSI.

In chapter 7 forms the general discussion for the project, and summarises the key findings from this project in relation to the published literature.

Chapter 2 - Background

2.1 Introduction

Chapter two sets out to describe the background to the present study. It will consider three broad themes; the background to the study, particulate matter, and the ecological effects of particulate matter on plant health. In particular the background to this study will examine the Integrated Pollution Prevention and Control (IPPC) model scenario, the improvement condition, the Corus works location and the location and nature of the adjacent South Gare and Coatham Sands Site of Special Scientific Interest (SSSI). The particulate matter section will firstly define particulate matter, it will then examine how suspended particulate matter is deposited, how the deposition of dust can be monitored, how the dust can be characterised and how the dust can be modelled. Finally the third section will investigate the situation regarding the potential sources of particulate matter, dust generation, suspension and deposition across the Corus works and dust suppression techniques employed on-site, and then the ecological effects of dust deposition to plant health. At the end of the present chapter the research hypotheses will be outlined.

2.1.1 Site background

The Corus works, Teesside, UK is located 7 miles to the north-east of Middlesbrough, 3 miles to the north-west of Redcar, and on the southern bank of the river Tees UK (subsequently referred to as the "Corus works" see Chapter 3 Figure 3.1 (456480, 525360 British National Grid)). Adjacent to the Corus works is South Gare and Coatham Sands, which is classified as a Site of Special Scientific Interest (SSSI) (subsequently referred to as the "SSSI" (456950, 526100 British National Grid)). The SSSI contains a rich diversity of invertebrate fauna, bird life and flora. This diversity is owed to the range of important habitats including fresh water marshes, salt marshes, sand dunes, and intertidal mud and sands. The sand dune community supports one of the largest continuous stands of lyme grass *Leymus arenarius* in Britain, along with sea couch grass *Elymus atherica* at the northern limit of its range. While the lime rich areas of tipped slag support the nationally rare grass the rush leaved fescue *Festuca arenaria*. The invertebrate fauna consists of several uncommon beetles including *Broscus cephalotes* and *Enochrus quadripunctatus* and rare spiders such as *Silometopus incurvatus* and *Dysdera crocata*. The intertidal areas of Coatham Sands support an internationally important community of

Sanderlings (*Calidris alba)*, which was around 1200 in 1988, approximately 8% of the West European population. The foreshore also supports around 2% of the western European population of Knots which feed on the intertidal areas, the breakwater and the mussel beds of the German Charlies (slag banks exposed at low tide) and Coatham Rocks.

2.1.2 Project background

To comply with the EU Integrated Pollution Prevention and Control (IPPC) Council Directive (96/61/EC), the Corus works, Teesside was required to submit an application for a permit to operate. The methodology to examine each of the emissions from the Corus works was agreed in discussions between the Environment Agency and Corus. The agreed methodology for one of the emissions, particulate matter (PM) with an aerodynamic diameter of 10 micrometres or less (PM_{10}), was a modelled emissions scenario of the expected environmental concentration of PM_{10}. The application was submitted to the Environment Agency for review in 2001. The modelled scenario highlighted that the expected environmental concentration of PM_{10} exceeded the limit set by the Expert Panel on Air Quality Standard (EPAQS) of 50 $\mu g\ m^{-3}\ s^{-1}$ as a 24 hour running average (EPAQS, 1995; QUARG, 1996), over a small area of the Corus works and the adjacent SSSI. To determine the potential threat of particulate emissions to the flora and fauna of the SSSI, the deposition of particulate matter to the SSSI needs to be quantified. Therefore, the Environment Agency issued a permit to Corus (Permit No. BK0493) with the following improvement condition (1.4.27):

"With regard to particulate emissions from the Installation, the operator shall carry out an assessment of the effect of this emission on South Gare and Coatham Sands."

The aim of the present study was to address this improvement condition. The first aim was to validate the modelling, although all model scenarios contain some degree of uncertainty, there were no ground measurements available to confirm the modelled PM_{10} concentration on the SSSI. Therefore the project aimed to undertake model development in order to validate the accuracy of the original model scenario predictions. Secondly the project aimed to accurately determine the dust deposition to the SSSI by undertaking an on-site monitoring study, to further validate the model scenario. Thirdly the project aimed to determine the potential effects of particulate emissions to South Gare and Coatham Sands SSSI.

2.2 Particulate matter

2.2.1 Definition of particulate matter

Particulate matter is an extremely diverse material as it can be classified by its properties in a number of different ways. These include particulate shape or phase, physical behaviour in the air, size, biological activity or chemical species (Environment Agency, 2004; Grantz *et al.*, 2003; QUARG, 1996). Despite this the most common method of defining particulate matter is by the aerodynamic diameter, (see Table 3.1).

Table 3.1 Fractions of particulate matter, defined by aerodynamic diameter (micrometers) (DEFRA, 2007).

Particulate matter fraction	Aerodynamic diameter of particulate matter (micrometers)
Total suspended particulates (TSP)	≤ 10 µm
PM_{10} or coarse fraction	$\geq 2.5 \leq 10$ µm
$PM_{2.5}$ fraction	$\geq 1 \leq 2.5$ µm
PM_1 or fine fraction	$\geq 1 \leq 0.1$ µm
Ultra fine fraction (UFP)	≤ 0.1 µm

The present report is broadly concerned with the total suspended particulate matter (TSP) and the coarse particulate matter fraction (PM_{10}). The coarse fraction of particulates remain airborne for short periods and are therefore deposited very close to the source of dust generation and suspension (Grantz *et al.*, 2003; QUARG, 1996). However, the particulates may become entrained in airflow and carried short distances by the wind to a settling point (QUARG, 1996). The Environment Agency are concerned that the particulate emissions from the Corus works may become entrained in airflow and carried on to South Gare and Coatham Sands SSSI.

Particulate matter can be generated by the movement or transport of raw materials, fugitive emissions from the storage of materials on-site (wind scouring of stockpiles), the handling and processing of materials (abrasion or crushing processes), or vehicles may re-suspend deposited particulates (Environment Agency, 2004; Grantz *et al.*, 2003). There are quantifiable PM_{10} emissions on the Corus works, such as those from stacks and stockyards, but fugitive emissions from stock piles can be difficult to determine accurately as they are subject to continual movement. Stack emissions are now strictly monitored to adhere to air quality standards, however fugitive dust emissions from stock piles, stock processing and suspended dusts are difficult to monitor. The IPPC permit has shown the environmental concentration of PM_{10} from the Corus works

exceeds the air quality standard and could potentially effect the flora and fauna of South Gare and Coatham Sands SSSI, which is of international importance, in particular the population of Sanderlings (*Calidris alba)*.

2.2.2 Environmental standard for particulate matter

The Expert Panel on Air Quality Standards (EPAQS) recommends 50 $\mu g\ m^{-3}\ s^{-1}$ as a 24 running average for PM_{10} (DEFRA, 2007; EPAQS, 1995), because of the concerns of the adverse human health impacts of airborne particulate matter. Epidemiological studies have found links between airborne concentrations of particulate matter and increased morbidity and mortality, more specifically respiratory and cardiac diseases. There is no environmental standard for environmental emissions of particulate matter.

2.2.3 Deposition of particulate matter

The processes which remove particulates from the air to the surface are defined as deposition (QUARG, 1996). There are three different forms of deposition wet, dry and occult deposition. They are independent of each other and influenced differently by meteorological, topographic and vegetative characteristics (Grantz *et al.*, 2003).

Wet deposition is a process resulting from the incorporation of atmospheric particles and gases into cloud droplets by nucleation, and their subsequent precipitation as rain or snow or from the scavenging of particles and gases by raindrops or snowflakes as they fall (Grantz *et al.*, 2003; Lovett, 1994; QUARG, 1996). The process of wet deposition operates on atmospheric gases and particulates in the range of 0.05 to 2.0 μm in diameter (Lovett, 1994; QUARG, 1996). This process of particulate matter deposition cleanses the air and deposits a significant amount of particulate matter to the surface (Grantz *et al.*, 2003).

Wet deposition is relatively unaffected by surface properties, but heavily dependant upon precipitation and ambient pollution concentrations, making it easy to quantify (Grantz *et al.*, 2003). The surface properties of leaves, such as wetability, exposure and roughness determine the retention of liquid and hence dissolved particulate matter on the leaf surface (Grantz *et al.*, 2003). The residence time of the dissolved particulate matter on the leaf depends upon the time taken to dry the leaves or until it is re-deposited by rainfall (Grantz *et al.*, 2003). Rainfall is responsible for the deposition of

particulate matter and also the re-distribution of previously dry deposited particulate matter on foliar surfaces (Grantz *et al.*, 2003). The concentration of particulate matter on the foliar surface is typically highest at the onset of a precipitation event and declines with duration of the precipitation event (Lindberg & McLaughlin, 1986).

Periods of heavy or sustained rainfall are responsible for a heavy chemical burden to the soil, as it transfers particulate matter from the foliar surface to the soil (Grantz *et al.*, 2003; Lovett & Lindberg, 1984) and can affect the potential uptake by the roots of the vegetation (Winner, 1994). However, in subsequent periods, dry deposition is substantially reduced due to the cleansing effect of wet deposition on the atmosphere (Grantz *et al.*, 2003; Lovett & Lindberg, 1984). Therefore low intensity precipitation can result in higher concentrations of deposited particulate matter on the foliar surface (Grantz *et al.*, 2003). Hence any study of particulate deposition should consider the collection of meteorological information to fully appreciate the foliar and soil loading.

Dry deposition is the slowest, yet continuous process of deposition which deposits material to any exposed surface of plant, soil or water (Grantz *et al.*, 2003). Dry deposition is controlled by air flows and gravity, which act in the lower atmosphere to bring particulate matter back to the surface almost continuously. It is extremely difficult to measure and model due to the huge diversity of influencing factors including; particulate size, diversity of canopy surface and structure, leaf microstructure, cell physiology, atmospheric chemistry, meteorological effects, and a variety of chemical constituents (Grantz *et al.*, 2003; Lovett, 1994). However, it is mainly controlled by atmospheric stability, wind speed, macro and micro-surface roughness and the diameter and surface characteristics of the particulate to be deposited (Grantz *et al.*, 2003; QUARG, 1996). The rate of deposition is expressed as Deposition Velocity and it is calculated by the following equation:

Equation 2.1

$$\text{Vd (m/s)} = \frac{\text{Flux density to surface (g m}^{-2}\text{ s}^{-1}\text{)}}{\text{Concentration at reference height (g m}^{-3}\text{)}}$$

Large particulates greater than 5 μm in diameter are transported by turbulent eddies in the lower atmosphere, created by fluctuations in surface temperature. These larger particulates are deposited by gravitational sedimentation and inertial impaction, whereas smaller particulates, in the range of 0.2 – 2.0 μm in diameter, can travel in the atmosphere for long distances until they are incorporated, most likely into wet deposition

(Lovett, 1994). The smallest particulates, less than 0.2 μm in diameter, are transferred by Brownian diffusion across the Planetary Boundary Layer (PBL - the first kilometre of the atmosphere, adjacent to the earths surface) (Lovett, 1994; QUARG, 1996), until they make contact with the surface, which is usually mediated by impaction (Grantz *et al.*, 2003). Once the particulates touch the surface (usually vegetation, soil or any surface feature), surface forces retain the particulates, even after multiple bounces. Methods to measure dry deposition are not sufficiently robust, since the mechanisms and factors governing dry deposition are not fully understood due to the considerable variation in particle size, canopy surfaces, and the chemical constituents of particulate matter which determine the rate of dry deposition (Grantz *et al.*, 2003). The foliar washing technique is one of the best available methods for determining dry deposition to foliar surfaces. After a pro-longed dry period, measurements of the through-fall (the process of water shedding from leaves to the ground surface) and stem-flow (the flow of water down the trunk or stem of a plant) of particulates, compared to parallel measurements of wet deposition can be used to determine the magnitude of dry deposition between precipitation events (Grantz *et al.*, 2003).

Occult deposition is the process of gaseous pollutant species dissolving into water droplets of fog or cloud i.e. coastal fogs, and are deposited to the surface by non-precipitating droplets (Fowler, 1980; Fowler *et al.*, 1991; Grantz *et al.*, 2003; Lovett & Kinsman, 1990; Lovett, 1994). As the fog forms it accretes and removes particles from the air, aqueous oxidation reactions assist particulate growth, removing airborne particulates and enhance deposition (Grantz *et al.*, 2003). A gas/liquid phase equilibrium develops due to the atmospheric stability which allows the droplets to persist (Grantz *et al.*, 2003).

There are two processes of deposition which act on different sized particulates; the first is gravitational sedimentation, which is responsible for the deposition of the larger particulates (Lovett, 1994). The second is by penetration of the canopy layer, this is caused as the wind moves over the surface of the vegetation, eddies are generated allowing the mixing of the droplet-laden air into the canopy (Lovett, 1994). Once within the canopy the sedimentation or inertial impaction allows the droplets to penetrate the leaf and stem boundary layers (Lovett, 1994). It is an extremely efficient method of transporting dissolved and suspended material directly to vegetative surfaces. The concentration of particulates is far higher within cloud or fog than precipitation or ambient air; particulates are delivered directly to the foliar surface in a hydrated and

bio-available form, whilst also re-hydrating previously dry deposited particulates through deliquescence, increasing their persistence on the surface of the leaf (Grantz *et al.*, 2003).

Occult deposition is influenced by factors that control cloud chemistry, meteorological factors that control cloud formation, atmospheric chemistry, and water content (Lovett, 1994). The proportion of particulate matter in fog droplets is deposited proportionally to wind speed, droplet size, concentration and liquid water content of the cloud or fog (Grantz *et al.*, 2003). The rate of occult deposition is also influenced by the receptor surface in three main ways (Lovett, 1994):

1. Gross canopy structure affects the intensity of turbulent mixing.
2. Shape, orientation and spatial arrangement of leaves and the stems of the vegetation determines the efficiency of transfer across the boundary layers.
3. Canopy density determines the surface area available for deposition (Lovett, 1994).

2.2.4 Particulate monitoring

2.2.4.1 Active monitoring

There are three main types of active monitoring which can be used to monitor the ambient suspended particulate matter concentrations in the atmosphere; Semi-automatic monitoring; automatic monitoring and optical sensor systems. The monitors require large sample sizes to provide continuous measures of the concentration of particulate matter, however they provide accurate and reliable results (Namiesnik *et al.*, 2005).

Semi-automatic samplers are usually low in cost, reliable and easy to operate. They are capable of providing daily averages, although some methods can be labour intensive, requiring laboratory analysis (DEFRA, 2005). The pollutant is collected by either physical or chemical means for analysis, usually by filtering a known volume of air for a known period of time through a chemical solution or filter (DEFRA, 2005). Gravimetric samplers filter particulate matter over a period of 24 hours and the mass collected on a filter is determined by weighing (QUARG, 1996). The samplers have an omni-directional narrow entry slot which allows the particulate matter to penetrate the filter in wind speeds up to $10\ m\ s^{-1}$ however, it requires a connection to a mains electricity supply (QUARG, 1996).

Automatic monitors provide high resolution data typically over an hour, yet they are relatively expensive requiring a trained operator and regular servicing which increases the overall maintenance costs (DEFRA, 2005). Samplers include the Tapered Element Oscillating Microbalance (TEOM) or the β-attenuation instrument, which analyse their samples in real-time, making them reliable and accurate (DEFRA, 2005). The TEOM measures the change in effective mass of a heated (50°C) oscillating tapered glass tube, whereby the deposition of particulate matter on the surface of a filter will cause a change (decrease) in the resonant frequency, which is proportional to the mass of the deposited particulate matter (Environment Agency, 2004; QUARG, 1996). The β-attenuation instrument measures the reduction in the intensity of beta particles passing through a filter, due to the accumulation of particulate matter on the filter (paper or fixed) (Environment Agency, 2004; QUARG, 1996). The accuracy of the results depends upon the geometry of the measuring head, the uniformity of the filter thickness and the strength of the beta source (Environment Agency, 2004). However, it is flawed as it is calibrated with the mass absorption co-efficient of Quartz, yet that of ambient aerosols can vary by up to ± 20 % of this, providing less accurate results than the semi-automatic gravimetric samplers and at a much higher price (Environment Agency, 2004; QUARG, 1996).

Optical sensor systems can be used portably and can provide spot measurements due to the low-sensitivity of the equipment. These instruments measure particulate matter by changes in the visible light in a sensing region (QUARG, 1996). This requires calibration and is subject to considerable uncertainty if the nature of the particulate changes, as the reading depends upon the size distribution, shape and refractive index of the particulates (QUARG, 1996). The Optical Scattering Instantaneous Respirable dust Indicating System (OSIRIS) monitor measures the ambient atmosphere using the principle of a narrow forward-angle of light scattering, which is proportional to the dust concentration and it is capable of providing 15 minute mean concentrations (Energy and the Environment Programme, 1999). A pump continuously draws an air sample through the nephelometer, which sizes individual particulates as they pass through a laser beam, and then collects them on a filter (Parsons & Salter, 2000). The filter can be weighed to calibrate the results gravimetrically, and chemically analysed or inspected using Scanning Electron Microscopy (SEM) (Parsons & Salter, 2000).

Although spatial and temporal real-time monitoring of the total suspended particulate matter on the SSSI would be very beneficial, exposing expensive equipment on the site is not realistic due to constraints on safety, resources and power supply.

2.2.4.2 Passive monitoring

The passive monitoring of ambient atmospheric particulate matter involves measuring the concentration of any analyte as a weighted average over the sampling and/or extraction time, which requires significantly less time than that consumed in active monitoring (Namiesnik *et al.*, 2005). Passive monitoring systems are cheap, simple and quick to use, producing accurate results, and can operate without mains electricity (Namiesnik *et al.*, 2005). There are five types of dust deposit gauges routinely used in the UK.

The British standard deposit gauge has an upward facing glass bowl supported by a metal stand at a height of 1.2m from the ground, the design was originally based on a rain gauge but increased in height to avoid collection of saltated material from the ground (Hall *et al.*, 1993). It samples ambient deposition vertically by dry or wet deposition. The drawbacks of this gauge is that it is susceptible to high losses since it is not optimally aerodynamic in strong winds, due to circulatory flows removing deposited particulates (Vallack, 1995a). It is only suitable for long exposure periods of one year with individual exposure periods of one month, which will obscure peaks in deposition. This gauge is now in limited use as the glass bowl can no longer be purchased and developments in dust gauge design have improved sampling methods (Environment Agency, 2004).

The International Standard deposit gauge (ISO, 1975) (see Figure 2.1.a) was designed to improve collection efficiency over that of the British Standard Gauge. It consists of an upward facing cylindrical collecting container with a bevelled edge at 45° and a bird guard (Environment Agency, 2004). It can be exposed for a period of one month, but its collection efficiency is limited as it is ineffective at slow wind speeds and is subject to loss of particulate matter at high wind speeds (I R Hanby, pers. comm.).

The Bergerhoff dust deposit gauges (see Figure 2.2.b) are typically exposed for one week. This is the cheapest and simplest of all the deposit gauges, it consists of a 5 litre collecting bottle mounted on a stand fitted with a removable bird guard, in accordance with the German Standard VDI 2119. This gauge is particularly sensitive to loss of material at high winds (I R Hanby, pers. comm.).

The British standard directional dust gauge (see Figure 2.1.c) is used to measure the dust flux into four vertical tubes aligned at 90° to each other over a period of 10 days to 1 month (Hall *et al.*, 1993). Once effectively positioned, it can distinguish dust from four different compass points. The four cylinders have a vertical slot which leads into their own collecting bottle. However, this means the measurements can only be applicable when there is one large dust source with a reproducible density and

composition (Environment Agency, 2004). The Corus site at Teesside is located within a mixed industrial area and this would be extremely unsuitable. Although effective at determining the direction of source depositing material, the directional dust gauge cannot directly indicate local deposition (Hall *et al.*, 1993).

The dry foam Frisbee dust deposit gauge (subsequently referred to as the "Frisbee" gauge) is the most recent of many prototypes designed to measure dust deposition (mg m^{-2} day^{-1}) (see Figure 2.1.d). An anodized aluminium Frisbee (see Figure 2.2) is supported by a steel tripod at 1.7m above ground level, within the tripod an internal opaque drain pipe leads from the base of the Frisbee to a 5 or 10 litre rainwater collecting bottle situated at ground level in the centre of the tripod (Vallack, 1995a). The Frisbee has a 227 mm diameter aperture and has been aerodynamically designed to flatten the airflow above the gauge, hence the wind speed of the air passing over the Frisbee is reduced to allow material to deposit out into the gauge (Hall *et al.*, 1993) (see Figure 2.2).

A stainless steel bird guard is supported above the Frisbee, this uses nylon thread crossed in a star formation to prevent birds landing on the gauge, and to reduce the risk of contaminating samples with bird strikes (Vallack & Shillito, 1998). The tripod can also support a cylindrical sticky pad adaptor which allows for directional sampling (see surface soiling Chapter 2 section 2.4.3). The Frisbee contains a black polyester foam dust trap designed to reduce sample contamination from falling leaves, insects or bird droppings (Vallack & Shillito, 1998) and also prevents dust previously deposited lost by rain splashes ('splash-out') or strong winds ('blow-out').

Although the specific efficiency of collection for the Frisbee dust deposit gauge has not been published, development at the Stockholm Environment Institute (SEI), York has shown that they are 36 % more efficient in comparison to the British Standard dust gauge (Vallack, 1995a), which was previously accepted as an efficient method of dust deposition (Hanby, pers. comm.). The SEI protocol on exposure, collection and analysis of the Frisbee dust deposit gauge has been published (Vallack, 1995b).

The passive dust deposition monitoring gauges are particularly susceptible to erroneous results from non-dust deposits including bird droppings, leaves and vandalism, but passive monitoring devices provide a considerably cheaper and realistic alternative to real-time monitoring for the present study. The favoured device for the present study is the Frisbee dust deposit gauge as it is cheap and can be repeated easily.

Figure a

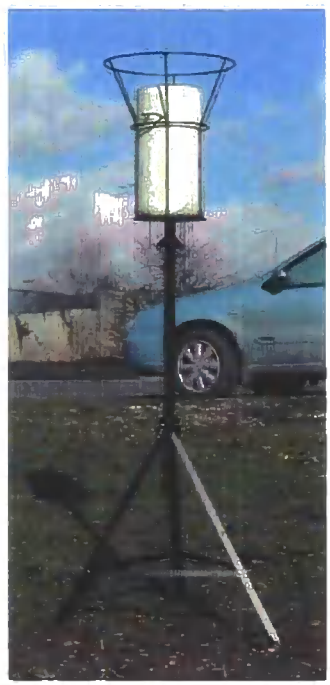

Figure b

Figure c

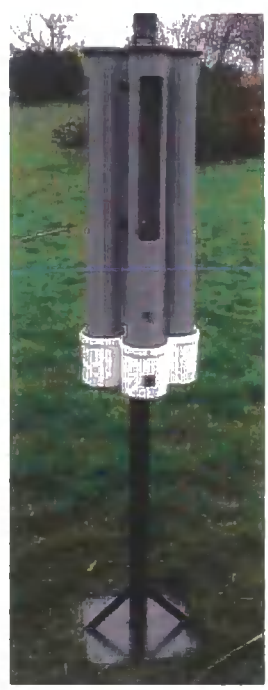

Figure d

Figure 2.1 Dust deposition Gauges. Figure a. The ISO dust deposit gauge. Figure b. The Bergerhoff Dust Deposit Gauge. Figure c. The directional dust gauge. Figure d. The dry foam Frisbee dust deposit gauge (Images from www.hanby.co.uk/ Ian Hanby, 2007).

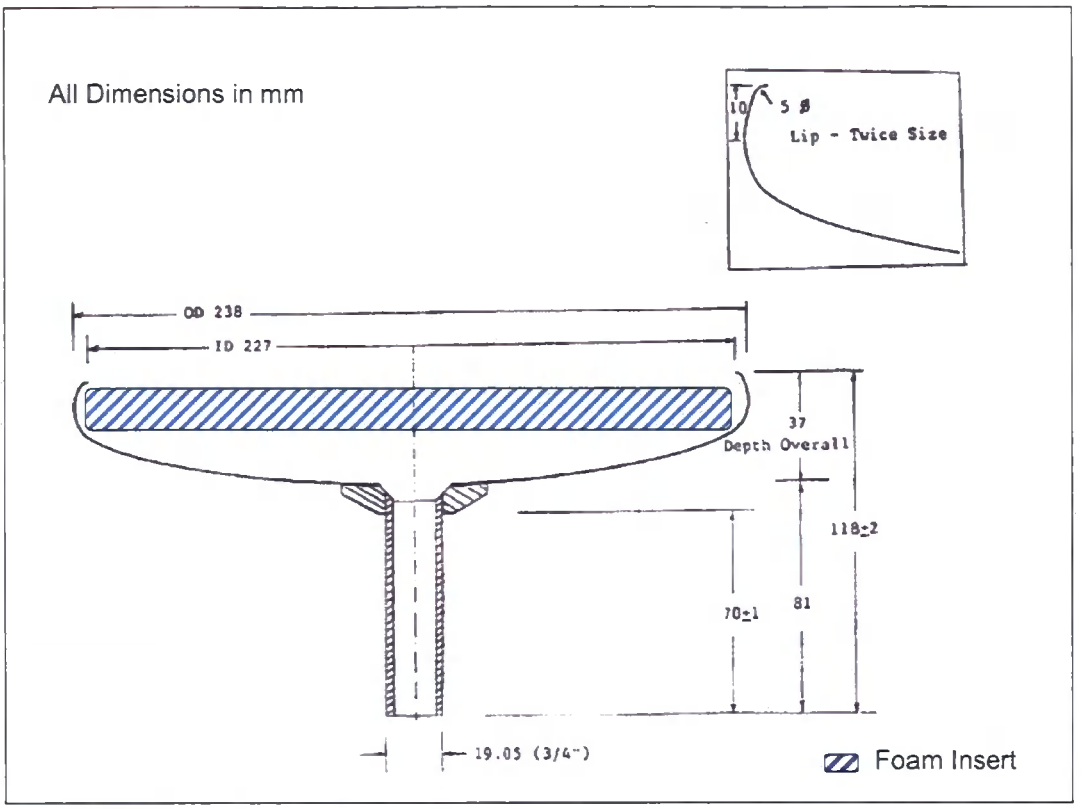

Figure 2.2 Cross-section diagram of the dry foam Frisbee dust deposit gauge, where all dimensions are in mm (Hall *et al.*, 1993). The blue hatched area shows the foam insert.

2.2.4.3 Surface soiling

Surface soiling measurements are designed to assess the nuisance value of dust (Adams, 1997). The Evans Electroselenium Smokestain Reflectometer (EEL) (Diffusion Systems Ltd, London, UK), also termed a gloss meter or photometer, can be used to measure the reduced surface reflectance after exposure to the ambient atmosphere, measured in Soiling Units (SU). The main drawback of this method is that surrogate surfaces, which were typically glass slides, were not thought to adequately represent the natural surface features of vegetation and hence could not readily produce reliable estimates of particulate deposition (Grantz *et al.*, 2003).

The glass slide soiling method is simple and effective way to determine the change in soiling rates of a surface over a period of time (Beaman & Kingsbury, 1984; Brooks & Schwar, 1987; Schwar, 1994; Schwar, 1998) followed by photometric analysis. It does not provide an overall measure of dust deposition since they are susceptible to the loss (by precipitation) or re-entrainment of particles. They are exposed for approximately one week and the dustiness of the slide is measured with a reflectometer, such as the EEL Smokestain Reflectometer. The reduction in reflectance is calculated using a pre-

exposure and post-exposure value. It is an extremely cost effective and repeatable method, which allows for particulate characterisation (finger-printing) using optical microscopy or SEM analysis. However, the reflectometer is subject to variability due to the thickness of the glass slides, any contaminants on the reverse of the slide, and only one measurement is taken per slide, not accounting for variability within a sample (Adams, 1997).

The sticky pad method is a non-intrusive method (Beaman & Kingsbury, 1981), designed to be exposed for a period of 2 to 7 days. White (or any other colour) Fablon self-adhesive vinyl stickers are used as the sampling medium, which are mounted on flat boards, that when placed horizontally will measure dust deposition or vertically will measure dust flux[1]. The change in reflectance, relative to a clean sticky pad is measured using a sticky pad reader (I R Hanby, Newark, UK). The sticky pad reader is designed to emulate readings from an EEL Smokestain Reflectometer and measure the percentage effective area coverage (% EAC). The reader has three tungsten filament bulbs, equally spaced to ensure uniform brightness across the sample (Hanby, 2007b). Measurements are taken at the centre of an illuminated circle 6 mm in diameter in the locating mask, at the base of the reader (Hanby, 2007a).

The sticky pad reader has achieved a linear relationship between reflected light energy and meter reading, by converting the photocurrent to voltage at zero photodiode voltage. The linearity of this relationship allows a two point calibration method, yet poor calibration can result if two points of similar meter readings are used.

The commercial company Dustscan provides a durable, passive and uncomplicated directional dust gauge, which monitors fugitive dust from 360° around the sampling head. It has an adhesive dust collection sheet mounted at 2 m, it is an ergonomically designed and protected by a rain guard. It is simple and cheap to install while also durable and discreet to avoid vandalism. Reliable samples can be taken quickly. The sticky pads are ideally exposed for a period of one week, up to a maximum of two weeks. For analysis the head is removed and placed into a carrying flask to prevent further exposure or damage. The sticky pad is then scanned and analysed using specialised equipment. The results can also be sent for geochemical, mineralogical or other analysis post-scanning. It will determine two measures of nuisance dust;

[1] A sticky pad is a directional deposition gauge, but the term dust flux is used in the present thesis to differentiate from dust deposition collected by the Frisbees.

1. Absolute Area Coverage (AAC %) a measure of the density of deposited dust (as presence or absence on the sample slide) irrespective of dust colour.

2. Effective Area Coverage (EAC %) a measure of the loss of reflectance or 'blackness' of the deposited dust.

It can also provide an estimate of mass deposition per unit area (as measured by a deposition gauge) and can be derived using standard formulae calibrated from site-specific information. For each sample 150,000 data points are individually assessed, making it a sensitive, repeatable and a powerful nuisance dust monitoring method. Up to 5° or 15° degree resolution allows indication of dust origin onto, across or out of a site and can provide a directional dust rose plotted across the site. These data can then be examined with meteorological data, to determine the prevailing meteorological conditions during the period of exposure. The sticky pads are then be sealed transparently allowing analysis of visual properties such as dust colour and particulate shape and size, and stored for later analysis if required.

2.2.5 Chemical characterisation of particulate matter

Detailed particle information can be obtained from single particle analysis techniques. These techniques can determine the potential origin, formation, transport, reactivity, transformation reactions and hence the potential environmental impact of the emitted particles (Jambers *et al.*, 1995). Determination of the specific chemical characteristics is therefore an important tool for assessing the affects of particulate emissions once deposited to foliar surfaces and the soil of the SSSI. Although different types of electron microscopes are available for single particle analysis, they all rely on electron beams to create various signals, and measure the change in the signal as an indication of the particle nature (Jambers *et al.*, 1995). Scanning electron microscopy coupled with energy dispersive x-ray detection or wavelength dispersive x-ray detection (SEM-EDX and SEM-WDX) has been used extensively to examine morphological and elemental information of particles (Bourrier & Desmonts, 2007; Lorenzo *et al.*, 2006; Xie *et al.*, 2005; Yue *et al.*, 2006). Manual methods have been an extremely useful tool however, they are very time-consuming to ensure sufficient particles are analysed for statistical testing (Jambers *et al.*, 1995). Automated methods of Computer Controlled Scanning Electron Microscopy (CCSEM) have yielded a greater number of particles analysed in a

time-efficient manner (Choel *et al.*, 2007; Katrinak *et al.*, 1995; Xhoffer *et al.*, 1991) although the detection limits and working conditions are less favourable (Jambers *et al.*, 1995).

Within the current literature the chemical characterisation of particulate matter primarily rich in iron has been attributed to sources of emissions in ferrous metallurgic processes (DeBock *et al.*, 1994; Katrinak *et al.*, 1995; Michaud *et al.*, 1993; Post & Buseck, 1984; Van Malderen *et al.*, 1996a; Xhoffer *et al.*, 1991). Determining the chemical characterisation of the dust deposited to the SSSI would be useful in assessing the contribution of particulate emissions to the SSSI, and also the effects of particulate matter on the plants and soil of the SSSI.

Analysis of dust samples collected on the Corus site and comparing the chemical character or 'finger-print' with samples of deposited dusts, it is possible to identify the origin of the particles, crudely as originating from Corus or not originating from Corus. Scanning Electron Microscopy and Energy Dispersive X-ray analysis (SEM-EDA) will be used on samples of reference and deposited dusts.

2.2.6 Modelling particulate matter

There are many different sources of particulate material, with diverse chemical characteristics; therefore models cannot fully describe the generation and spatial and temporal variation for all particulates. However, there are a variety of dispersion models available which can predict a range of temporal and spatial variations in particulate matter (AQEG, 2005), and the modelling of particulate emissions is an effective method for determining particulate emissions. These models are able to predict future scenarios and predictions under various mitigation strategies. Given the pollutant emission data and atmospheric information, dispersion models can calculate the concentration of pollutants to across a specified area or to a specific site. The amount of pollutant released can be calculated by either actual measurement or process knowledge. Gaussian plume dispersion models can be used to explain observed concentrations of air borne pollutants. They can be used to test scenarios of atmospheric stability to determine the downwind air pollutant at the local scale.

There are a range of effective atmospheric dispersion models available for modelling particulate emission scenarios for example box models (e.g. AURORA), Gaussian models (e.g. CALPUFF, AEROPOL, AERMOD, ADMS), Lagrangian/Eulerian models (GRAL, TAPM) and CFD (Computational Fluid Dynamic) models (e.g.

FLUENT, ARIA local) see Holmes & Morawska (2006) for more detailed information. Previous model scenarios conducted by Corus used the Atmospheric Dispersion Modelling System (ADMS) and therefore to obtain comparable results, ADMS was chosen to model particulate emissions for the present study. ADMS is an advanced Gaussian atmospheric dispersion model which can be used to model the potential emissions from industrial installations, and has performed well in validation studies (Carruthers *et al.*, 2000; Hanna *et al.*, 2001; Holmes & Morawska, 2006; Riddle *et al.*, 2004; Timmis *et al.*, 2000). The model can be used to assess a variety of different sources including point, area, line, volume and jet emissions. Options for the model include dry and wet deposition, NO_x chemistry, hills, buildings, puffs, fluctuations, odours, radioactivity, plume visibility, coastline and time varying sources.

2.3 Particulate matter at the Corus works, Teesside

2.3.1 The steel production process

The Corus works, Teesside is an integrated iron and steel manufacturing plant, with coke ovens, a sinter plant, a blast furnace, a Basic Oxygen Steel-making plant (BOS), and steel rolling mills. There are several processes that take place on the site for processing the raw materials. Firstly the coal is heated in the Coke ovens, which are airless ovens, to over 2000 °C to remove any volatiles and convert the coal into coke, while the iron ore, usually hematite or magnetite, is processed in the sinter plant to produce pellets of iron ore. The coke is added to the top of the blast furnace, while hot air is blown into the base of the blast furnace. Within the blast furnace the iron ore is then reduced with the coke to molten iron. To remove any impurities in the iron ore a flux, usually silicon dioxide but sand, silicates, limestone or dolomite are also used, is added to the blast furnace, which produces the waste slag. The waste slag sits on top of the molten iron, due to the high temperatures of the blast furnace, and hence the two products can be drawn off separately. The molten iron is then transferred by large vats termed torpedoes to the BOS plant, where the carbon content of the molten iron is reduced. Depending on the required final quality, the molten iron can be pre-treated by either desiliconisation or desulphurisation before going into the BOS plant furnace.

The BOS plant furnace is charged with a ratio of 4:1 molten iron to steel scrap. A cooled lance blows pure oxygen into the furnace, which ignites the dissolved carbon

producing carbon monoxide and carbon dioxide. This process heats the vessel to approximately 1700 °C and melts the steel scrap. Burnt lime or dolomite is then added to absorb any impurities in the steel; this forms a slag which can be poured off separately. The steel is poured into a ladle, a process called tapping, and specific alloys can be added to give specific qualities to the final required product.

2.3.2 The Corus works, Teesside

Steelmaking began in Teesside in 1875 when Bolckow Vaughan and Co, Ltd. installed acid converters at the South Bank works. In the years that followed this was replaced by open-hearth steelmaking (1911), and then accompanied by the Warrenby Steelworks and Plate mills (1916). Although Dorman Long and Co, Ltd. had purchased six blast furnaces in 1929 at Redcar, these two companies merged in 1929.

At some time between the turn of the century and 1914, blast furnace and steelmaking slag, together with refractory materials and demolition rubble, were consolidated to begin reclaiming land from the sea. This area includes the current Redcar blast furnace and the adjacent sand dunes of Coatham Sands and South Gare SSSI.

Development of the Lackenby site, which included an open hearth steel plant and universal beam mill, began in 1946, after the purchase of 600 acres of land between Redcar and Cleveland. In 1967 the Iron and Steel Act nationalised the iron and steel making works across the UK and established the British Steel Corporation (BSC).

The present day ironworks underwent further development throughout the 1970s. The Redcar works was developed with the construction of the marine ore reception terminal and ore unloading facilities, burden preparation facilities, including ore stockyards, blending facilities, sinter plant, pellet plant, coke ovens, blast furnace and power plant. While the Lackenby works developments included the commissioning of the Basic Oxygen Steelmaking (BOS) and the continuous casting plant. The works were developed further in the 1980s for secondary steelmaking facilities. By 1988 the Cleveland, Lackenby and Redcar sites were integrated as one steel works, and the BSC was privatised as British Steel plc (previously Corus, now Tata Steel).

In 2006, the Corus works produced 4,100,254 tonnes of sinter, 1,220,402 tonnes of coke from the Redcar coke ovens and 555,408 tonnes of coke from the South Bank coke ovens. The Corus works produced 3,182,077 tonnes of liquid steel and 3,122,511 tonnes of top-hole iron in 2006.

2.3.3 Dust at the Corus works, Teesside

The Corus works, Teesside is an integrated iron and steel plant, where a wide range of potential dust generating activities and processes are undertaken. Stack emissions are monitored to adhere to strict stipulations of particulate matter emissions, but probably do not contribute significantly to dust deposition on the SSSI as the emissions are most likely entrained in air flows carrying them beyond the Corus works and the SSSI to the North Sea. It is most likely that the fugitive particulate emissions, of the coarse dust fraction, which are deposited to the surface quickly, contribute to the potential deposition of particulates on the SSSI. Large quantities of coarse dust are known to be created from the loading, unloading, transport and storage of materials on industrial sites, especially the handling facilities for dry bulk cargoes such as coal and iron ore (Gupta *et al.*, 2005).

Few studies have investigated the loss of raw material from wind erosion of open storage yards at steelworks, yet these dust emissions are known to contribute a significant proportion of the total level of suspended particulates (Badr & Harion, 2005). Despite the application of latex sprays to the material stockpiles, the continual rotation of material exposes a new face from which particulates can be raised and carried by the wind (Farmer, 1993), which reduces the overall effectiveness of the latex. The erosion from stock piles is dependant upon wind energy and the available eroding particles along with stored bulk density, surface crust, moisture content, particle size distribution, and pile geometry. The most vulnerable area of stock piles to erosion is the upper-half of the windward slop on sharp crested piles, hence conical piles with flat tops are more sheltered from the effects of wind erosion (Badr & Harion, 2005). Previous works have observed an abrupt drop in air pressure associated with sharp crested piles, which enables greater mass transport of material (Neuman *et al.*, 1997; Walker & Nickling, 2003). Hence the wind speed over stockpiles can be a rough estimate of dust emissions, which allows for predictions for areas of deflation and deposition (Badr & Harion, 2005).

Although some studies have investigated the fugitive dust emissions from steelworks and coal power stations, they have focussed on the shelter effect of porous barriers or windbreaks (Badr & Harion, 2005; Borges & Viegas, 1988; Lee & Kim, 1999; Lee *et al.*, 2002; Stunder & Arya, 1988). The size of stockyards and the unpredictability of meteorological conditions can make barriers and windbreaks ineffective relative to their cost (Badr & Harion, 2007). Therefore, the most efficient technique to minimise particulate emissions lift-off from stockpiles would be to arrange stockpiles according to

the dominant wind characteristics to minimise sediment transport (Badr & Harion, 2005; Badr & Harion, 2007).

A considerable area of Corus works are for material stock piling. The Corus works consumes large volumes of material annually, during 2006 approximately 5,000,000 tonnes of iron ore, 2,500,000 tonnes of thermal and coking coal, 62,000 tonnes of coke, over 100,000 tonnes of Olivine sands and over 730,000 tonnes of limestone were received (G Williams, pers. comm.). These stock piles are subject to continuous addition, re-distribution, blending and removal of material.

The Corus works also use dust suppression techniques to prevent the initial suspension and re-suspension of particulate matter. Dust suppression with water, fine mists and sprays with binding agents are all effective tools for reducing the fugitive dust emissions from vehicles, roads and stockpiles (Environment Agency, 2004; Goldbeck & Marti, 1996).

There are many potential activities and processes on the Corus works which could contribute to fugitive emissions include the unloading facilities at the shipyards, the blast furnace, the BOS plant, the sinter plant and the ponding station. Therefore there are many sites, activities and processes on the Corus works which can lead to fugitive dust emissions. Therefore characterisation analyses of deposited dusts are difficult to attribute to a single on-site source.

2.4 The effect of particulates on vegetation

Particulate matter can have both chemical and physical effects on the soil, flora and fauna of communities (Talley *et al.*, 2006). The potential chemical effect of dust is greatest when the dust contains toxins, acids, bases or metals (Farmer, 1993; Pagotto *et al.*, 2001; Talley *et al.*, 2006). Plants coated with non toxic dusts display symptoms of leaf shading, blocked stomata, leaf injury (necrosis), increased diffusion resistance, increased leaf temperature, inhibition of transpiration, reduced photosynthesis, increased water loss, reduced vegetative growth and reduced reproductive output and reduced fruit set which are exacerbated by chemically active dusts (Czaja, 1961; Eller, 1977; Eveling, 1969; Farmer, 1993; Grantz *et al.*, 2003; Hirano *et al.*, 1995; Sharifi *et al.*, 1997; Talley *et al.*, 2006). A study on the effects of urban dusts on the Fir *Abies alba* were compounded by nitrous oxides and lead from car exhaust emissions (Braun & Flückiger, 1987). The physical smothering of plants depends upon the emission rate of particulates, meteorology and leaf surface conditions, and require measurements of absolute dust

levels to be recorded, but even low concentrations of dust have been shown to effect plant health (Farmer, 1993).

At the species level, particulate matter has been shown to cause the decline and extinction of species, in addition to changes in community structure. At the community scale it has been shown to have caused a change in the dominant tree species of *Acer rubrum*, *A. saccharum, Quercus prinus, Q. rubra* (Brandt & Rhoades, 1972), and the community structure of epiphytic lichens (Gilbert, 1976). Typical responses at the plant level include the development of chlorotic and necrotic spots on the leaves (visible injury – usually as the cell contents become disorganised), foliar senescence, reduced photosynthesis, reduced stomatal conductance, change in root-shoot ratio, reduced growth and reproduction (Grantz *et al.*, 2003; Winner, 1994). It is important to note that some of the most sensitive components of an ecosystem are masked by averaging and compensatory mechanisms, so monitoring of the effects of deposition should incorporate sensitive individuals (Winner, 1994).

Dust can also have a significant effects on the plants indirectly through secondary stresses such as drought or pathogens, as they alter the competitive balance between species, alter the soil chemistry and soil microbial communities (Farmer, 1993). Dust also provides a medium for the growth of fungal diseases and also reduces the effectiveness of pesticide sprays for crop plants (QUARG, 1996). This can reduce the capacity of the plants to respond to other environmental stresses, such as soil chemistry (Winner, 1994). It is important to obtain a range of indicative stress characteristics for particulate matter as it could be confused with non-pollutant stresses, such as nutrient deficiencies (Farmer, 1993). Although some studies on individual organisms have revealed much regarding the effect of air pollutants on plants. Linking these to adverse impacts to populations and communities would provide information on the ecosystem response to stress (Sigal & Suter, 1987). Changes to the population structure are very slow to appear, hence species diversity has become one of the most frequently measured parameters, although changes in biomass and nutrient content of the litter may provide some valuable insight into the properties of the community (Grantz *et al.*, 2003; Sigal & Suter, 1987).

Chemical attack, directly on the plant or indirectly on the soil can have detrimental effects on plant growth, especially chemical attack on the soil which will have much longer detrimental effects due to the alteration in soil chemistry and pH, nutrient cycling, disturbance to the transpiration stream and the plants ability to absorb minerals (Farmer, 1993; Grantz *et al.*, 2003; Petavratzi *et al.*, 2005). Trombulak &

Frissell (2000) found that increased ambient dust levels near roads had a number of ecological effects including altered hydrology, geomorphology and invasive species spread.

In a study by Dixit (1988) *Amaranthus dubius* and *Phaseolus vulgaris* leaves, dusted with bauxite and cement dusts showed visible injuries including chlorosis and necrosis, in addition to premature senescence. These responses were similar to the response found to ozone (Swanson *et al.*, 1973; Thomson *et al.*, 1966) and to water, temperature and light stresses (Wise *et al.*, 1983).

In a recent study on the effects of dust on the Valley Elderberry *Sambucus mexicana* (Talley *et al.*, 2006), there was a weak correlation between dust deposition and symptoms of stress including water stress, dead stems and reduced leaf size, overall plant size was reduced, the water content of the leaves were lower and the leaves were thicker.

A study conducted on the shrub *Viburnum tinus* (Thompson *et al.*, 1984) found dust application to the upper surface of leaves, caused leaf shading and reduced photosynthesis, while dust application to the lower surfaces of the leaves impeded diffusion. However, to elicit this response dust loading between 2.5 and 5 times higher was required. Gale and Easton (1979) also found photosynthesis was reduced by up to 10 % on three arid shrubs, and the increase in light intensity in summer months was not sufficient to compensate for the effect of leaf shading, although the study did not account for the potential chemical effect of limestone dust. Another study on desert shrubs found a reduction in photosynthesis by 21 % in *Larrea tridentate*, 44 % in resinous leaves and photosynthetic stems of *Atriplex canescens* and 58 % in non resinous C_4 leaves of *A. canescens* (Sharifi *et al.*, 1997). Dusting leaves was also found to reduce the maximum leaf conductance, reduced transpiration, reduced instantaneous water use efficiency, increased leaf temperature (due to increased absorption of infra-red radiation and increased PAR reflectance. The *Larrea* and *Atriplex* shrubs exposed to high levels of deposition had reduced leaf areas and greater leaf specific masses, which indicate the short term effects of reduced photosynthesis and decreased water use efficiency are resulting in lower primary production in desert plants (Sharifi *et al.*, 1997).

2.5 Research hypotheses

The null hypotheses to be tested in the present study were identified as the following:

1. There is no deposition of particulate matter to South Gare and Coatham Sands SSSI.
2. There is no flux of particulate matter to South Gare and Coatham Sands SSSI.
3. The deposition and flux of particulate matter is not affected by meteorological conditions including wind speed, wind direction and rainfall.
4. There is no deposition or flux of particulate matter emissions from the Corus works to South Gare and Coatham Sands SSSI.
5. The model scenario is not relevant for predicting particulate matter deposition onto South Gare and Coatham Sands SSSI.
6. There is no impact of particulate matter emissions on the flora of South Gare and Coatham Sands SSSI.

2.6 Summary of Chapter 2 - Background

The present project was concerned with the potential fugitive emissions of particulate matter from the Corus works, Teesside. The first section of this chapter presented the site and project background. In the second section particulate matter was examined, firstly how it can be defined, the human health standard, processes which lead to deposition, monitoring methods (active, passive and surface soiling techniques), the chemical characterisation and finally the modelling of particulate matter emissions. The third section covered the steel production process, a background to steel production at the Corus Teesside works, and potential sources of dust generation at the Corus works. The fourth section presented the ecological effects of particulate matter on flora and finally the fifth section presented the research hypotheses for the present study.

As there is a huge diversity of particulate matter, it is important to consider the chemical character of the particulate emissions in comparison to the chemical character of particulate matter deposited on the SSSI, to enable an assessment of the contribution of emissions to the total deposition. The present study will examine the chemical characteristics using SEM-EDA. Modelling the expected environmental concentration of particulate matter in comparison to actual measurements of deposited particulate matter enables an assessment of the relevance of particulate modelling. The particulate emissions from the Corus works will be modelled using ADMS, to compare with previously modelled scenarios.

The present research will adopt two monitoring techniques, the passive Frisbee deposit gauge and the sticky pads. These particulate monitors are accurate, precise, efficient, reliable, cost-effective, easy to use and repeatable. Although high spatial and temporal resolution real-time data would be preferable, the site limitations make this unfeasible and beyond the scope of the current project.

Dust deposition can affect flora by both direct effects on the foliar surface and indirect effects on the soil chemistry. The effects of particulate emissions on the SSSI will be examined by determining the soil iron concentration and the effects on plant gas exchange.

Chapter 3 - Dust deposition and flux

3.1 Introduction

A primary aim of the present study was to determine the total dust deposition to the area surrounding the Corus works. To achieve a resource-effective dust monitoring study, Frisbee dust deposition gauges were used in combination with directional sticky pad analysis. This combined approach enabled an examination of dust deposition and dust flux to six different sites. Taking account of the site limitations, including security, access, electricity and financial resources, the combined sticky pads and Frisbee dust deposit gauge monitoring approach represents an effective study of fugitive dust emissions.

This chapter will set out the fieldwork program designed to quantify the dust deposition and flux, split into two sections. The first section will discuss the deposition of dust to six Frisbee dust deposit gauges, while the second section will examine the dust flux to six sticky pads. The study is based at six monitoring sites which were located on and surrounding the Corus works, Teesside.

3.2 Dust deposition

3.2.1 Introduction

The first section of the present chapter will examine the dust deposition to monitoring sites on and surrounding the Corus works, Teesside. As discussed in Chapter 2, the dust deposited to Coatham Sands and South Gare SSSI has been modelled but there are no ground measurements available to qualify the model scenario. For a detailed description of passive monitoring techniques see Chapter 2 section 2.2.4.2.

A passive dust monitoring programme was designed using Frisbee dust deposit gauges. The protocol for using the Frisbee dust deposit gauge has been developed by the Stockholm Environment Institute (SEI), York, Warren Spring Laboratory, Stevenage and Selby District Council, North Yorkshire (Vallack, 1995b). The Frisbee dust deposit gauge has been used successfully to monitor dust deposition (Vallack & Chadwick, 1992; Vallack & Chadwick, 1993; Vallack, 2004) and is now a preferred method for dust deposition studies (Environment Agency, 2004).

The present section of this chapter will present the results of a passive dust monitoring study conducted with Frisbee dust deposit gauges exposed at six monitoring sites. The total dust deposition will be compared; at one site to assess variation between Frisbees; in relation to meteorological conditions measured on the Corus works and at Loftus meteorological station, and at one site to a specific activity on the Corus works.

3.2.2 Field site

The field work for this study was undertaken at the Corus integrated iron and steel works, Teesside, UK (subsequently referred to as the "Corus works" (456480, 525360 British National Grid)) and the adjacent sand dune ecosystem; Coatham Sands and South Gare SSSI (subsequently referred to as "the SSSI" (456950, 526100 British National Grid)). The site is located 7 miles northeast of Middlesbrough, and 3 miles northwest of Redcar on the south bank of the river Tees.

The location of the Corus works, Teesside is within close proximity to a group of Special Areas of Conservation (SACs), Special Protection Areas (SPAs) and Sites of Special Scientific Interest (SSSIs) which are collectively termed "Teesmouth and Cleveland Coast" (see Figure 3.1). The SSSI covers an area of approximately 381.2 ha. The SSSI was first notified by Natural England (formerly English Nature) as a site of international importance in 1971 under section 23 of the National Parks and Access to the Countryside Act, 1949 and later revised following an extensive habitat survey in 1988 (Woolven & Radley, 1988). The SSSI meets the criteria for both the European Community Directives on the Conservation of Wild Birds and the list of Wetlands of International Importance under the Ramsar Convention. The SSSI is located between the Corus works to the south, the North Sea to the north, the Tees Estuary to the northwest and Redcar to the southeast.

The SSSI supports a wide range of important habitats which have developed since the South Gare breakwater was constructed in the 1860's. The SSSI contains an extensive range of habitats including intertidal mud and sand, sand dunes, rocky foreshore, saltmarsh and freshwater marsh which are important for their flora, invertebrate fauna and bird life.

The main dune system runs for approximately 5 km from the Tees estuary in the northwest of Figure 3.1 towards the town of Redcar in the southeast. The dunes are dominated by marram grass *Ammophila arenaria,* lyme grass *Leymus arenarius* and sea couch-grass *Elymus atherica.* The dune slacks are abundant with the northern marsh

orchid *Dactylorhiza purpurella*, the early marsh orchid *D. incarnata* and the fragrant orchid *Gymnadenia conopsea*. Along the dune system, areas of tipped slag, rich in lime, support another community of plants including the yellow wort *Blackstonia perfoliata*, lesser centaury *Centaurium pulchellum*, knotted hedge parsley *Torilis nodosa*, carline thistle *Carlina vulgaris*, strawberry clover *Trifolium fragiferum* and rush leaved fescue *Festuca arenaria*. The areas of saltmarsh include sea wormwood *Seriphidium maritimum*, lesser sea spurrey *Spergularia marina*, lax-flowered sea lavender *Limonium humile*, sea purslane *Atriplex portulacoides* and smallest hare's ear *Bupleurum tenuissimum*. While the fresh water marsh communities are dominated by Bulrush or Great reedmace *Typha latifolia*, there are other species of rushes *Juncus* ssp. and sedges *Carex* ssp. and parsley water dropwort *Oenanthe lachenalii*.

The North-East of England has a temperate climate. In the summer months the North-East of England receives an average of 170 sunshine hours and an average minimum and maximum temperature of 10 °C and 19 °C respectively. The winter months average 50 sunshine hours and an average minimum and maximum temperature of 0.5 °C and 6 °C respectively. The coastal location of the Corus works minimises the number of frost days experienced on the sand dunes, however the North of England usually receives around 57 days of frost annually. Precipitation is low receiving around 750 mm annually, and only 129 days receive 1 mm or more rainfall annually. The prevailing wind direction is from the south-west.

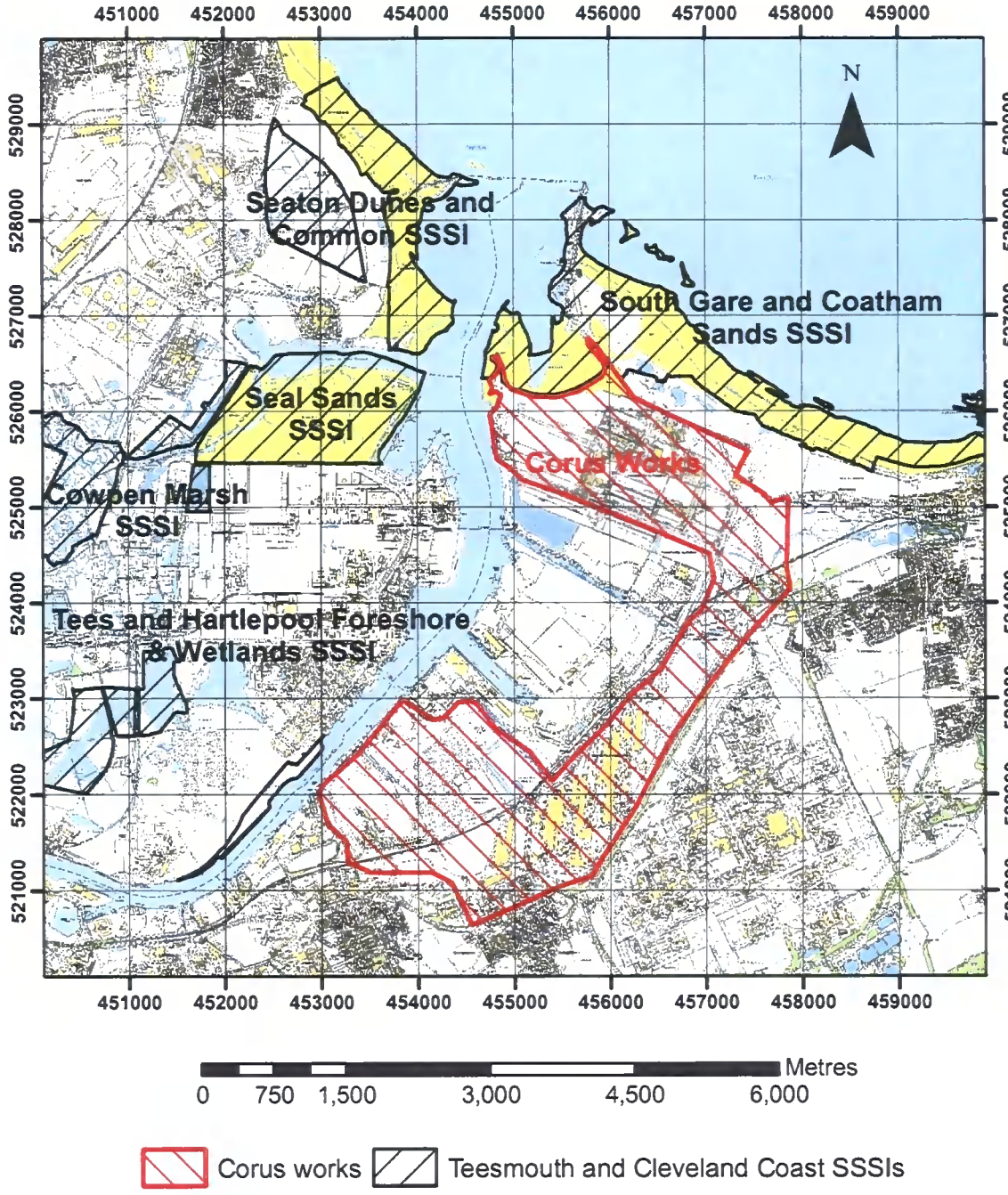

Co-ordinate System: British National Grid. Projection: Transverse Mercator.
Datum: OSGB 1936.

Figure 3.1 Location of the Sites of Special Scientific Interest (SSSI's) in proximity to the Corus Works. Black hatched areas show the SSSI's and the red hatched area shows the Corus works.

3.2.3 Methods

3.2.3.1 Locating the passive dust deposition monitoring programme

A passive dust monitoring programme was established in March 2006 at six locations on the Corus works, Teesside using dry foam Frisbee dust deposition gauges (I R Hanby, Newark, UK). The dry foam Frisbee dust deposition gauge, was developed by the Stockholm Environment Institute (SEI) University of York and other collaborators.

The aim of the monitoring programme was to quantify the potential level of dust deposition onto the SSSI. Although it was important to arrange the Frisbee deposition gauges to account for wind and dust deposition from all directions, it was of primary interest to monitor the deposition from wind carrying material in the direction of the prevailing south-westerly winds across the Corus works onto the SSSI. To monitor the dust deposition upwind of the Corus site, Frisbee gauges were located south-west of the Corus works and beyond the SSSI. The criteria used to select monitoring locations were as follows:

1. The area had to be safe for regular access.
2. The area had to be secure from vandalism.
3. Located in an area away from large buildings or objects which could disrupt wind flow and hence deposition to the gauge.

It was not possible to locate a gauge on the SSSI itself due to public access from the road which runs along the Corus perimeter fence to the South Gare breakwater. Although the SSSI is used for leisurely pursuits of dog walking or bird spotting, it is also prone to antisocial activities. In a previous study on the SSSI using sulphur dioxide diffusion tubes, less than two thirds of the exposed tubes were collected for analysis, due to loss from vandalism (Haines, pers. comm.).

As a preliminary study, a model scenario produced by Corus in 2001 of the expected environmental concentration of particulate matter from emissions on the Corus site (see Chapter 5 for a more detailed examination of this modelled scenario produced for the Integrated Pollution Prevention and Control (IPPC) permit application) was used to examine the validity of the site selection criteria. This modelled scenario was used to assess the range of potential deposition to the six selected sites. The model scenario showed that the selected monitoring sites were representative of a range of predicted environmental concentrations of particulate matter. Frisbee B was located close to the

area of the Corus works expected to receive 50 μg m^{-3} PM_{10} (see Figure 5.1 in chapter 5 section 2), at the north-western perimeter of the Corus works. It was not possible to locate a monitoring site in the area expected to receive 45 μg m^{-3} PM_{10} because it did not meet the selection criteria. Frisbee A was located in an area expected to receive 40 μg m^{-3} PM_{10} south-east of the blast furnace. Frisbee C was located within the Corus works adjacent to the SSSI in an area expected to receive 40 μg m^{-3} PM_{10}. Frisbee D was located upwind of the Corus site in an area expected to receive 40 μg m^{-3} PM_{10}. Frisbee E was located at the end of the South Gare breakwater and Frisbee F was located in a residential area to the south-east of the Corus works, both these areas were expected to receive 40 μg m^{-3} PM_{10}.

3.2.3.2 Exposing the passive dust deposition monitors

Monitoring was undertaken at Frisbee A from 1st March 2006 to 30th March 2007. Frisbee A was located 1020 m south-east of the blast furnace, and between 500 to 800 m from the SSSI (see Figure 3.2 and Table 3.1). Within the vicinity of Frisbee A were the sinter stock yards to the south-west. Frisbee B was exposed from the 14th March 2006 to 1st May 2007. Frisbee B was located adjacent (within 10 m) to the coke stock yards, 550 m north-west from the blast furnace, and only 50 m from the SSSI. Frisbee C was exposed from the 14th March 2006 to 1st May 2007, it was located 800 m south-east of the blast furnace, and within 60 m of the SSSI. Frisbee D was located in a secure cage off the Corus works on Coatham Marsh, it was exposed from the 14th March 2006 and was collected in on the 30th March 2007. Frisbee D was located 150 m from the SSSI, 120 m from the Corus fence, and 1330 m south-east of the blast furnace. Frisbee E was exposed from the 14th March 2006 to 6th December 2006; it was removed prior to the termination of the monitoring programme due to limitations on site accessibility. Frisbee E was located 2650 m to the north-west of the blast furnace, approximately 1000 m from the SSSI and 2300 m from the Corus boundary. Frisbee F was exposed from the 12th April 2006 to the 30th March 2007. Frisbee F was 2000 m from the Corus works and 2900 m south-east from the blast furnace. Frisbee G and H were exposed over the period from the 30th March 2007 to the 1st May 2007. Each Frisbee was located 7.5 m from Frisbee C (see Figure 3.2 and 3.3).

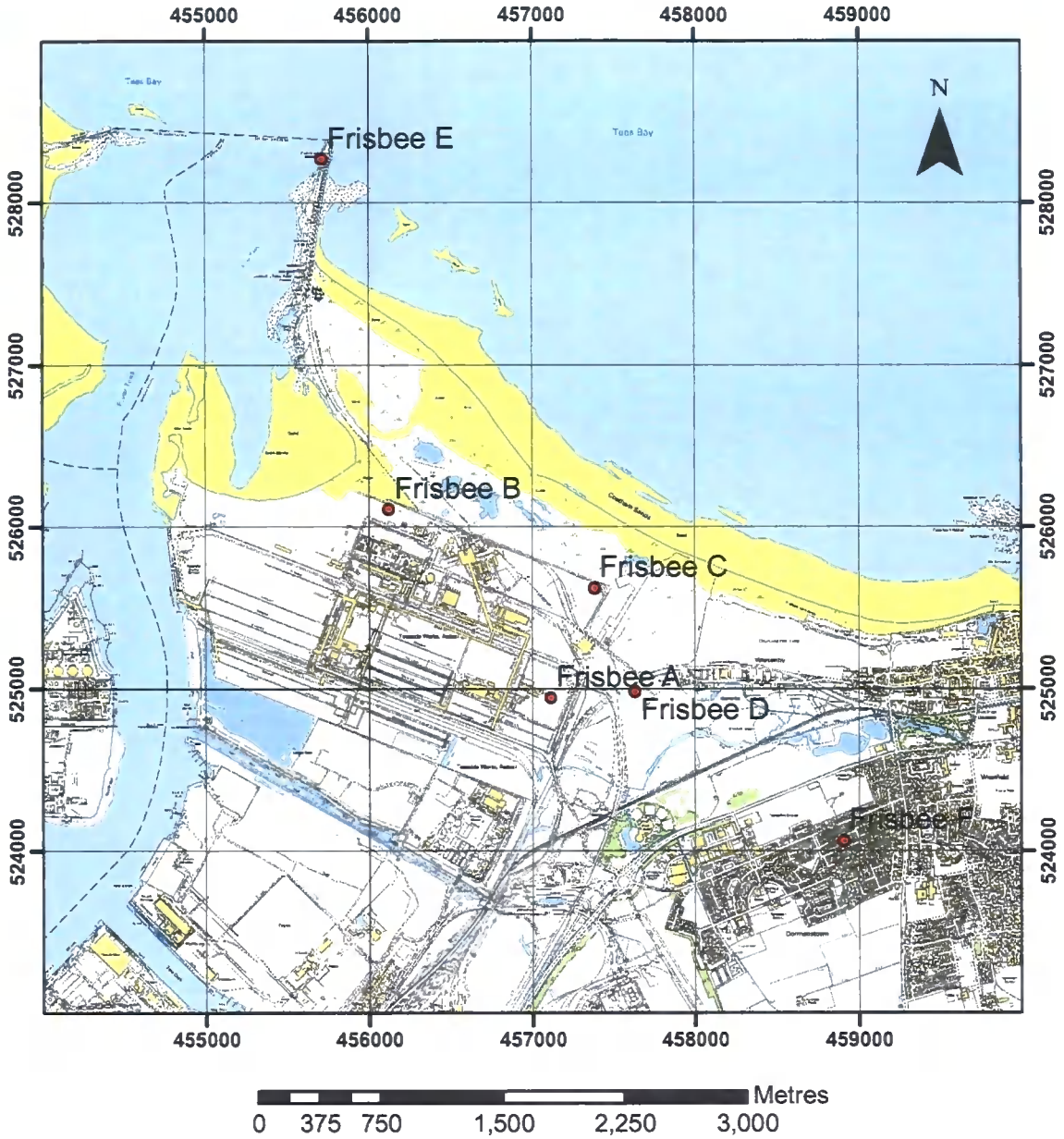

Co-ordinate System: British National Grid. Projection: Transverse Mercator.
Datum: OSGB 1936.

Figure 3.2 Locations of the six Frisbees exposed across the Corus works and Coatham Sands and South Gare SSSI.

Table 3.1 British National Grid co-ordinates for the locations of the Frisbees.

Frisbee	British National Grid Co-ordinate
A	457114, 524943
B	456122, 526108
C	457381, 525622
D	457631, 524982
E	455714, 528269
F	458907, 524062
G	457375, 525627
H	457387, 525619

3.2.3.3 Passive dust monitoring protocol

The method outlined below is based upon the SEI Protocol for using the Dry Frisbee (with Foam insert) dust deposit gauge (Vallack, 1995b).

The Frisbee-shaped collecting bowl (anodized spun aluminium) was supported at the top of a tripod at a height of 1.7 m above the ground. The tripod was secured to the ground with guy ropes to ensure the Frisbee was vertical (see Chapter 2 Figures 2.1.d and 2.2.). The collecting bowl was lined with 10 mm thick, 240 mm diameter disc of black open-celled polyester foam and surrounded by a bird strike preventer. Water and deposited material drained through a hole in the centre of the Frisbee through the central opaque drainage pipe into the opaque 5 litre HDPE collecting bottle fixed at the bottom of the tripod.

3.2.3.4 Frisbee location

Frisbees were located on an ostensibly flat area, with no object greater than 2 m in height such as buildings, trees within 5 m of the gauge. Any high buildings or objects were ensured to subtend to an angle less than 30^{o} with the horizontal at the sampling point to minimise disturbance to wind flow over the gauge (Vallack, 1995b). Areas with overhead wires where birds could perch were avoided.

3.2.3.5 Frisbee exposure

The Frisbee was fitted with a clean dry foam insert, and a 5 litre collecting bottle, which was marked with the Frisbee designation (A-F) and date of exposure. After approximately one month the foam disk was inspected and any leaves, bird droppings or other extraneous material on the surface were noted and removed. The foam insert was placed into the collecting bottle, and the Frisbee was thoroughly cleaned with 1 litre distilled water using a small brush to loosen material. The collecting bottle was labelled with the date of retrieval, returned to the laboratory and stored at 4 °C until filtration within 1 to 3 days. A clean foam insert and collecting bottle were replaced on the Frisbee, and marked with the Frisbee designation name (A-F) and date of exposure.

3.2.3.6 Recovering dust from the Frisbee gauge

Glass microfibre filters (9 cm diameter Whatman GF/A pre-weighed (to the nearest 0.1 mg)) were dried in foil packets in an oven for 1 hour at 80 °C, and left to equilibrate for a minimum of 2 hours in a desiccator. Care was taken when handling the filters; tweezers were used to place the filters into the foil packets and care taken not to place a filter directly onto unclean surfaces.

The contents of the collecting bottle were filtered under suction, using a Whatman three-piece funnel leading into a 5 litre Buchner flask. Deposits left inside the collecting bottle were loosened with a brush and distilled water, and passed through the filter. The volume of water collected was recorded.

The foam insert was thoroughly rinsed in 1 litre of distilled water which was passed through the filter. Any large extraneous material (originating from domestic or industrial processes) was noted and weighed separately. The filter was then dried, equilibrated and reweighed as above.

All apparatus was thoroughly cleaned between samples to avoid cross-contamination.

During each exposure period a control (non-exposed) Frisbee was analysed using distilled water.

3.2.3.7 Calculating the rate of dust deposition

The mean rate of dust deposition (undissolved solids) was calculated as follows:

Equation 3.1

$$\frac{(W2-W1) \times 24.7}{T} \text{ (mg m}^{-2} \text{ day}^{-1})$$

Where: W1 = initial dry weight of filter (in mg)

W2 = final dry weight of filter paper plus dust (in mg)

And: T = length of exposure period (in days)

3.2.3.8 Frisbee variation

The methodology followed to assess Frisbee variation was based upon the SEI Protocol for using the Dry Frisbee (with foam insert) dust deposit gauge, to confirm the validity of this three deposit gauges were exposed at one monitoring site. Designed to determine the variation in dust deposition to the Frisbee dust deposit gauges, the Frisbees G and H were exposed alongside Frisbee C in April 2007 (see Figure 3.3).

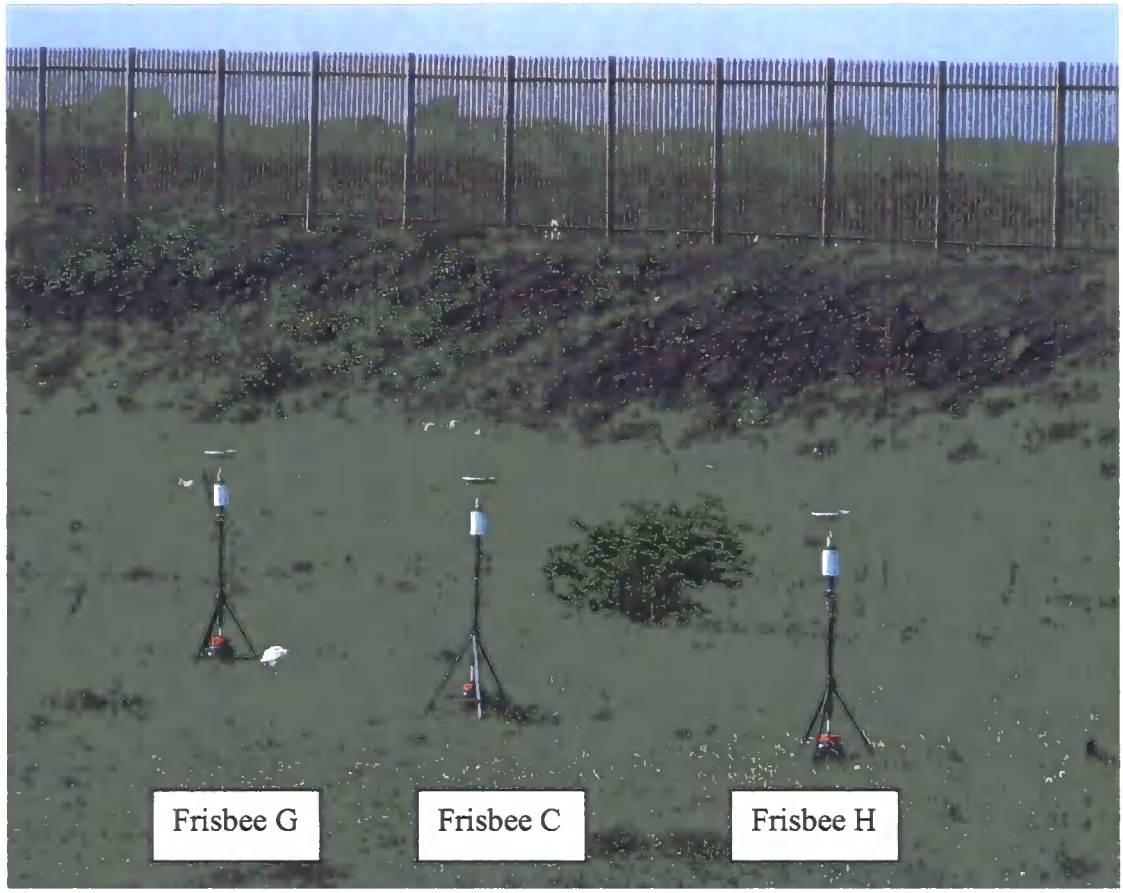

Figure 3.3 Frisbees C (457381, 525622), G (457375, 525627) and H (457387, 525619) exposed from April 2007, at the north-eastern boundary of the Corus works (see Figure 3.2).

3.2.3.9 Accurate geo-location of the deposition monitors

A GeoXT handheld (Trimble GmbH, Germany) Global Positioning System (GPS) device was used to take the GPS locations of the Frisbees on site. In real-time, data collection at sub-metre accuracy was achieved, with correction from the Satellite Based Augmentation System (SBAS). Locations recorded with this feature gave sub 0.9 m horizontally accuracy, otherwise, uncorrected GPS positions were taken and were post processed using base station data from the Ordnance Survey national GPS network. The base station files were downloaded for the specific times when measurements were taken using GPS Pathfinder Office v3.1 (Trimble GmbH, Germany). The GPS locations were corrected to sub-metre accuracy and imported into ArcGIS (Environmental Systems Research Institute, Redlands, California).

3.2.3.10 Collection of on-site meteorological data

Meteorological data were collected on the Corus works to allow analysis with locally measured wind speed and direction data. Wind speed and direction were measured using a Skye wind hog (Skye Instruments, Llandrindod Wells, UK) which comprises a potentiometer wind vane (wind direction), an anemometer (wind speed) and a two channel WindHog data logger. The anemometer had a race of 0.3 to 75 metres per second and was accurate to 1 % of the reading, while the wind vane had an accuracy rating of 10° typical maximum instantaneous error. The wind hog was set up to sample every 30 seconds, and then log an average of those readings at 30 minute intervals. Recorded data were downloaded using an RS232C cable in an ASCII output. The WindHog began collecting data from the 19th October 2006 to the 1st May 2007.

3.2.3.11 Collection of Loftus meteorological data

Meteorological data for this study were supplied by the British Atmospheric Data Centre (BADC, Chilton, UK). Data for the period March 2006 to May 2007 were taken from the closest meteorological station at Loftus, which was located 10 miles southeast of the Corus works. The nearer Coulby Newham station was no longer operational due to a past vandalism attack. Loftus was considered to be the most representative data available for the meteorological conditions at the Corus works.

3.2.3.12 Collection of ponding information

Ponding is a term used by the steel industry to describe the management of molten iron during an interruption to the steel production process. Molten iron is continually produced from the blast furnace, and transported in large vats, referred to as torpedoes. On occasion, for example when the BOS (steelmaking) plant is offline, the molten iron can be discharged into reservoirs, allowed to cool, broken up, loaded for transport and returned to the blast furnace. The very nature of ponding is sporadic, unpredictable and the potential emissions are strongly related to the short-term localised meteorological conditions. The reservoirs used to discharge the molten iron are located to the northeast of the Corus works (457206, 525558 British National Grid).

Information on the total volume of ponded iron and slag was obtained from the Redcar blast furnace reports. When the torpedoes are filled with molten iron, the time and weights are recorded. Although the exact time at which ponding occurs, and hence the emissions are not recorded, the time when the torpedo returns to the blast furnace for re-filling is available. The lifetime of the molten iron in the torpedo can be anywhere between 8 and 12 hours (Boydell, pers. comm.). However, the majority of torpedoes return to the blast furnace within 5 hours, and often within 3 hours. It was therefore estimated that five hours after the torpedo had left the blast furnace the ponding event would occur. The total molten iron ponded was calculated for exposure period for Frisbee C.

3.2.3.13 Data analysis

Data were analysed using SPSS statistical software (SPSS Inc. Chicago, Illinois, USA) and presented using Sigma Plot v.10 (Systat Software Inc. San Jose, California, USA). The dust deposited at Frisbee F in June 2006 was excluded from the analysis as extraneous material was found on the foam insert. The dust deposition data were tested for normality (Kolmogorov-Smirnov) and were found to be normally distributed ($KS > 0.117$, $n = 8, 11, 12, 13$, $p > 0.06$). The total water collected in the Frisbees were tested for normality (Kolmogorov-Smirnov) and were found to be normally distributed ($KS > 0.43$, $n = 8, 12$ $p > 0.6$).

Paired T-tests were conducted on all dust deposition data to determine if there was any difference in deposition between locations. Paired T-tests were conducted on the total water collected in the six Frisbees to determine if there was any effect of rainfall on deposition between locations. A component of wind speed and direction was calculated from the meteorological data measured at the meteorological stations located at Loftus and on the Corus works. Stepwise regressions were undertaken on the monthly dust depositions with the wind components and rainfall measured at Loftus and on the wind components measured at the Corus works. The dust deposition at Frisbee C was also regressed against the total iron ponded.

3.2.4 Results

3.2.4.1 Variation in dust deposition between Frisbees at a single monitoring site

The quantities of dust deposited at Frisbees C, G and H in April 2007 were found to be 738.5, 847.3 and 807.2 mg m^{-2} day^{-1} respectively (see Figure 3.4). The total dust deposited to the three Frisbees was similar. Frisbees G and H were within 5 % of each other, Frisbee C and H were within 10 % of each other, and Frisbee C and G were within 15 % of each other.

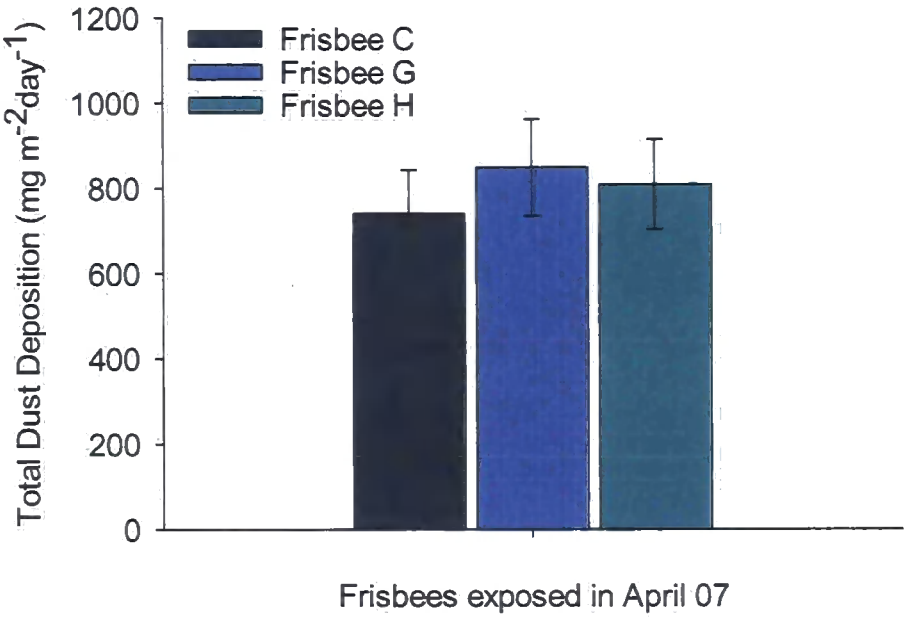

Figure 3.4 The total dust deposition (mg m^{-2} day^{-1}) for Frisbee C, G and H exposed in April 2007. Error bars show ± 1 SE.

3.2.4.2 Dust deposition

The mean dust deposition from April 2006 to March 2007 for the six monitoring locations were found to be significantly different to the non-exposed (control) Frisbees (results not presented); Frisbee A ($\bar{x}$ = 530.2 mg m^{-2} day^{-1}, σ = 177, df = 11, t = 11.0, $p < 0.001$); Frisbee B ($\bar{x}$ = 932.4 mg m^{-2} day^{-1}, σ = 384, df = 11, t = 8.2, $p < 0.001$); Frisbee C ($\bar{x}$ = 562.5 mg m^{-2} day^{-1}, σ = 205, df = 11, t = 9.6, $p < 0.001$); Frisbee D ($\bar{x}$ = 180.2 mg m^{-2} day^{-1}, σ = 62, df = 11, t = 10.5, $p < 0.001$); Frisbee E ($\bar{x}$ = 152.4 mg m^{-2} day^{-1}, σ = 53, df = 7, t = 8.1, $p < 0.001$) and Frisbee F ($\bar{x}$ = 102.5 mg m^{-2} day^{-1}, σ = 25, df = 11, t = 10.8, $p < 0.001$).

Overall the highest rate of dust deposition was measured at Frisbee B, with 1715.9 mg m^{-2} day^{-1} in September 2006 (see Figure 3.5.b). The level of dust deposition at Frisbee A was relatively high, with 914.4 mg m^{-2} day^{-1} recorded in March 2007 (see Figure 3.5.a). The highest dust deposition recorded at Frisbee C was 909.4 mg m^{-2} day^{-1} in August 2006 (see Figure 3.5.c). The highest level of dust deposition at Frisbee D was recorded in March 2007 with 279.9 mg m^{-2} day^{-1} (see Figure 3.5.d). Frisbee E was exposed from April to November 2006, and the highest level of dust deposition was recorded in August 2006 with 238.7 mg m^{-2} day^{-1} (see Figure 3.5.e). There was little variation in the dust deposition recorded at Frisbee F throughout the 12 month exposure period; with a difference of only 56.9 mg m^{-2} day^{-1} recorded between the highest and lowest months of dust deposition, the highest level of dust deposition was recorded in July at 124.7 mg m^{-2} day^{-1} (see Figure 3.5.f). The lowest dust deposition for most Frisbees was recorded in February 2007 where Frisbee A, B, C, D, and F recording deposition rates of 262.8, 414.1, 418.9, 81.95 and 67.8 mg m^{-2} day^{-1} respectively.

The dust deposition to Frisbee A ($\bar{x} = 506$ mg m^{-2} day^{-1}, $\sigma = 191$), Frisbee B ($\bar{x} = 892$ mg m^{-2} day^{-1}, $\sigma = 380$) and Frisbee C ($\bar{x} = 556$ mg m^{-2} day^{-1}, $\sigma = 209$) were significantly higher than the dust deposition to Frisbee D ($\bar{x} = 173$ mg m^{-2} day^{-1}, $\sigma = 65$, $df = 11$, $t \geq 6.5$, $p < 0.0005$), Frisbee E ($\bar{x} = 147$, $\sigma = 52$, $df = 7$, $t \geq 6.0$, $p < 0.0005$) and Frisbee F ($\bar{x} = 102$ mg m^{-2} day^{-1}, $\sigma = 25$, $df = 10$, $t \geq 6.8$, $p < 0.0005$). The dust deposited to the Frisbees located on the Corus works (Frisbees A, B and C), and the Frisbees located off the Corus works (Frisbees D, E and F) were statistically similar.

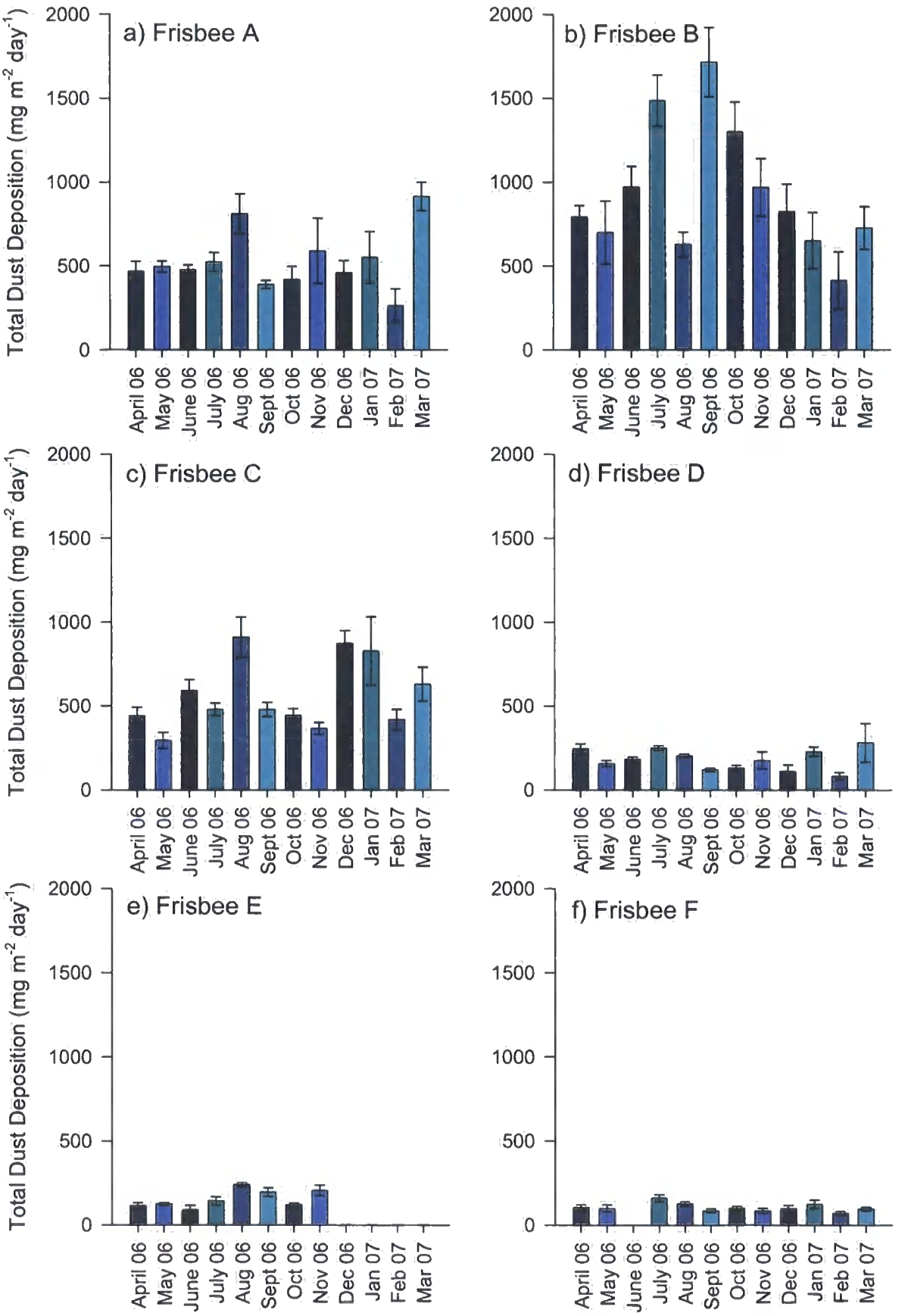

Figure 3.5 Total monthly dust deposition (mg m^{-2} day^{-1}) for Frisbees A to F (on graphs a. to f. respectively) exposed on and surrounding the Corus works. Error bars show ± 1 SE.

3.2.4.3 Investigating the potential relationship between dust deposition and local meteorological conditions – measured at Loftus

The wind components calculated from the meteorological data collected at Loftus were not related to the dust deposition at Frisbee B, C, E and F. The north-westerly wind component measured at Loftus was found to significantly increase the dust deposition from April 2006 to March 2007 for Frisbee A ($r^2 = 0.44$, $f = 7.9$, $p > 0.02$, $n = 11$) (see Appendix A – Figure 1.a) and Frisbee D ($r^2 = 0.47$, $f = 9.1$, $p > 0.05$, $n = 11$) (see Appendix A – Figure 1.b).

The precipitation calculated from the meteorological data collected at Loftus was not related to the dust deposition to Frisbee A, B, C, D, E and F (see Appendix A – Figure 4).

3.2.4.4 Investigating the potential relationship between dust deposition and local meteorological conditions – measured on the Corus works

The wind components calculated from the meteorological data collected on the Corus works were not related to the dust deposition at Frisbee A, B, C and E. The north-westerly wind component measured on the Corus works was found to significantly increase the dust deposition from November 2006 to March 2007 for Frisbee D ($r^2 = 0.80$, $F = 12.0$, $P > 0.05$, $n = 4$) (see Appendix A – Figure 1.c), which confirms the significance found using the Loftus data. The westerly wind component measured on the Corus works was found to significantly increase the dust deposition from November 2006 to March 2007 for Frisbee F ($r^2 = 0.79$, $F = 11.3$, $P > 0.05$, $n = 4$) (see Appendix A – Figure 1.d).

The precipitation calculated from the total water collected in each of the six Frisbees were found to be significantly similar despite location ($\bar{x} = 3046, 2643, 2612, 2644, 2431$ & 2595 ml month^{-1}, $\sigma \geq 988$, $df = 8, 12$, $t \leq 2.0$, $p > 0.05$) (see Figure 3.6.a).

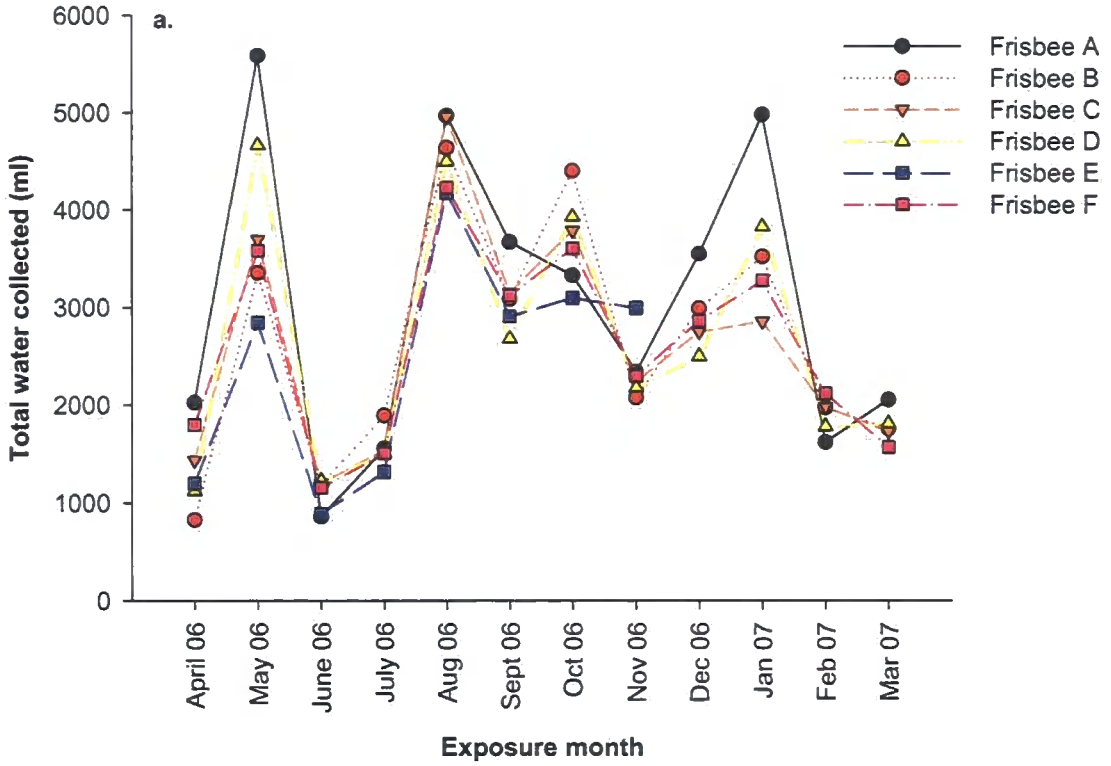

Figure 3.6 Total water collected for the six Frisbees exposed from April 2006 to March 2007. Where black shows Frisbee A, red shows Frisbee B, orange Frisbee C, yellow shows Frisbee D, blue shows Frisbee E and purple shows Frisbee F.

3.2.4.5 Investigating the potential relationship between dust deposition and the iron ponded on the Corus works

The total weight of iron discharged at the ponding station (see Figure 3.7.a) was found not to significantly affect the total deposition at Frisbee C ($r^2 = 0.25$, $f = 3.4$, $p = 0.10$, $n = 12$) (see Figure 3.7.b), although there was a positive relationship found between increased iron discharged at the ponding station and increased deposition at Frisbee C (see Appendix A – Figure 1.e).

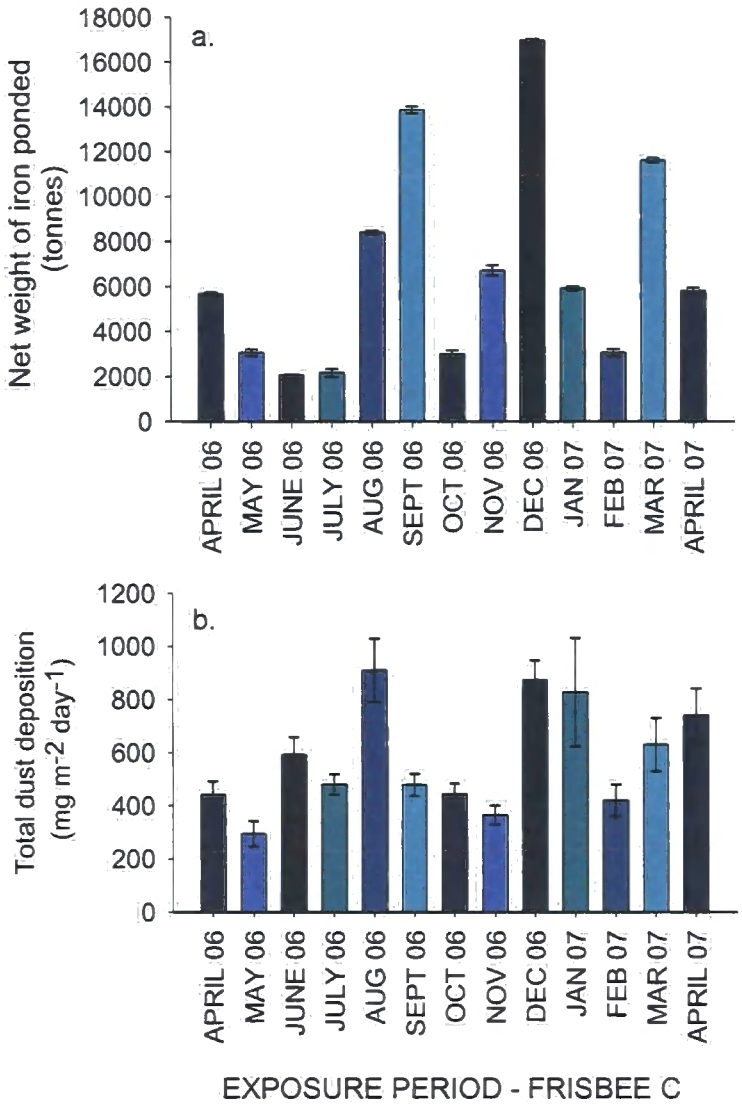

Figure 3.7 Graph a shows the total net weight of iron ponded (tonnes) at the Corus works, Teesside from April 2006 to April 2007 (Data sourced from Corus, Teesside). Graph b shows the total dust deposition (mg m^{-2} day^{-1}) to Frisbee C from April 2006 to April 2007. Error bars show ± 1 S.E.

3.2.5 Discussion

3.2.5.1 Dust deposition variation at a single monitoring site

The comparison of the three Frisbee deposition gauges exposed in April 2007, at one monitoring site, revealed that the total dust deposited was similar. Although there was between 5 and 15 % variance in the total dust deposited, these results can be considered similar (Hanby, pers. comm.; Vallack, pers. comm.) (Vallack & Shillito, 1998). This provides a certain degree of confidence in the results obtained from the Frisbee deposition gauges and the filtration process.

3.2.5.2 Dust deposition on and surrounding the Corus works

Frisbee A was located to the south-east of the blast furnace, and to the north-west of the sinter stock yards. The dust deposited to Frisbee A was relatively high throughout the 12 month exposure period, with the two peaks in deposition occurring in March 2007 and August 2006, which correspond to strong westerly winds.

Frisbee B was located on the Corus works, adjacent to the SSSI, at the north-western boundary of the Corus site, and to the north-east of the coke stock yards. The highest dust deposition across the Corus works was recorded at Frisbee B. The months which experienced the highest depositions were July, September, and October 2006, which did not correlate to the peaks in dust deposition at Frisbee A and C. It is possible that the fugitive emissions which contribute to the dust deposition at B do not contribute to the dust deposition at Frisbee A or C. However, the peaks in deposition at Frisbee B correspond to peaks in southerly and south-westerly winds, while the peaks in dust deposition at Frisbees A and C, and the relatively low deposition to Frisbee B, during August 2006 and March 2007 correspond to peaks in westerly winds.

Frisbee C was located on the Corus works, adjacent to the SSSI, at the north-eastern boundary of the Corus works. The Frisbee was east of the blast furnace, north-east of the ponding station and north of the sinter stock yards. The total dust deposited at Frisbee C was relatively similar to the total deposition at Frisbee A, with a corresponding peak in deposition during August 2007, although the total dust deposition in December 2006 and January 2007 were also relatively high for Frisbee C. These months with

relatively high dust deposition to Frisbee C correspond to strong westerly and south-westerly winds.

Frisbee C was located within close proximity (less than 200 m) to a number of potential dust generating activities. The general area around the Frisbee is also used as a stock yard for scrap metal and also broken up ponded material. Activities in this area include ponding, the breaking up of the ponded material, relocating this material to stocking grounds close by, and the eventual transfer of this material back to the blast furnace by trucks. The dust deposition at Frisbee C was probably a result of these different activities which occur in the vicinity of Frisbee. Dust generated by these activities is likely to be deposited into the gauge under a wide range of wind directions, and meteorological conditions.

Frisbee D was located to the south-east of the Corus works, but off-site within a secure cage. Although it was close to the SSSI, it was separated from the dunes by a man-made embankment, approximately 20 m high, which ran parallel to the dunes. The centre of the Corus works (Redcar) is located to the north-west of the sampling point at D, including the coke ovens, ponding stations and blast furnace. The level of dust deposition at Frisbee D was considerably lower than to the Frisbees located on the Corus works. The dust deposited to Frisbee D was relatively low throughout the 12 month exposure period, with the two peaks in deposition occurring in March 2007 and April 2006, which correspond to strong north-westerly winds.

Frisbee E was located in a secure area at the end of the South Gare breakwater, to the north of the Corus works. Within this area there were buildings and machinery which may have affected the flow of wind to the gauge. The dust deposited to Frisbee E was higher in the latter half of 2006, specifically August, September and November, but the total dust deposition was much lower than the three Frisbees found on the Corus works.

The location of Frisbee F was located in a residential area of Dormanstown, to the southeast of the Corus works. The dust deposited to Frisbee F was relatively low throughout the 12 month exposure period, but peaks in deposition during April 2006, August 2006 and January 2007 corresponded to peaks in strong westerly winds. However, to the west of Frisbee F, there were a number of potential dust-generating industrial sites and activities, which included Corus.

The total dust deposition to the Frisbees on the Corus works, which were either adjacent or close to the SSSI (within 500 m) were found to be significantly similar. The total dust deposition to Frisbees D, E and F was also found to be significantly similar,

although the specific location and immediate environment of each of the three Frisbees differed.

3.2.5.3 The potential relationship between dust deposition and local meteorological conditions

The dust deposition over the 12 month exposure period to Frisbee A and D was found to be related to a function of the wind in a north-westerly direction, recorded at the Loftus meteorological station. When compared with the meteorological data recorded on the Corus works, the dust deposition to Frisbee D was again found to be related to a function of the wind in a north-westerly direction. The dust deposition to Frisbee F was also found to be related to a function of the wind in a westerly direction, recorded on the Corus works. To the north-west of Frisbee A and D was the centre of the Corus works, including the coke ovens, blast furnace, the coke stock yards (Frisbee A only) and the ponding station (Frisbee D only). Although the Corus works are in a westerly direction from Frisbee F, there could be other potential sources of fugitive emissions from the Teesside area to Frisbee F.

The dust deposited to Frisbee B, C and E was found not to be related to a function of the wind in any direction, recorded at either the Loftus or the on-site (Corus) meteorological station. It is possible that at Frisbee B and C, the direction of the wind is less important for dust deposition, due to multiple potential sources of fugitive emissions located in different directions from the monitoring sites, including the blast furnace, multiple stock yards, ponding station and coke ovens. It is possible at Frisbee E that similar levels of dust deposition are expected from all directions, indicating that any potential emissions from Corus are not transported to the South Gare breakwater. However, to confirm these hypotheses, the dust flux needs to be examined which is presented in the second section of the present chapter.

The total water collected in the six Frisbees was found to be significantly similar; therefore any variation in the total dust deposited to the Frisbees was not attributable to variation in rainfall at each monitoring site. The total precipitation at Loftus was not correlated to the total dust deposition for the exposure periods at the Frisbees A, B, C, D, E and F.

3.2.5.4 The potential relationship between dust deposition and the total iron ponded at the Corus works

The deposition of dust to Frisbee C was not significant to the total weight of iron discharged at the ponding station. Typically ponding occurs in short bursts, lasting only a few minutes, but it has the potential to generate fugitive dust emissions. However, the deposition of these emissions is dependant on localised short-term meteorological conditions. It is possible that emissions generated from a ponding event could be carried over the Frisbee gauge, and deposited beyond the Corus boundary onto the SSSI or beyond in the North Sea. It is worth noting that over the 12 month exposure, increased ponding activity and increased deposition of dust to Frisbee C was approaching significance, yet there was considerable noise in the data. However, it is difficult to establish a relationship as the ponding events are short-term events and the dust deposition is measured over a monthly exposure period.

3.2.5.5 Overall value of dust deposition studies

The Frisbee dust deposition gauges (with dry foam insert) were cheap, reliable, repeatable and one of the most effective passive dust monitoring devices available commercially. For the present study the Frisbee deposit gauges were an efficient use of resources, in terms of both time and money. The gauges were also efficient dust collectors, for specific sites.

The Frisbee deposition gauges are designed to measure the average monthly deposition to a specific point hence the chronic deposition, so episodes of acute fugitive dust deposition are not highlighted within the exposure period. In order to determine the potential contribution of sources of acute fugitive emissions a real-time monitoring study would be required to be undertaken, which was not within the scope of the present study.

The Frisbee gauges do not provide any directional information, or collect from specific wind directions. They are open to collecting dust deposited from all directions of wind flow, and these dusts are measured over a monthly averaging period. Despite this the gauges provide an accurate indication of the total deposition to a specific site, irrespective of wind direction.

Frisbees are passive monitors with a long averaging period; the gauges are not designed to monitor the potential impact of short-term events which may induce a phase

of acute fugitive dust emissions. Such events, including ponding events, are not easy to identify in monthly averages of dust deposition.

Passive dust deposit and flux monitors have a valuable contribution to make to dust deposition studies. The longer sampling period enables a view of the chronic deposition to a specific site. More over the fugitive dust emissions at a specific site can be examined with the combination of meteorological data on wind speed and direction, and the rate of specific activities. For the present study, the simultaneous monitoring of dust deposition and flux across a wide area, enabled easy identification of direction-specific sources of emissions.

3.3 Directional dust flux

3.3.1 Introduction

The second section of the present chapter will examine the dust flux[2] to the six monitoring sites on and surrounding the Corus works. The Frisbee dust deposition gauges provide valuable information on dust deposition across the Corus works and surrounding area, however, they do not provide directional information. The primary benefit of conducting a simultaneous deposition and passive dust flux monitoring study is the combined value of information on the total dust deposited and the directional dust flux to a single monitoring site. For a more detailed description of surface soiling measuring techniques see Chapter 2 section 2.4.3.

A sticky pad reader was used to measure the surface soiling for the present study. Designed to emulate readings from an Evans Electroselenium (EEL) smoke-stain reflectometer, the sticky pad reader was developed (Beaman & Kingsbury, 1981; Beaman & Kingsbury, 1984) and standardised as a non-intrusive reflectometer (Farnfield & Birch, 1997). The sticky pad reader has shown a high degree of correspondence with the alternatively commercially available DustScan (Datson & Birch, 2007).

The present section will compare the dust flux to three sticky pads located at one monitoring site; compare the dust flux to six sites on and surrounding the Corus works over a 12 month collection period; and compare the dust flux to the speed and direction of the wind, a potential dust generating activity located on the Corus works.

3.3.2 Methods

3.3.2.1 Locating the passive dust flux monitoring programme

A PVC cylindrical sticky pad holder was fixed with locking screws at 1.2 metres on the tripod supporting the Frisbee (see Figure 3.8). Sticky pads were exposed at each of the Frisbees located on the Corus works (see Figure 3.2 and Table 3.1 for the specific locations and section 3.2.3.1 for a detailed description of the monitoring sites). The sticky pad holder was orientated to North and marked to ensure that sticky pads were attached and orientated in the same direction for each exposure period. The white Fablon self-adhesive vinyl sticky pads (I R Hanby, Newark, UK) measure 317 mm in length and

[2] A sticky pad is a directional deposition gauge, but the term dust flux is used in the present thesis to differentiate from dust deposition collected by the Frisbees.

148 mm in width. Once exposed the sticky pad represents a full 360° degree exposure, enabling dust flux measurements for any direction.

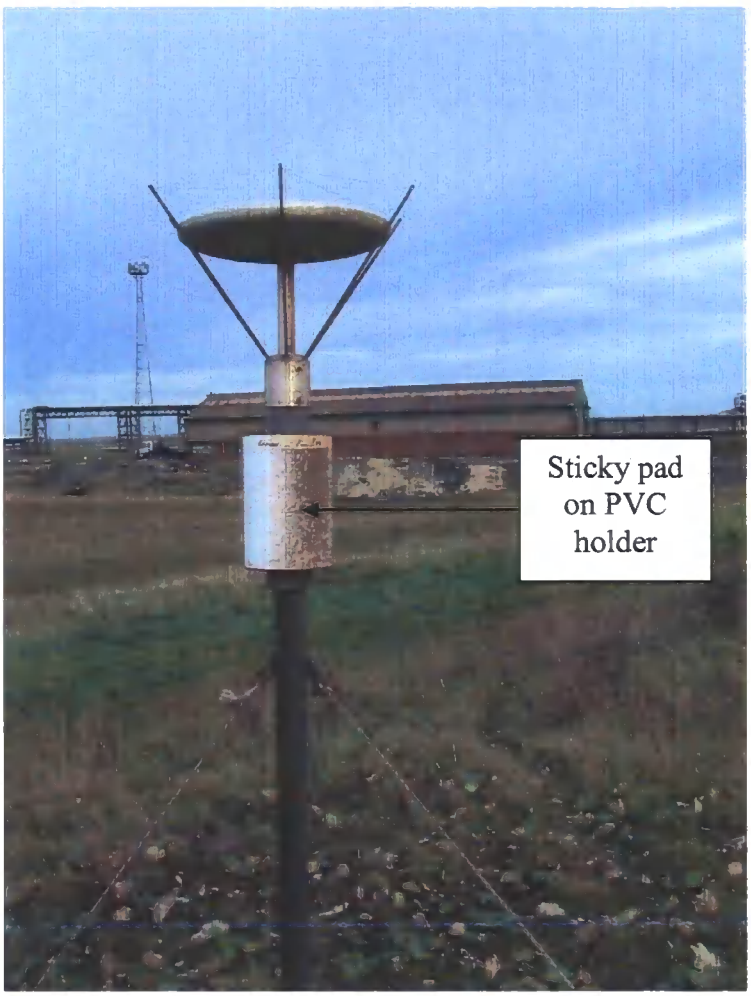

Figure 3.8 A cylindrical PVC sticky pad holder located on a tripod supporting the dry Frisbee deposition gauge.

3.3.2.2 Exposing and recovering a sticky pad

To ensure the sticky pad was located with the correct orientation the protective backing paper was cut 15 mm from the upper edge. This acted as an unexposed reference area, and was marked with the location and date of exposure and collection. The sticky pad holder was cleaned prior to exposure to ensure that material was not trapped on the reverse of the sticky pad. The sticky pads were exposed for approximately one week, although exposure periods regularly varied between 5 and 14 days due to site accessibility problems. The backing paper was replaced on the sticky pad and returned to the laboratory for analysis. Sticky pads were exposed from April 2006 to March 2007 at the six monitoring sites (A-F).

3.3.2.3 Sticky pad reader calibration procedure

A sticky pad reader subsequently referred to as the "reader" (I R Hanby, Newark, UK) is a non-intrusive method used to measure the dust deposition on an area of sticky pad. The reader has three tungsten filament bulbs, equally spaced to ensure uniform brightness across the sample (Hanby, 2007b). A reading was taken from the centre of an illuminated circle 6 mm in diameter in the locating mask, at the base of the reader.

The following calibration procedure is the suppliers preferred method for the Sticky Pad Reader (Hanby, 2007a). It emulates readings produced by an Evans Electroselenium Smokestain Reflectometer (EEL) (Diffusion Systems Ltd, London, UK) (see Chapter 2 section 2.4.3) when it is not possible to measure the samples on the EEL meter. This is the most accurate and reliable method for calibrating the reader, but other calibration methods could have been used.

All work using the reader was carried out on a white board with uniform background reflectance (see Figure 3.9). The calibration sheet was placed over the white board; the reader was switched on and allowed to settle for a few minutes. Once the reader had stabilized the locating mask was placed over the centre of the '99' area on the calibration sheet. The locating mask ensures the sample was held flat, and clearly identifies where the reading was taken. The reader was then placed over the locating mask and the reading noted as Y1. The locating mask and reader were then placed over the centre of the '33' area and the reading was taken as Y2.

To calculate the Zero-Error correction Equation 3.2 was applied, and rounded to the nearest integer:

$$Y2' = \frac{(Y1 - Y2)}{2} \qquad \textbf{Equation 3.2}$$

While the reader was placed over the '33' area, the left hand side screw labelled Z (Zero control), was adjusted with a small screwdriver to read Y2'. The reader was then returned to the '99' area and the right hand side screw labelled C (Calibration control) was adjusted to read 99. To ensure the reader had been calibrated correctly the reader was returned to the '33' area. This procedure was repeated to validate the accuracy of the calibration procedure. Finally to ensure the reader was adequately calibrated the reader

was placed over the intermediate values of 42, 54 and 83 to confirm that readings were correct to ±2.

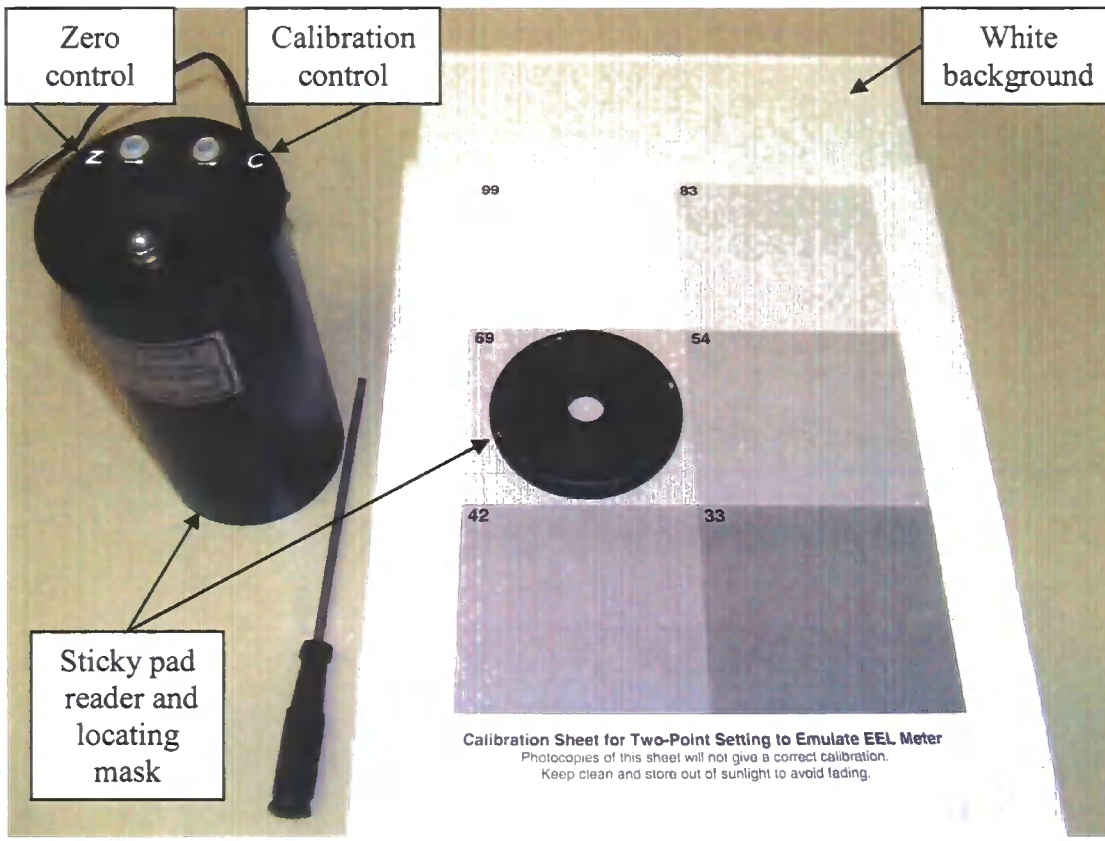

Figure 3.9 - Calibration sheet and sticky pad reader, the locating mask is shown on area '69'. The zero control and calibration controls are on the left and right hand side of the sticky pad reader (respectively). The calibration sheet for a two-point setting of a sticky pad reader, which emulates an EEL meter, showing the calibration areas 83, 54, 33, 42, 69 and 99 (clockwise from the top right).

3.3.2.4 Measuring dust flux on sticky pads

The reverse side sticky pad was cleaned before each reading was taken to ensure that any material remaining on the back of the sticky pad was removed, preventing erroneous results. Each sticky pad was placed on a white board as a standard background reflectance labelled with the compass points and reading intervals outlined below.

The remaining 15 mm band of backing paper located along the upper edge of the sticky pad was removed to measure clean unexposed values. Eight reference readings were taken 8 mm from the top of the sticky pad at equally spaced intervals, approximately every 19.5 mm along the sticky pad (representing N, NE, E, SE, S, SW, W and NW). For each exposed sticky pad the eight readings were averaged to give a clean, unexposed, value for the sticky pad.

The number of readings taken along the sticky pad was determined by the quantity and distribution of dust flux along the sticky pad. A minimum of eight compass points were used approximately every 19.5 mm along the sticky pad (N, NE, E, SE, S, SW, W and NW), with additional eight compass points when heavy dust flux occurs at the relevant intervals (NNE, ENE, ESE, SSE, SSW, WSW, WNW, NNW). At each of these compass points six equally spaced readings were taken down the sticky pad at 26 mm, 48 mm, 70 mm, 92 mm, 115 mm, and 137 mm. These six readings were then averaged for each compass point to calculate the Effective Area Coverage (EAC). By controlling the method for measuring the sticky pad, the potential for subjective measuring was overcome.

The average EAC for each compass point was subtracted from the clean unexposed value. The difference between these two numbers was divided by the total number of days when the sticky pad was exposed. This final value percentage Effective Area Coverage per day (% EAC day^{-1}) gives an indication of the dust flux for each of the compass points (8 to 16) for that exposure period at that specific location. Any change in reflectance which results in larger % EAC day^{-1} indicates the direction of most frequent and or heaviest dust flux.

3.3.2.5 Dust flux variation

Although the methodology for the sticky pad follows the protocol from I Hanby (Hanby, 2007a), to confirm the accuracy of the sticky pads, a study to determine inter-sticky pad variability was undertaken. Two sticky pads G and H were exposed on the 30th March to the 1st May 2007, within 7.5 m of sticky pad C (see Figure 3.3).

3.3.2.6 Data analysis

Data were analysed using SPSS statistical software (SPSS Inc. Chicago, Illinois, USA) and presented using Sigma Plot v.10 (Systat Software Inc. San Jose, California, USA).

The Wilcoxon signed rank test was used to examine the sticky pads at monitoring sites C, G and H. Although these data were normally distributed ($KS > 0.33$, $n = 10\text{-}17$, $p > 0.05$), a non-parametric test was used conservatively due to the small sample sizes.

The values for mean directional dust flux were tested for normality (Kolmogorov-Smirnov) and were found to be normally distributed ($KS > 0.51$, $n = 8$, $p > 0.05$). Paired

T-tests were conducted on all dust flux directions to determine if there was any difference between the fluxes to different monitoring sites.

The wind speed and direction data were used to calculate an average wind component for the 8 cardinal compass points. The average wind speed for the eight compass points were calculated for each exposure period, and tested for normality. Despite employing numerous standard transformations (square root, logarithm, inverse, reflect and square root, reflect and logarithm and reflect and inverse), these data were found to be non-normally distributed. This was attributable to infrequent northern and north-easterly winds, the poor resolution in the wind direction measurements (with only 10^{o} resolution), and the short exposure periods of less than 7 days. Hence it was not possible to conduct a regression with the meteorological and dust flux data, as there is not an equivalent non-parametric test available. Therefore, for each exposure period the average wind speed for the eight compass points were ranked. The dust flux for each of the 8 cardinal compass points were ranked for all of the exposure periods. A Spearman-Rank correlation was performed on the average wind direction and dust flux for each compass point. The Spearman-Rank correlation was an appropriate alternative to the parametric regression test, as these data would have violated the test assumptions.

3.3.3 Results

3.3.3.1 Dust flux variation between sticky pads

The sticky pads C, G and H were correlated against each other to examine for any significant differences between the dust fluxes to the three sticky pads at one monitoring site. The dust flux during the three weeks when the sticky pads were exposed was considerably variable, hence the difference in scale on the radial axis of graphs a. to c. in Figure 3.10. Irrespective of the total dust flux, the directional dust flux was statistically similar for all three sites ($z \geq -1.82$, $n = 6$ $p > 0.05$) (see Figure 3.10).

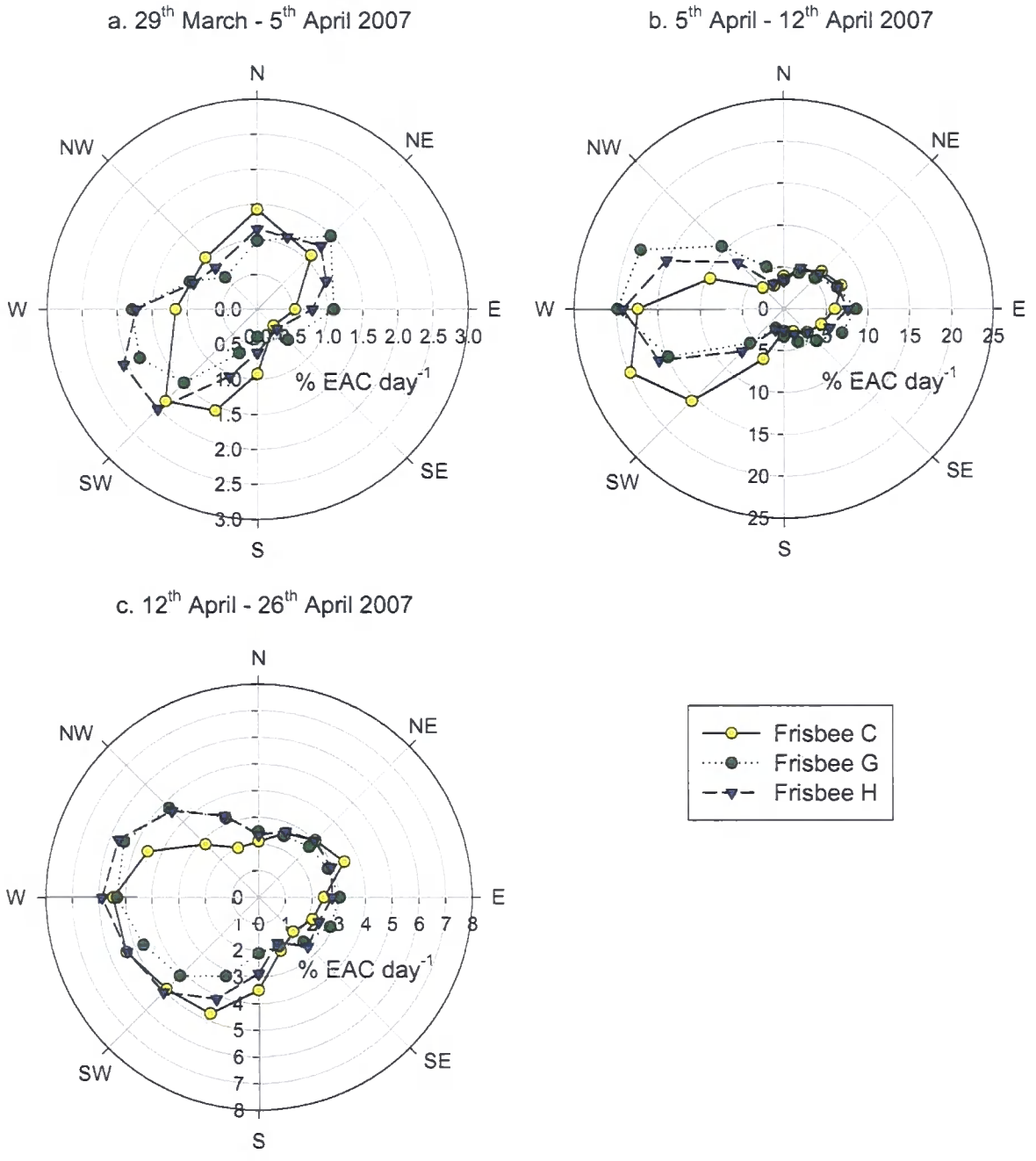

Figure 3.10 Percentage Effective Area Coverage (% EAC day^{-1}) on the sticky pads exposed in April 2007, where yellow indicates sticky pad c, green indicates sticky pad G and blue indicates sticky pad H. Where graph a shows the 29th March to 5th April, graph b shows 5th April to 12th April and graph c shows the 12th April to 26th April, note the difference in radial scales for each graph.

3.3.3.2 Dust flux

The mean flux to sticky pad A was relatively similar for most directions and ranged between 2.3 % EAC day^{-1} for the south-eastern flux and 4.7 % EAC day^{-1} for the western flux ($\bar{x} = 4.03$, $\sigma = 1.69$). The only exception to this was the south-western flux which was 7.8 % EAC day^{-1} (see Figure 3.11.a) also the dust flux contained considerably more variance than all other directions.

The highest mean dust flux was at sticky pad B. The mean dust flux ranged between 3.3 % EAC day^{-1} for the northern flux and 7.0 % EAC day^{-1} for the southern flux (see Figure 3.11.b). Despite this the flux to sticky pad B was not significantly higher than the fluxes to sticky pad A and C. However, it was significantly higher than the fluxes to sticky pads D, E and F ($\bar{x} = 5.2$, $\sigma = 1.5$, $df = 7$, $t \geq 6.38$, $p < 0.001$). The largest dust fluxes were the southern, south-eastern, south-western and western, and of these the south-eastern and southern fluxes contained the greatest variance.

The mean flux to sticky pads A and C were of relatively similar magnitude. The mean dust flux at sticky pad C ranged between 2.2 % EAC day^{-1} for the northern flux and 3.4 % EAC day^{-1} for the southern flux ($\bar{x} = 3.89$, $\sigma = 2.19$). The only exceptions to this were the south-western flux which was 7.8 % EAC day^{-1} and the western flux which was 6.9 % EAC day^{-1} (see Figure 3.11.c). The southern and south-western fluxes to sticky pad C contained the greatest variance.

The mean dust flux to sticky pad D (see Figure 3.11.d) was significantly lower than the fluxes to sticky pads at A, B and C ($\bar{x} = 1.7$, $\sigma = 0.69$, $df = 7$, $t \geq 3.58$, $p \leq 0.01$), and significantly higher than the dust fluxes to sticky pads at E (see Figure 3.11.e) and F (see Figure 3.11.f) ($t \geq 2.9$, $p < 0.02$). There was little variation in the majority of the fluxes varying between 1.1 % EAC day^{-1} to the south-east and 1.9 % EAC day^{-1} to the north-west, but there was considerable variation and the highest flux for the western flux which was 3.2 % EAC day^{-1}.

The dust flux to sticky pad E was similar for most directions, ranging between 0.6 % EAC day^{-1} for the western flux and 1.1 % EAC day^{-1} for the southern flux, with considerable variance in the south-east, south and south-western fluxes. The mean flux to sticky pad E was significantly lower than the flux to sticky pads A, B, C and D ($\bar{x} = 0.81$, $\sigma = 0.18$, $df = 7$, $t \geq 2.93$, $p \leq 0.02$), and significantly higher than the flux to sticky pad F ($t = 7.35$, $p < 0.001$).

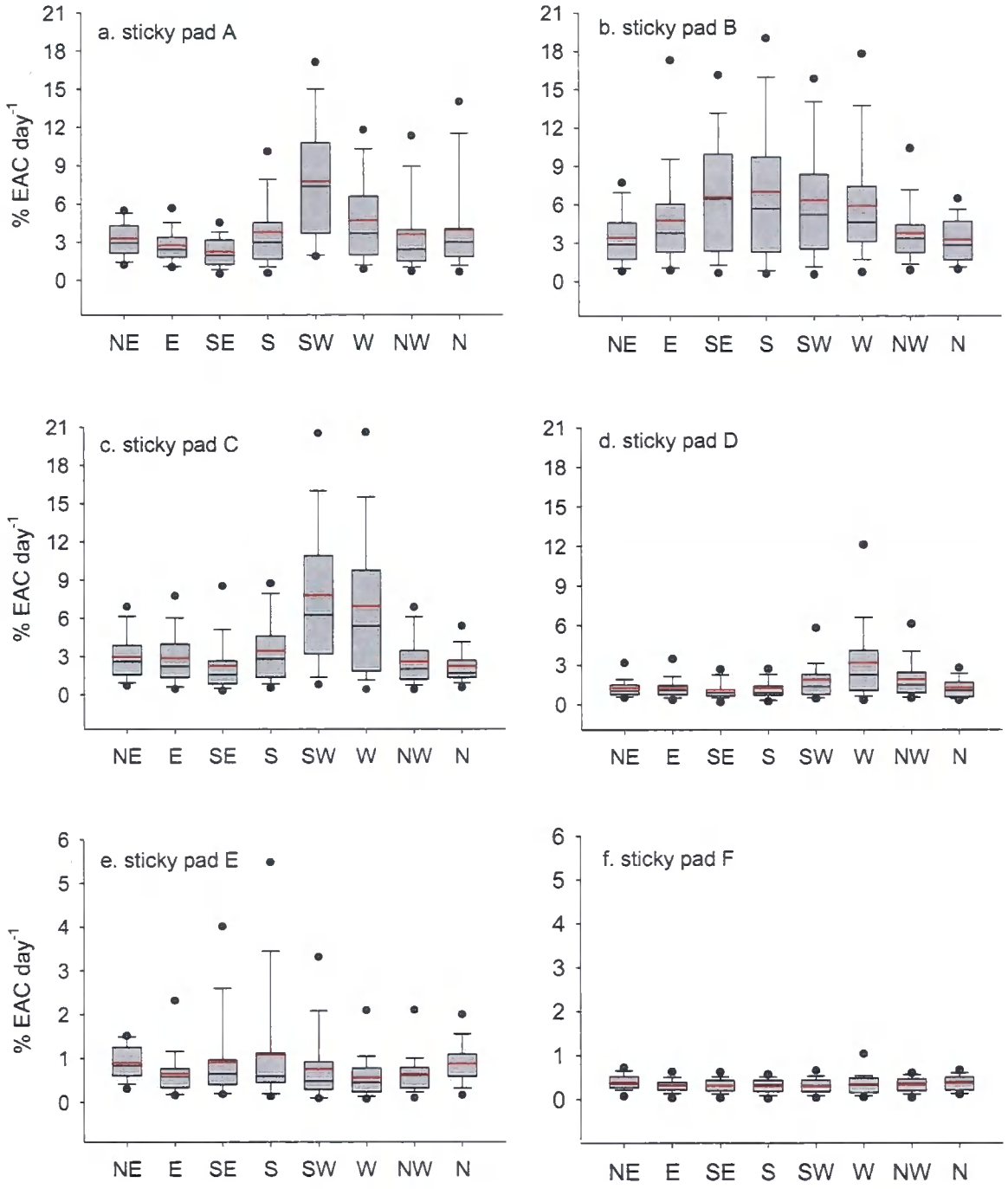

Figure 3.11 Dust flux represented as percentage Effective Area Coverage (% EAC day^{-1}) to sticky pads at six monitoring sites for the period April 2006 to March 2007. Where graph a shows sticky pad A (n=47), graph b shows sticky pad B (n=51), graph c shows sticky pad c (n=50), graph d shows sticky pad D (n=47), graph e shows sticky pad e (n=26), and graph f shows sticky pad F (n=26). The plots show the mean (red line), median (black line), 25 % and 75 % percentile (box plot), 10 % and 90 % percentile (whisker plot) and 5 % and 95 % percentile (black circle). The y axis scale bar on graphs a, b c and d is different to the scale bar for graphs e and f.

The dust flux to sticky pad F was significantly lower than the dust flux to all the other sticky pads ($\bar{x} = 0.34$, $\sigma = 0.03$, df = 7, $t \geq 4.57$, $p < 0.001$). The mean flux for all directions varied between 0.30 % EAC day^{-1} for the south-western flux and 0.39 % EAC day^{-1}, and there was very little variance in the all of the fluxes.

3.3.3.3 Investigating the potential relationship between dust flux and local meteorological conditions – measured at Loftus

The most frequent strong positive correlations of dust flux to the component of wind was for the south-western flux, which included sticky pad A ($n = 47$, $r_s = .85$, $p < 0.001$), sticky pad B ($n = 51$, $r_s = .73$, $p < 0.001$), sticky pad C ($n = 49$, $r_s = .83$, $p < 0.001$) and sticky pad D ($n = 47$, $r_s = .82$, $p < 0.001$). There were strong positive correlations for the dust flux and the wind component for the southern flux to sticky pad A ($n = 47$, $r_s = .74$, $p < 0.001$), sticky pad B ($n = 51$, $r_s = .84$, $p < 0.001$) and sticky pad E ($n = 26$, $r_s = .80$, $p < 0.001$). The dust flux and wind component for the western flux were also strongly positively correlated at sticky pad A ($n = 47$, $r_s = .83$, $p < 0.001$), sticky pad C ($n = 49$, $r_s = .79$, $p < 0.001$) and sticky pad D ($n = 47$, $r_s = .80$, $p < 0.001$) (see Appendix A Figures 2 and 3 for correlation graphs). There was no strong correlation between dust flux and the wind component for any direction of dust flux at sticky pad F.

It may not be a coincidence that the fluxes of dust in the southern, south-western and western directions are most often strongly positively correlated to the component of wind, because the prevailing winds were from the south-west.

3.3.3.4 Investigating the potential relationship between dust flux and the iron ponded on the Corus works

The dust flux at sticky pad C was correlated against the volume of iron discharged at the ponding station. This showed that there was no relationship between the direction of dust flux and total iron ponded.

3.3.4 Discussion

3.3.4.1 Variation between sticky pads

The comparison of three sticky pads exposed over the same exposure period at one dust monitoring site revealed that the dust flux for all directions were statistically similar. This provided the study with confidence in the results obtained from the sticky pads, and the sticky pad reader.

3.3.4.2 Measurements of dust flux

The dust flux measured on and surrounding the Corus works, varied spatially and temporally, due to the variance recorded in the fluxes measured. Overall the highest dust fluxes were recorded at sticky pad B. However, the highest individual directional dust flux was measured for the south-western fluxes at sticky pad A and C. The south-western flux for sticky pads B, D and E were also relatively high but contained considerable variance.

The dust flux at sticky pad A was quite high for the western flux, which could potentially result from fugitive emissions from the stock yards. The north-western and northern fluxes which were reasonably high but contained considerable variance, pointed to the general direction of the centre of the Corus works including the blast furnace.

The majority of directional dust fluxes at sticky pad B were relatively high and contained considerable variance; the western flux could potentially be related to the ore terminal, the south-western flux could potentially be related to the coke stock yards, the flux to the south could potentially be related to the general area of the Corus works and the flux to the south-east could potentially be related to the blast furnace.

The dust flux to sticky pad C was of relatively similar quantity to the flux at sticky pad A, however, there was considerably more variance for all directions of dust flux. However, the two highest dust fluxes for the south-west and west could potentially be related to the potential emissions from the blast furnace and ponding station, respectively.

The dust fluxes measured at sticky pad D were of relatively similar value and variance, except the western fluxes. The Corus works are located directly to the west of Frisbee D and fugitive dust emissions are likely to be the main contributing factor to the

flux of dust. However, the fluxes to sticky pad D are significantly lower than the fluxes to the sticky pads located on the Corus works, hence the distance which particles are entrained could potentially be quite short.

The highest dust flux at sticky pad E was recorded for the southern and south-eastern fluxes of dust, which could correspond to wind-blown material from the Corus works, or alternatively other industrial activities in the Teesside area.

The dust fluxes recorded at the residential sticky pad F were similar irrespective of direction, although there was more variance in the western fluxes.

3.3.4.3 Correlating the potential relationship between dust flux and local meteorological conditions and on-site ponding of iron

For the sticky pads A, B, C and D, the south-west points in the general direction of the Corus works. The sinter bed stocks were to the southwest of sticky pad A, the coke stock yards were to the southwest of sticky pad B, the ponding stations and the general area of Corus works were to the southwest of sticky pad C and the general areas of the Corus works were to the southwest of sticky pad D. This combined with the fact that the south-westerly winds are from the prevailing wind direction indicates that this was most likely to be the case.

All of the directions of dust flux to sticky pad C were not related to the amount of iron discharged at the ponding station during the exposure periods. As a discharging event usually only lasts a few minutes, it is heavily dependant upon the short-term meteorological conditions. Therefore, it is possible that potential emissions from a discharging event are carried over the monitoring site, and discharged beyond the monitoring site.

3.3.4.4 Dust flux studies

Dust flux measurements are a valuable tool for determining the direction of source material to deposition gauges. As the present study has shown, the dust flux to the sticky pads on the Corus works primarily received material from the southern, south-western and western fluxes. Whereas sticky pad F has shown all directions of dust flux are equal in their contribution to overall dust flux to a specific point. Without this directional

information, it would be difficult to attribute the deposition to the Frisbee gauges to specific directions and sources.

Although the sticky pads are an important tool in dust flux studies, there are important limitations which must be considered. The most important limitation is that once a specific area of the sticky pad has trapped a particle, it can no longer continue to trap material. Hence, exposure periods have to be kept to a minimum in order to prevent sticky pad saturation. Another important limitation is the possible loss of material during heavy rainfall. However, the original purpose of dust flux monitoring was to determine the perceived nuisance value of dust to public including windows and cars, which are also subject to loss of material in heavy rainfall.

Dust flux studies are an important tool for determining the overall contribution of a specific directional source of dust emissions, to the dust flux and deposition at a particular site. It has shown in the present study that on the Corus works the majority of dust flux comes from specific directions, contrasting to a residential site, where the dust flux was generally uniform, and therefore potentially representative of background material.

3.4 Summary of Chapter 3 – Dust deposition and flux

The key outcomes of the dust deposition to the Frisbee monitoring sites on and surrounding the Corus works were identified as the following:

Six Frisbees (with dry foam insert) were exposed at six dust monitoring sites established across the Corus works and surrounding areas from April 2006 to March 2007.

Three Frisbee gauges (C, G, and H) were exposed at one site monitoring site in April 2007. There was good agreement between the total dust deposited to the three gauges, although there was variation in the deposition to the three deposition gauges.

The highest dust deposition was measured at Frisbee B. The total dust deposited at Frisbees A, B and C was significantly higher than the total dust deposited at Frisbee D, E and F.

The dust deposition at Frisbee A and D was found to correlate to the north-westerly winds, while the dust deposition at Frisbee F was found to correlate to the westerly winds. The dust deposited at Frisbee A, B, C, D, E and F were not correlated with the precipitation measured at Loftus for the 12 months exposure. The total dust deposited to all of the six Frisbees was not related to the total water collected in the Frisbee gauge or the total precipitation over the exposure period. The dust deposited to Frisbee C was found to be approaching significance in relation to the total weight of iron ponded.

The key outcomes of the dust flux to the sticky pad monitoring sites on and surrounding the Corus works were identified as the following:

Sticky pads were exposed at the six dust monitoring sites (A-F) from April 2006 to March 2007 to determine directional dust flux. A sticky pad reader was used to assess the percentage Effective Area Coverage (% EAC day^{-1}) of dust for the eight cardinal compass points for each exposure period.

When three monitoring gauges (C, G & H) were exposed at one monitoring site, the sticky pads found significantly similar dust flux for each direction of dust flux.

Therefore, the results for the directional dust flux can be interpreted with reasonable confidence.

The largest dust flux measured on the sticky pads located on the Corus works (A, B and C) were from the south-western (A, B & C), southern (A & B) and western (A & C) fluxes. These dust fluxes were all in the direction of the Corus works, and potential fugitive dust generating activities or stockyards. The largest dust fluxes on the Corus works were those to sticky pad B.

The dust fluxes measured at the sticky pads located off the Corus works (D, E and F) were significantly lower than the dust fluxes measured on the Corus works. The highest flux to sticky pad D and F was the western flux; and the highest flux to sticky pad E was the southern flux. These fluxes were all in the direction from the Corus works, relative to the Frisbees. However, the dust fluxes to Frisbee F were equal in their contribution to the total directional dust flux.

The peaks found in the dust fluxes to Frisbee A, B, C, D and E were all in the direction from the Corus works, and towards the SSSI. Therefore there is potential for dust generated on the Corus works to be deposited onto the SSSI. The northern and north-eastern fluxes to Frisbees B, C and D, in the direction from the SSSI towards the Corus works were relatively low, and therefore there is less potential for dust generated on the SSSI to contribute to the total dust deposition to the Frisbees.

Overall the combination of dust deposition and flux provide a valuable contribution to the present study, especially for the dust flux, as they enable the identification of potential sources of fugitive emissions, whilst also measuring the total deposition to a specific site.

The potential sources of dust flux and deposition to the six monitoring sites require a comprehensive study of the chemical characterisation of the particulate matter. This work is presented in the following chapter.

Chapter 4 - Dust characterisation

4.1 Introduction

Determining the chemical composition and morphology of the particulate matter emissions is an important step in determining the potential effects of deposition to plant health. Studies have shown direct (leaf damage) and indirect (soil chemistry) effects from deposited dusts on plant health (see Chapter 2 section 4 and chapter 6 for an examination of the effects of dust on plant health). Hence it is important to determine the chemical composition of the dust deposited to the area on and surrounding the Corus works, Teesside to appreciate the potential effects to the vegetation on South Gare and Coatham Sands SSSI.

Some studies on the chemical composition of airborne particles have been limited to bulk analysis (Yue *et al.*, 2006), which only provides the average information of many particles. Individual particle analysis methods are a valuable alternative to bulk analysis methods (Yue *et al.*, 2006). Scanning Electron Microscopy with Energy Dispersive X-ray Spectrometry analysis (SEM-EDX or SEM-EDS) can determine morphological and elemental information on individual particles (Yue *et al.*, 2006). The SEM-EDA technique of single particle analysis has been used effectively for studies of dust emissions (Bourrier & Desmonts, 2007; Lorenzo *et al.*, 2006; Xie *et al.*, 2005). Recent studies on chemical characterisation have used an automated Scanning Electron Microscope with Energy Dispersive X-ray Spectrometry (SEM-EDA, SEM-EDS or SEM-EDX) which enable a more comprehensive study of particle chemical composition. In a study by Lorenzo *et al.* (2006) sample collection was controlled for specific wind speeds and directions, a total of nearly 11,000 particles were analysed using computer controlled Scanning Electron Microscopy (CCSEM), and clustered into five particle classes, to determine the contribution of railway traffic to particle emissions. A study published in 1991 by Xhoffer *et al.* (1991) used an automated sampling strategy which examined approximately 500 particles per sample for the chemical characterisation of aerosol particles over the North Sea and English Channel. A study on the influence of a steel works on the deposition of iron-rich particles examined approximately 1000 particles per sample, for over 11,800 particles using CCSEM-EDX (Choel *et al.*, 2007) and found that iron-rich particles were of large abundance in air masses which passed over a steel works. Katrinak *et al.* (1995) also studied more than 1000 particles per sample using CCSEM to identify aerosol particle types in Phoenix, Arizona. The work

presented in the current chapter used an SEM-EDA, as an effective method of analysis of single particles spectra.

The use of hierarchical cluster analysis as a multivariate data reduction technique, employing Ward's method has been proven highly successful in many studies on dust characterisation which have classified the particles into clusters based on similarity (DeBock *et al.*, 1994; Katrinak *et al.*, 1995; Paoletti *et al.*, 1999; Paoletti *et al.*, 2003; Van Malderen *et al.*, 1996a; Van Malderen *et al.*, 1996b) and in particular utilising a squared Euclidean distance approach (Osan *et al.*, 2002; Xie *et al.*, 2005). Although other multivariate analysis techniques have been used and proven successful, the present study used hierarchical cluster analysis.

Corus has conducted similar work at another site in the UK from which a dust directory has been compiled for the chemical composition of site materials. Although, the material will not vary considerably between sites the present study is the first to consider the specific chemical characteristics of fugitive dust at the Teesside Corus works and surrounding area.

The main aims of the present chapter are to characterise the chemical composition of the individual particles of dust deposited to the Frisbees, and the dust flux to the sticky pads; use the chemical composition of the particles to identify the possible sources of fugitive dust emissions to each of the six different locations.

4.2 Methods

4.2.1 Sample collection

The dust deposition samples were collected in a dry Frisbee (foam insert) dust deposit gauge and filtered under suction through a glass microfibre filter (see Chapter 3 section 2). The dust flux samples were collected from a sticky pad mounted around a cylindrical holder on the Frisbee gauge (see Chapter 3 section 3). To ensure the particles analysed were not contaminated in these collection procedures by the sampling mediums a clean and unexposed sample of the glass microfibre filter, sticky pad and foam insert were selected for analysis.

Seven dust deposition and six dust flux samples collected on and around the Corus works were taken from the six Frisbee monitoring sites (Chapter 3 Figure 3.2 and Table 3.1). Frisbee A, B and C were located on the Corus works; Frisbee D was located to the southeast of the works adjacent to the SSSI. Frisbee E was located to the north of

the Corus works at the end of the South Gare breakwater and Frisbee F was located to the southeast of the Corus works in the residential area of Grangetown.

It was ensured that the dust flux exposure period corresponded to the dust deposition exposure period for comparable results. On average dust deposition was sampled for exposure periods of one month, and dust flux was sampled for an exposure period of 7 days, although exposure periods for dust flux of 5 to 28 days did occur. One week of exposure was selected at random from each month of deposition (see Table 4.1). To avoid biased sampling of outliers samples were taken from different exposure periods, hence they are not directly comparable (see Table 4.1 and Chapter 3 section 3.2.4 Figure 3.5).

To analyse the dust deposition to each Frisbee an area of 15 mm^2 was removed from the glass microfibre filter. It was ensured that each filter used during the SEM-EDA analysis was of similar origin, the filters were taken from the same stage of sample filtration.

Table 4.1 Samples of dust deposition and dust flux used for SEM-EDA analysis.

Sampling Point	Dust deposition			Dust flux exposure period
	Exposure Period		Total deposition (mg m^{-2} day^{-1})	
A	July	03/07/06 – 01/08/06	523	05/07/06 – 12/07/06
B	October	02/10/06 – 31/10/06	1301	05/10/06 – 12/10/06
C	August	01/08/06 – 01/09/06	909	09/08/06 – 16/08/06
D	September	01/09/06 – 02/10/06	120	13/09/06 – 25/09/06
E	October	02/10/06 – 31/10/06	118	20/10/06 – 27/10/06
F	July	03/07/06 – 01/08/06	83	n/a
F	September	01/09/06 – 02/10/06	159	31/08/06 – 25/09/06

For the analysis of dust flux, an area of 15 mm^2 was removed from a position 13 cm down from the upper edge of the sticky pad, at 2, 8, 11, 17 and 27 cm from the left hand edge, to represent the compass points N, W, SW, S and NE respectively. Dust flux at Frisbee A was additionally sampled at 20 cm from the left hand edge to allow measurement of the deposition from a predominately SE direction.

For a thorough and representative investigation into the type and sources of dust at the Corus works a range of samples were taken from on-site activities. The samples were collected by sampling material from the different potential sources of dust. The samples were collected from stock or road-side piles, and sieved to remove the larger particles. This ensured that the sample collection procedure minimised cross-contamination from other sources and included the appropriate size fraction of airborne

particulate matter. Reference samples were taken from the coke stock yards (455750, 525500 British National Grid), the Redcar ore terminal sinter beds (457150, 525150 British National Grid) and the ponding station (457206, 525558 British National Grid). Three additional samples were taken from the roads adjacent to these three activities, within 10 m of the source. Individual particles were selected randomly for chemical characterisation to account for a range of sizes and morphology. This also accounted for any sampling bias in the collection of the reference samples.

4.2.2 Measurements taken with a Scanning Electron Microscope with Energy Dispersive Analysis (SEM-EDA)

Single particle analysis was conducted using a Scanning Electron Microscope (SEM). The size, shape and chemical composition of particles were observed using a Philips XL40 SEM, operated in accordance with the Corus work instruction CPR SUS 322. Energy Dispersive Analysis (EDA) was used to obtain images at an accelerating voltage of 15 kV, with a beam spot size of 6 at a working distance of 10 mm. A total of 1963 single particles were measured manually at random, with an average of 45 particles per sample (44 samples in total). Each sample was coated with a thin carbon film prior to examination. The X-ray spectra were recorded for seventeen elements including sodium, chlorine, aluminium, manganese, magnesium, zinc, titanium, calcium, barium, bismuth, chromium, copper, iron, silicon, sulphur, potassium and phosphorus. The individual particle spectra were used to calculate a percentage weight for all 17 of the elements. This work was carried out at the Corus Research, Development and Technology Centre, Swinden Technology Centre (STC), Rotherham.

4.2.3 Data analysis

Data were analysed using SPSS statistical software (SPSS Inc. Chicago, Illinois, USA) and presented using Sigma Plot v.10 (Systat Software Inc. San Jose, California, USA). The data were analysed using hierarchical cluster analysis, employing Ward's method, utilising a squared Euclidean distance approach. This classification algorithm is a hierarchical tree in which particle clusters are organised on the basis of increasing distances. For the dust reference, deposition and flux samples hierarchical cluster

analysis was conducted using the percentage weight for each of the 17 elements, hence particles of similar chemical composition were grouped together.

4.3 Results

4.3.1 Sampling medium

A sample of the glass microfibre filter (Whatman G/F A) and the foam insert were analysed to determine their chemical composition. The glass microfibre filter was analysed at three points (Table 4.2). The chemical composition of the filter was on average majority silicon with a percentage weight of 59 %, along with small amounts of sodium (10 %), barium (11 %), zinc (8 %), aluminium (6 %), potassium (3 %) and calcium (3 %).

Analysis using the SEM-EDA facility of the foam insert and sticky pad found that both samples contained a high percentage, by weight, of carbon and oxygen, which are beyond the limits of detection for SEM-EDA. The easily identifiable structure of the foam insert, combined with the spectra made it possible to avoid sampling in error. The sticky pad was also easily identified by the spectra and was not sampled in error as the outline of the particle was clear.

Table 4.2 Percentage weight of each element in the particle spectra for a glass microfibre filter (Whatman GF/A) used to filter the dust deposited to the Frisbee gauges.

Spectrum label	Percentage weight (to 2 decimal places)						
	sodium	aluminium	silicon	potassium	calcium	zinc	barium
L1	7.69	5.97	60.12	3.46	3.21	8.17	11.38
L2	15.16	6.11	57.56	2.69	2.44	6.77	9.26
L3	6.87	6.32	60.26	3.88	2.96	8.32	11.39

4.3.2 Reference samples

Six clusters were identified within the six reference samples collected on the Corus works. Each cluster is presented as a percentage composition of the particles analysed for each sample (Figure 4.3). All of the samples collected were found to have some carbon particles present, except at the sinter bed track site. The cluster of carbon particles was on average below 2 %, except at the coke stock yards where it accounted for 5 % of the particles analysed.

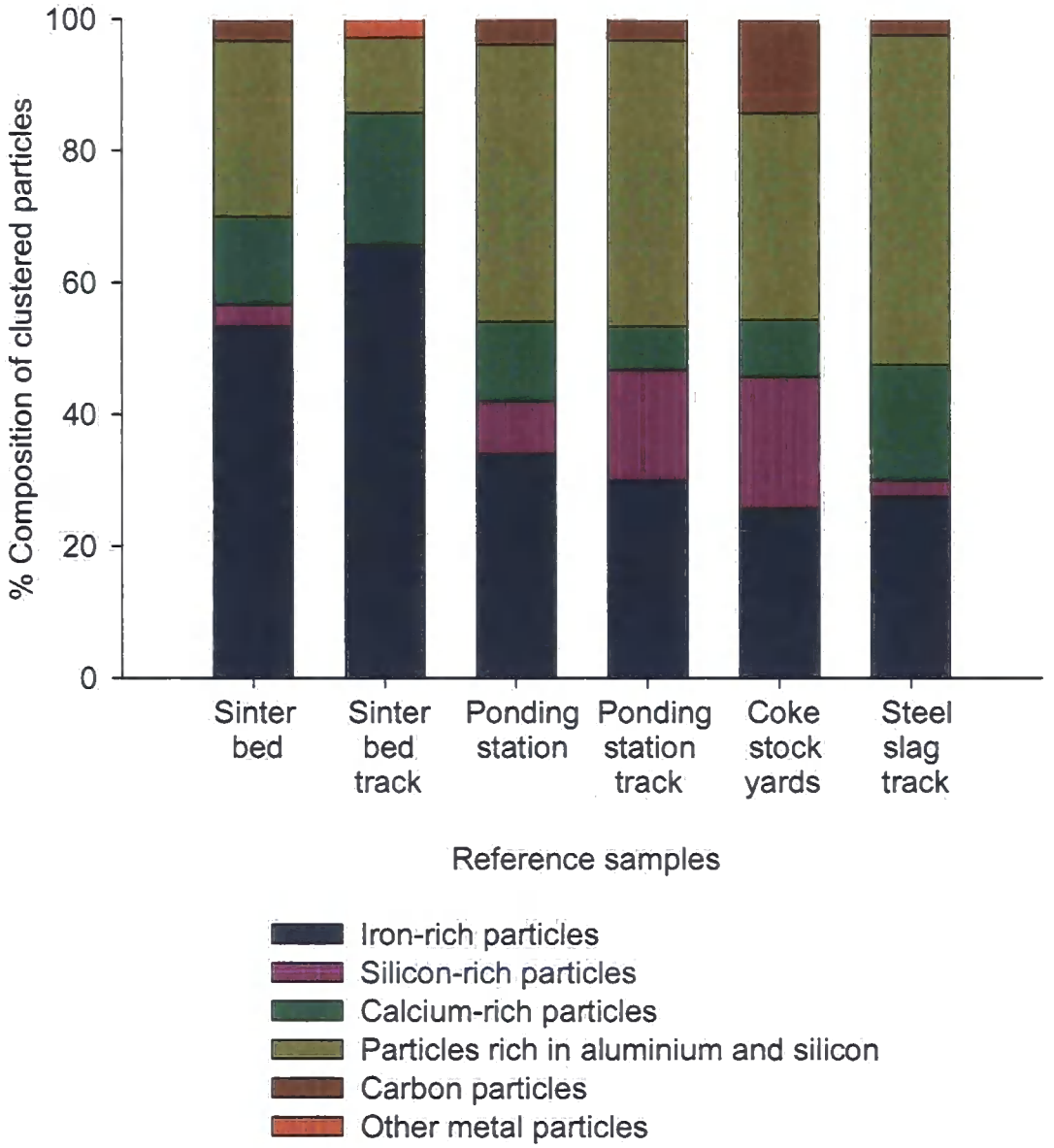

Figure 4.3 Cluster percentage compositions of 6 reference samples taken from the Corus works. Analysis was conducted using an SEM-EDA facility and processed using hierarchical cluster analysis. Where blue indicates iron-rich particles, purple indicates silicon-rich particles, green indicates calcium-rich particles, yellow indicates particles rich in aluminium and silicon, brown indicates carbon particles and orange indicates other metal particles.

The two samples taken from the sinter bed and sinter bed track were found to be of relatively similar chemical composition, because of a similarity in the percentage composition of clustered particles. The largest cluster was the iron-rich particles with 53 % at the sinter bed site and 66 % at the sinter bed track site. The second largest cluster for the sinter bed site with 26 % of the total particles analysed were the particles rich in aluminium and silicon, followed by 13 % of calcium-rich particles, 3 % carbon particles and 3 % silicon-rich particles. The second largest cluster for the sinter bed track site with

20 % of the total particles analysed was the calcium-rich particles, followed by 12 % of particles rich in aluminium and silicon and 3 % of particles containing other metals, which at the sinter bed track site was aluminium.

The samples taken at the ponding station and ponding station track were found to have similar chemical composition, with a similar percentage breakdown of clusters. The ponding station and the ponding station track samples contained 42 and 43 % particles rich in aluminium and silicon respectively. The second largest particle cluster was the iron-rich particles which accounted for 34 % of the particles from the ponding station site and 30 % of the particles from the ponding station track. The third largest particle cluster at the ponding station site was the calcium rich-particles accounted for 12 % of the particles analysed, followed by the silicon-rich particles which accounted for 8 % of the particles analysed. The third largest particle cluster at the ponding station track site were the silicon-rich particles which accounted for 17 % of the particles analysed, followed by the calcium-rich particles which accounted for 7 % of the particles analysed.

The samples taken at the coke stock yards and the steel slag track were found to be of different chemical composition, with a different percentage breakdown of the clusters. The percentage composition of clusters for the coke stock yards sample was 31 % of particles rich in aluminium and silicon, 26 % iron-rich particles, 20 % silicon-rich particles, 14 % carbon particles, and 9 % calcium-rich particles. The percentage composition of clusters for the sample taken at the steel slag track was 50 % of particles rich in aluminium and silicon, 28 % iron-rich particles, 18 % calcium-rich particles, 2.5 % silicon-rich particles, and 2.5 % carbon particles.

4.3.3 Dust deposition samples

Six clusters were identified from the seven samples of dust deposition collected on and surrounding the Corus works. Each cluster is presented as a percentage composition of the particles analysed for each sample (Figure 4.4). The six clusters revealed by hierarchical cluster analysis, were; iron-rich particles; calcium-rich particles; silicon-rich particles; particles rich in aluminium and silicon; particles rich in carbon and particles rich in other metals. The particles clustered into the particles rich in aluminium and silicon contained three subgroups which had relatively high levels of iron, calcium and aluminium; however they were clustered together at this stage of the analysis.

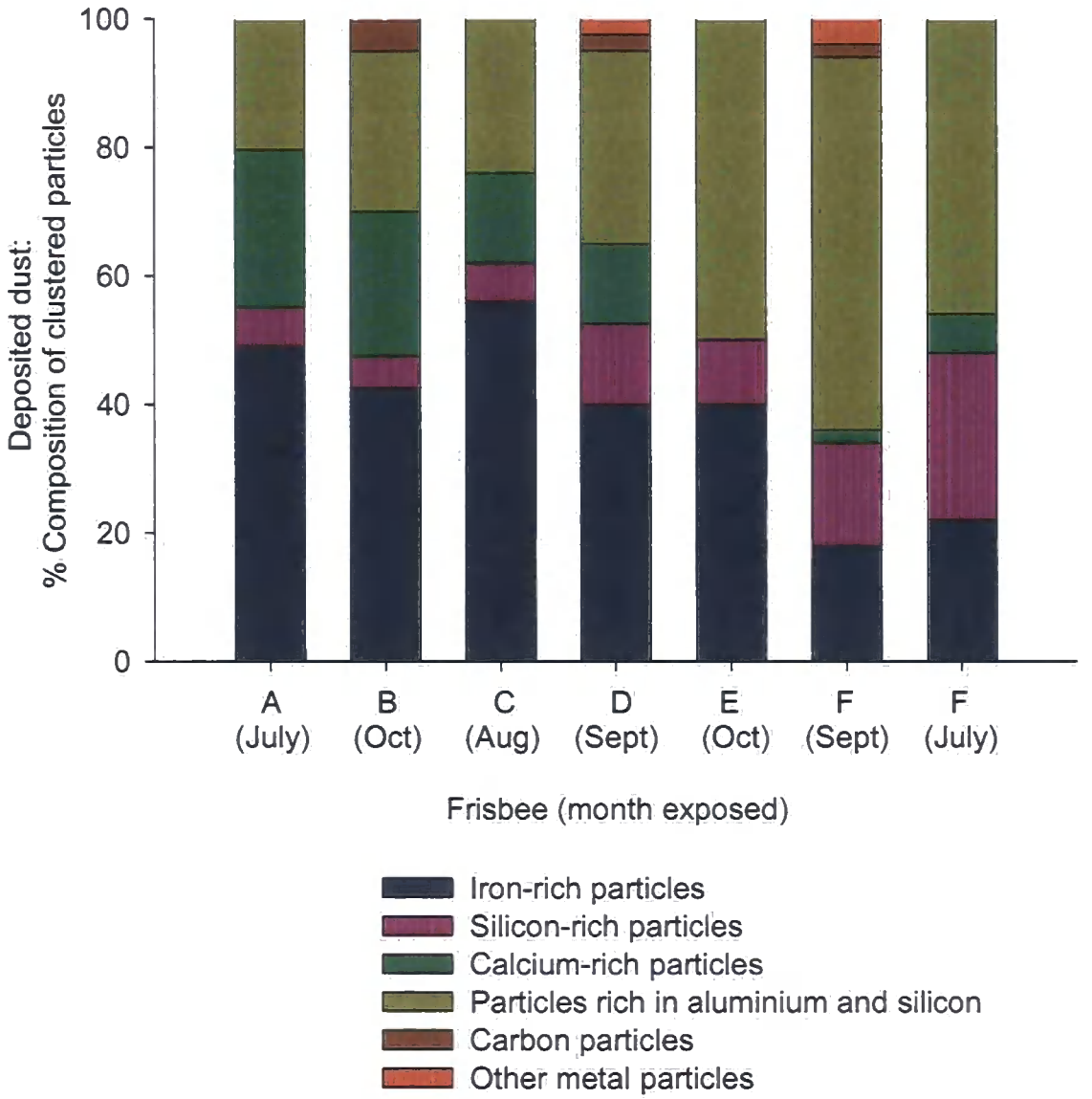

Figure 4.4 Cluster percentage compositions of 7 dust deposition samples taken from the Corus works and surrounding areas. Analysis was conducted using an SEM-EDA facility and processed using hierarchical cluster analysis. Where blue indicates iron-rich particles, purple indicates silicon-rich particles, green indicates calcium-rich particles, yellow indicates particles rich in aluminium and silicon, brown indicates carbon particles and orange indicates other metal particles.

The cluster analysis for the dust deposited at Frisbee A in July 2006 revealed four clusters of particles, of which: iron-rich particles accounted for 49 %; calcium-rich particles accounted for 25 %; particles rich in aluminium and silicon accounted for 20 % and silicon-rich particles accounted for 6 %.

The cluster analysis for the dust deposited at Frisbee B in October 2006 revealed five clusters of particles, of which: iron-rich particles accounted for 43 %; particles rich

in aluminium and silicon accounted for 25 %; calcium-rich particles accounted for 22 %; silicon-rich particles accounted for 5 % and carbon particles accounted for 5 %.

The cluster analysis for the dust deposited at Frisbee C in August 2006 revealed four clusters of particles, of which: iron-rich particles accounted for 56 %; particles rich in aluminium and silicon accounted for 24 %; calcium-rich particles accounted for 14 % and silicon-rich particles accounted for 6 %.

The cluster analysis for the dust deposited at Frisbee D in September 2006 revealed six clusters of particles, of which: iron-rich particles accounted for 40 %; particles rich in aluminium and silicon accounted for 30 %; calcium-rich particles and silicon-rich particles both accounted for 13 %, and carbon and other metal particle clusters both accounted for 2 %, of which titanium was the main component of the other metal particles.

The cluster analysis for the dust deposited at Frisbee E in October 2006 revealed three clusters of particles, of which: 50 % were particles rich in aluminium and silicon; 40 % were iron-rich particles and 10 % were silicon-rich particles.

The cluster analysis for the dust deposited at Frisbee F in July 2006 revealed six clusters of particles, of which: 58 % were particles rich in aluminium and silicon; 18 % were iron-rich particles; 16 % were silicon-rich particles; 4 % were other metal particles mainly titanium, and calcium-rich and carbon particle clusters both accounted for 2 % of the total particles analysed.

The cluster analysis for the dust deposited at Frisbee F in September 2006 revealed four clusters of particles, of which: 48 % were particles rich in aluminium and silicon; 26 % were silicon-rich particles; 22 % were iron-rich particles and 6 % were calcium-rich particles.

At the Frisbee sites A, B, C, and D the majority of particles analysed were mainly characterised by iron-rich particles, its lowest was at Frisbee B accounting for 43 % of the deposition and its highest was at Frisbee C accounting for 56 % of the deposition. The level of iron-rich particles was 40 % at both Frisbee D and E, which despite being located beyond the Corus works, are still in close proximity to the works at 120 and 2300 m respectively. The percentage of the iron-rich particle cluster at Frisbee F in July and September was very low in comparison to the other five sampling sites accounting for 18 and 22 % of the total particles analysed. The dominant particle cluster at Frisbee F was the particles rich in aluminium and silicon which accounted for 58 % of the particles analysed in July and 46 % of the particles analysed in September. Overall, the percentage

of the iron-rich particle cluster was highest on the Corus works, while the cluster of particles rich in aluminium and silicon was higher at sites surrounding the Corus works.

The cluster of calcium-rich particles was at its highest at Frisbees A and B, at 24 and 22 % of the total particles analysed respectively. The calcium-rich particle cluster declined to 14 and 13 % at Frisbees C and D, respectively. At Frisbee E the calcium-rich particles were notably absent form the deposited dust. However, at Frisbee F in July the calcium-rich particle cluster accounted for very little of the total deposited particles at only 2 % increasing to 6 % in September. The calcium-rich particles were mainly calcium silicates at Frisbees A, B, C and D, whereas at Frisbee F they were calcium sulphates.

4.3.4 Dust flux samples

Eight distinct particle clusters were identified from the six samples of directional dust flux as follows; as iron-rich particles (Figure 4.5); silicon-rich particles (Figure 4.6); calcium-rich particles (Figure 4.7); particles rich in aluminium and silicon (Figure 4.8); carbon particles (Figure 4.9); other metals (including aluminium, titanium, manganese, chromium, copper, barium, bismuth and zinc) (Figure 4.10); sulphur-rich particles (Figure 4.11); and particles rich in sodium and chlorine (Figure 4.12). The particles clustered into particles high in aluminium and silicon, had relatively consistent levels of silicon, but the cluster contained three broad subgroups of particles. There were particles which had relatively high levels of iron, calcium and aluminium; however they were clustered together at this stage of analysis.

The majority of the clusters were found at all six sites except for carbon particles which were only found at sticky pads A, B and F; sulphur-rich particles which were only found at sticky pads A, B, C and E and particles rich in sodium and chlorine which were found at sticky pads C, D and E.

The cluster analysis for the dust flux to the sticky pad at A, for the period from the 5th to the 12th July 2006, found that the most frequently occurring cluster was the iron-rich particle cluster for all directions. The iron-rich particle cluster accounted for 61 % of the western flux at its maximum, and 38 % of the north-eastern flux at its minimum (Figure 4.5.a). The second most frequently occurring cluster was the particles rich in aluminium and silicon which at its maximum accounted for 33 % of the north-eastern flux, and at its minimum 20 % of the western flux (Figure 4.8.a). The third largest cluster was the calcium-rich particles which accounted for 24 % of the south-eastern flux

at its maximum, and 9 % of the western flux at its minimum (Figure 4.7.a). The remaining particle clusters were present in very low percentages, accounting for less than 5 % of the total flux in any direction, these included silicon-rich particles (Figure 4.6.a), sulphur-rich particles (Figure 4.11.a), carbon particles (Figure 4.9.a) and other metals (Figure 4.10.a). The only exception to this was the north-eastern flux of silicon-rich particles which accounted for 14 % of the total flux.

The cluster analysis for the dust flux to the sticky pad at B, for the period from the 5th to the 12th October 2006, found that the most frequently occurring cluster was the iron-rich particle cluster for all directions. At its maximum the iron-rich particle cluster accounted for 60 % of the southern flux, compared to its minimum of 28 % of the northern flux (Figure 4.5.b). The second most frequently occurring cluster was the particles rich in aluminium and silicon which at its maximum accounted for 34 % of the north-eastern flux compared to its minimum of 14 % of the southern flux (Figure 4.8.b). The calcium-rich particles were the third largest cluster which accounted for 30 % of the northern flux at its maximum, compared to its minimum of 14 % of the south-western and north-eastern flux (Figure 4.7.b). The remaining particle clusters were present in very low percentages, accounting for less than 10 % of the total flux in any direction, these included silicon-rich particles (Figure 4.6.b), carbon particles (Figure 4.9.b) and other metals (Figure 4.10.b).

The cluster analysis for the dust flux to the sticky pad at C, for the period from the 9th to the 16th August 2006, found that there were two clusters that were the most frequently occurring. The iron-rich particle flux was predominantly from the south-west and west, while the flux for the particles rich in aluminium and silicon was predominately from the north and west. The iron-rich particle cluster at its maximum accounted for 48 % of the south-western flux, and at its minimum 9 % of the northern flux (Figure 4.5.c). The cluster for particles rich in aluminium and silicon cluster accounted for 41 % of the northern flux at its maximum and 9 % of the southern flux at its minimum (Figure 4.8.c). The calcium-rich particles were the third largest cluster which at its maximum accounted for 30 % of the north-eastern flux, and at its minimum accounted for 7 % of the south-western flux (Figure 4.7.c). The fourth largest cluster was the particles rich in sodium and chlorine which accounted for 28 % of the northern flux at its maximum, around 10 % of the southern and north-eastern flux, 6 % of the western flux and at its minimum absent in the south-western flux (Figure 4.12.c). The remaining particle clusters were present in very low percentages, accounting for less than 8 % of the total flux in any direction, these included silicon-rich particles (Figure 4.6.c), sulphur-rich

particles (Figure 4.11.c) and other metals (Figure 4.10.c). The only exception to this was the southern flux of sulphur rich particles which accounted for 26 % of the total flux.

The cluster analysis for the dust flux to the sticky pad at D, for the period from the 13th to the 25th September 2006, found that the most frequently occurring cluster was the cluster of particles rich in aluminium and silicon for all directions. The particles rich in aluminium and silicon cluster accounted for 51 % of the southern flux at its maximum, compared to 33 % of the northern flux at its minimum (Figure 4.8.d). The second most frequently occurring cluster was the iron-rich particles, which at its maximum accounted for 56 % of the western flux, compared to 28 % of the south-western flux at its minimum (Figure 4.5.d). The silicon-rich particles were the third largest cluster which was relatively small. At its maximum the silicon-rich particle cluster accounted for 16 % of the south-western flux, compared to 8 % of the western and northern flux at its minimum (Figure 4.6.d). The remaining particle clusters were present in very low percentages, accounting for less than 5 % of the total flux in any direction, these included calcium-rich particles (Figure 4.7.d), particles rich in sodium and chlorine (Figure 4.12.d) and other metals (Figure 4.10.d). The only exception to this was the northern and south-western flux of calcium-rich particles which accounted for 8 and 6 % of the total flux, respectively.

The cluster analysis for the dust flux to the sticky pad at E, for the period from the 20th to the 27th October 2006, found that the most frequently occurring cluster was the calcium-rich particles for all directions. At its maximum the calcium-rich particle cluster accounted for 40 % of the western flux, compared to 20 % of the south-western flux at its minimum (Figure 4.7.e). The second most frequently occurring cluster was the particles rich in aluminium and silicon which at its maximum accounted for 28 % of the north-eastern flux and 26 % of the northern flux, compared to 3 % of the southern flux at its minimum (Figure 4.8.e). The sulphur-rich particle cluster was the third largest cluster, at its maximum it accounted for 24 % of the southern flux, compared to 6 % of the western flux at its minimum (Figure 4.11.e). The fourth largest particle cluster was the iron-rich particles which at its maximum accounted for 20 % of the western flux, compared to the northern flux where it is absent (Figure 4.5.e). The remaining particle clusters were present in very low percentages, accounting for less than 10 % of the total flux in any direction, these included silicon-rich particles (Figure 4.6.e), particles rich in sodium and chlorine (Figure 4.12.e) and other metals (Figure 4.10.e). The only exceptions to this were the north-eastern and south-western flux of silicon-rich particles

which accounted for 16 and 11 % of the total flux, respectively, and the south-western flux of particles rich in sodium and chlorine which accounted for 11 % of the total flux.

The cluster analysis for the dust flux to the sticky pad at F, for the period from the 31st August to the 25th September 2006, found that the most frequently occurring cluster was the particles rich in aluminium and silicon for all directions. The particles rich in aluminium and silicon accounted for 66 % of the south-western and north-eastern flux at its maximum, compared to 28 % of the southern flux at its minimum (Figure 4.8.f). The second most frequently occurring cluster was the iron-rich particles which at its maximum accounted for 28 % of the southern flux compared to 8 % of the north-eastern flux at its minimum (Figure 4.5.f). The silicon-rich particles were the third largest cluster which at its maximum accounted for 20 % of the western flux, compared to 10 % of the north-eastern flux at its minimum (Figure 4.6.f). The fourth largest cluster was the calcium-rich particles which accounted for 30 % of the southern flux at its maximum, around 7 % of the south-western and 8 % of the northern flux (Figure 4.7.f). The remaining particle clusters were present in very low percentages, accounting for less than 5 % of the total flux in any direction, these included carbon particles (Figure 4.9.f) and other metals (Figure 4.10.f). The only exception to this was the northern flux of other metal particles which accounted for 8 % of the total flux.

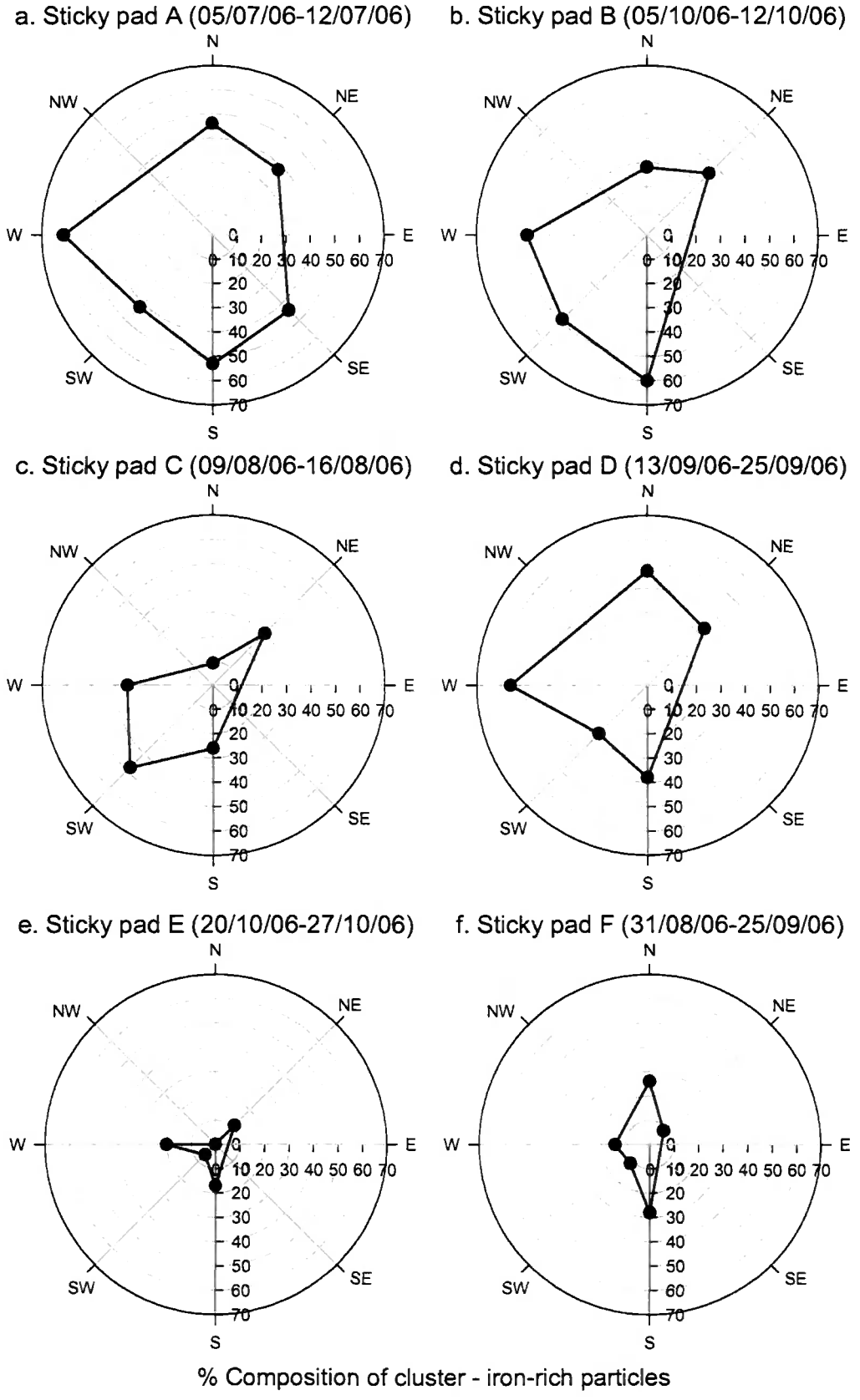

Figure 4.5 Percentage composition of the iron-rich particle cluster (blue) for directional dust flux, using single particle analysis of SEM-EDA data, analysed using hierarchical cluster analysis. Graphs a to f show the directional flux for sticky pads A to F respectively.

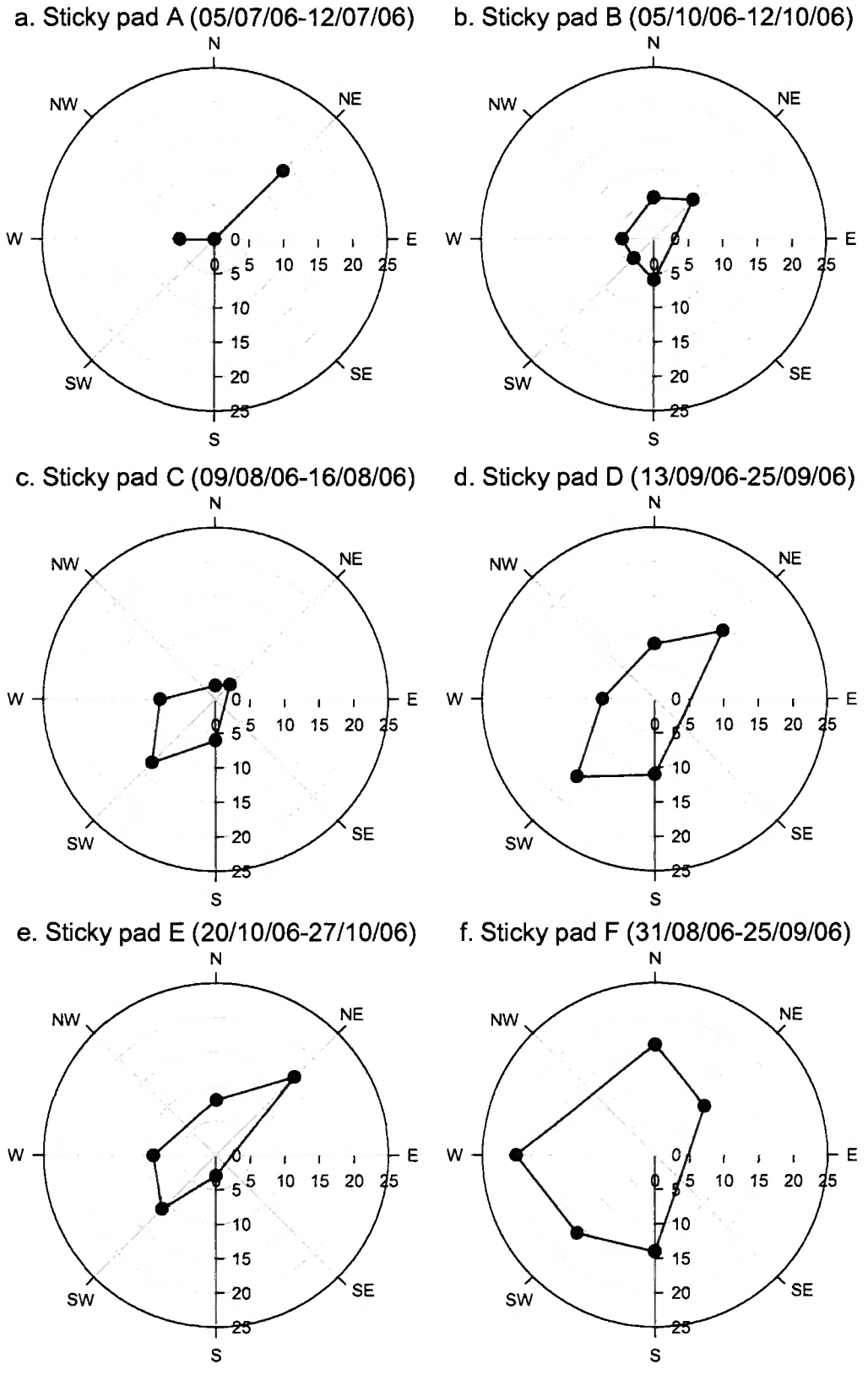

Figure 4.6 Percentage composition of the silicon-rich particle cluster (purple) for directional dust flux, using single particle analysis of SEM-EDA data, analysed using hierarchical cluster analysis. Graphs a to f show the directional flux for sticky pads A to F respectively.

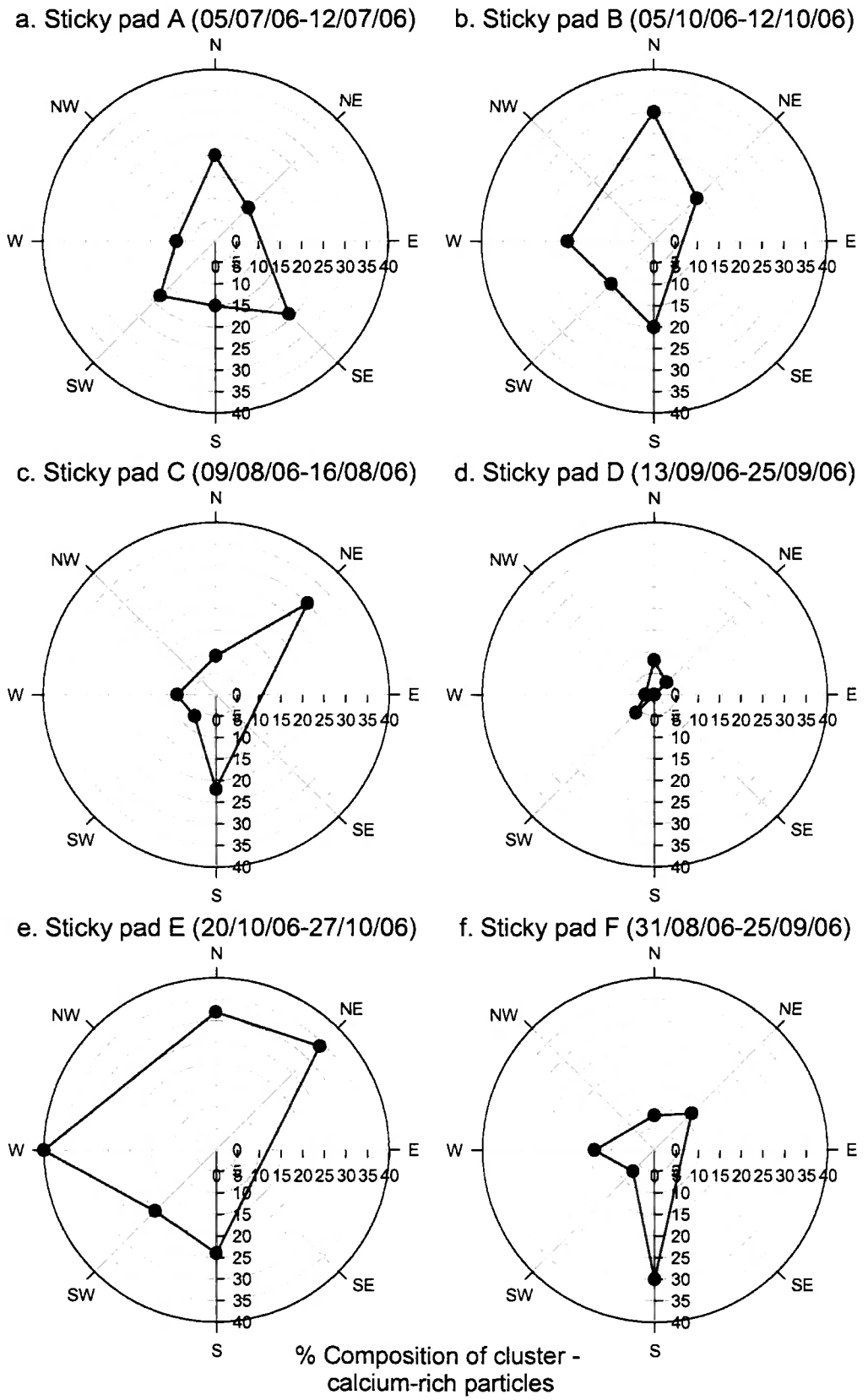

Figure 4.7 Percentage composition of the calcium-rich particle cluster (green) for directional dust flux, using single particle analysis of SEM-EDA data, analysed using hierarchical cluster analysis. Graphs a to f show the directional flux for sticky pads A to F respectively.

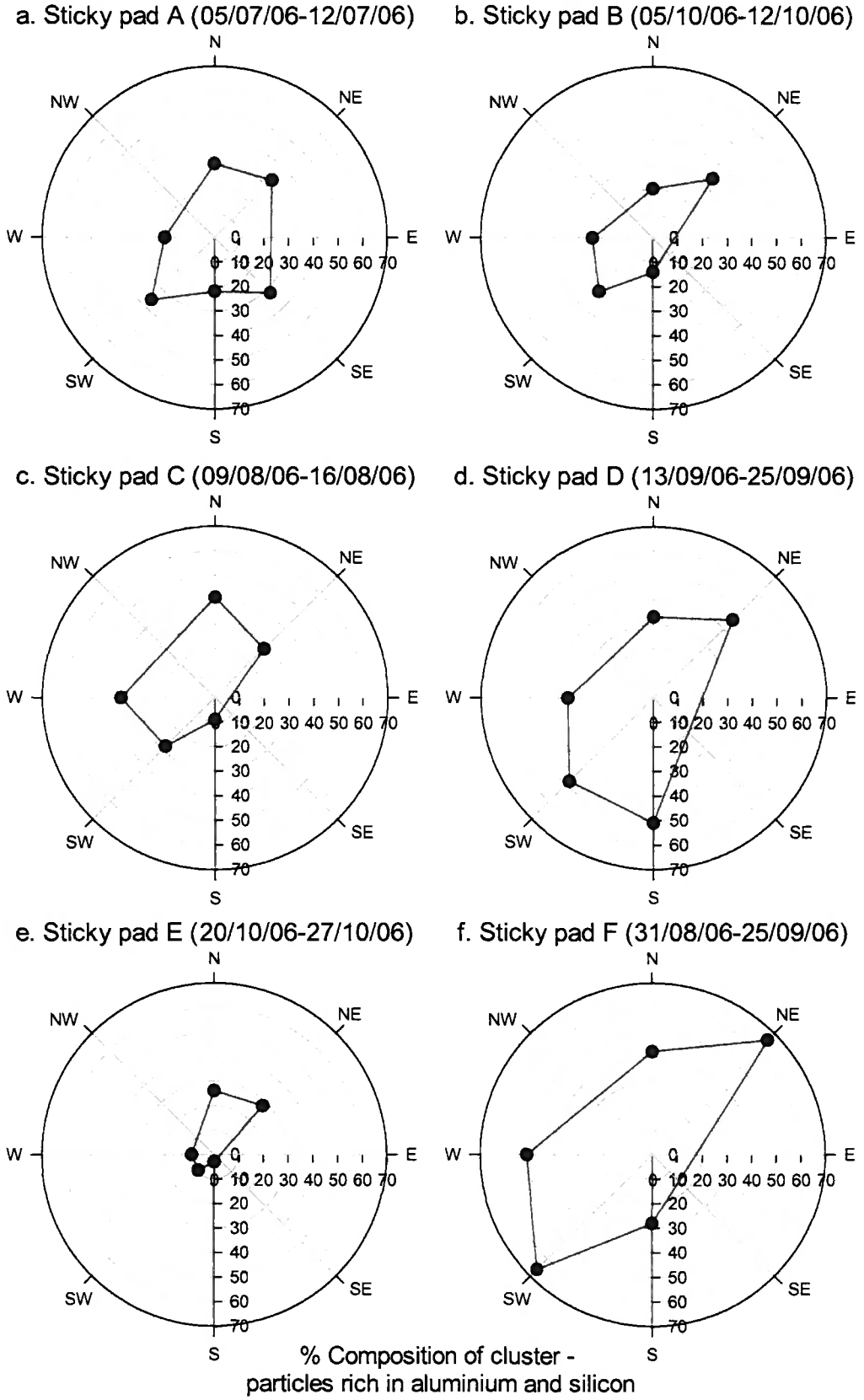

Figure 4.8 Percentage composition of the aluminium and silicon rich particle cluster (yellow) for directional dust flux, using single particle analysis of SEM-EDA data, analysed using hierarchical cluster analysis. Graphs a to f show the directional flux for sticky pads A to F respectively.

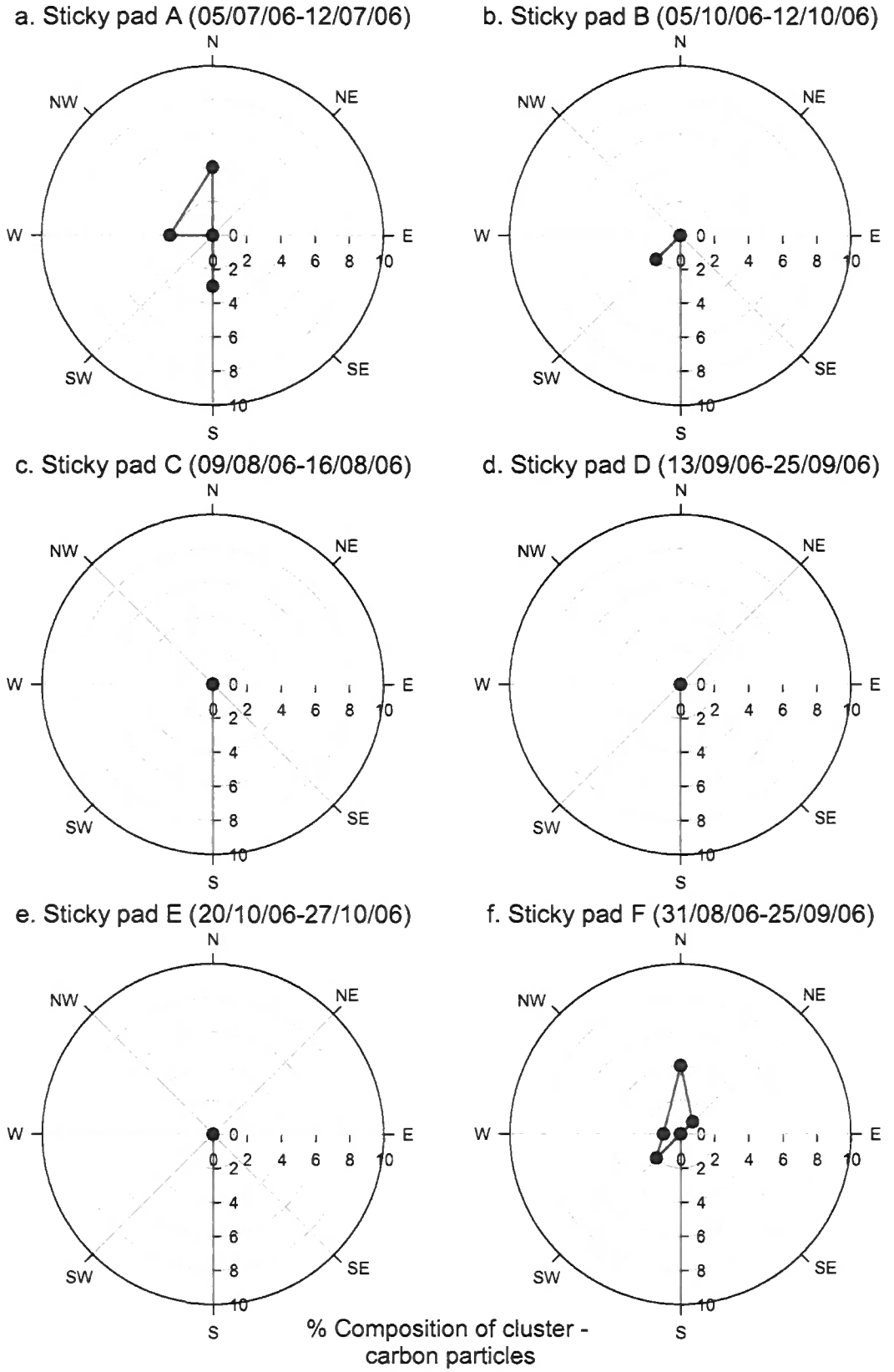

Figure 4.9 Percentage composition of the carbon particle cluster (brown) for directional dust flux, using single particle analysis of SEM-EDA data, analysed using hierarchical cluster analysis. Graphs a to f show the directional flux for sticky pads A to F respectively.

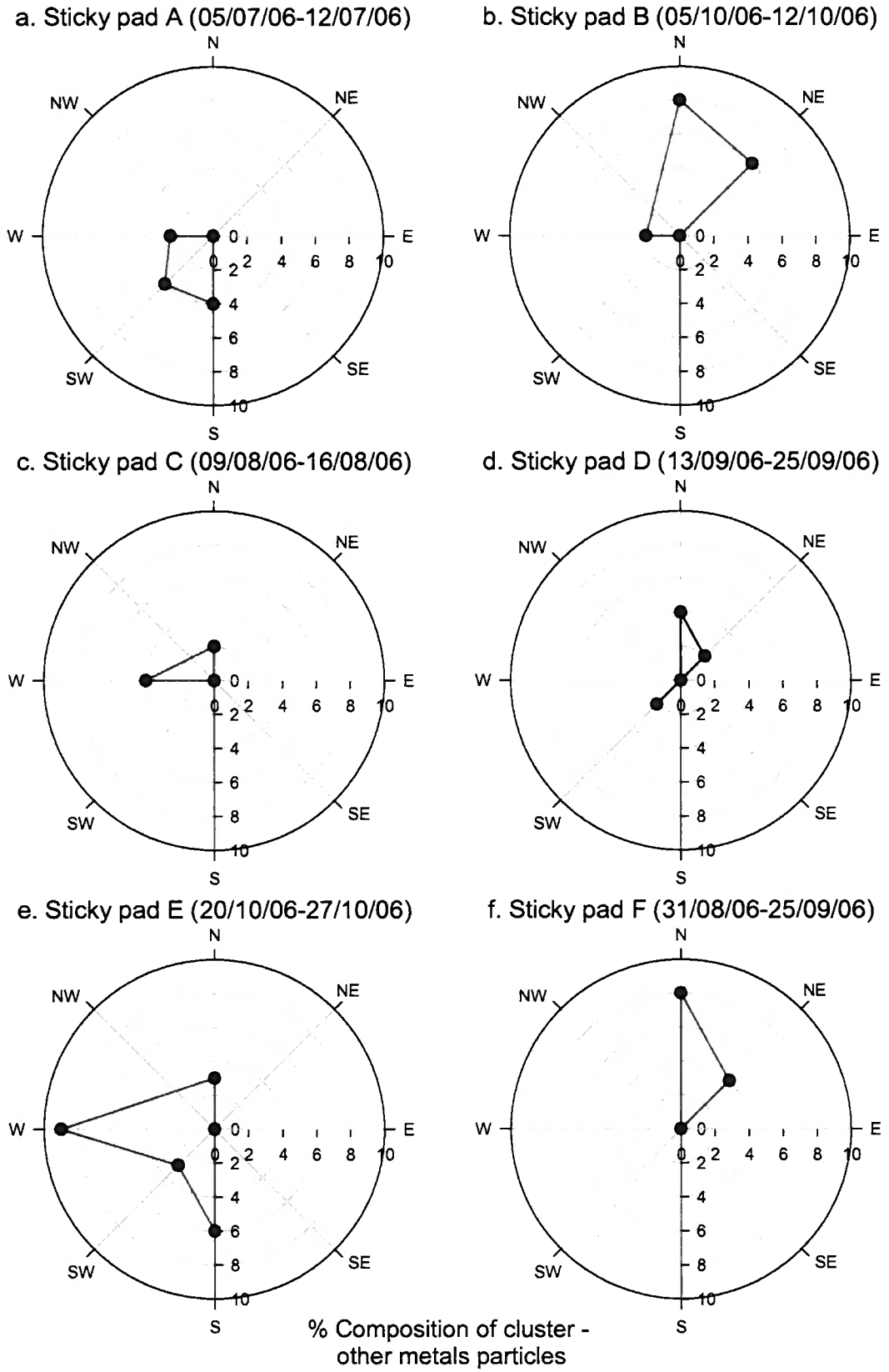

Figure 4.10 Percentage composition of the other metals particle cluster (orange) for directional dust flux, using single particle analysis of SEM-EDA data, analysed using hierarchical cluster analysis. Graphs a to f show the directional flux for sticky pads A to F respectively. Other metals include aluminium, titanium, manganese, chromium, copper, barium, bismuth and zinc.

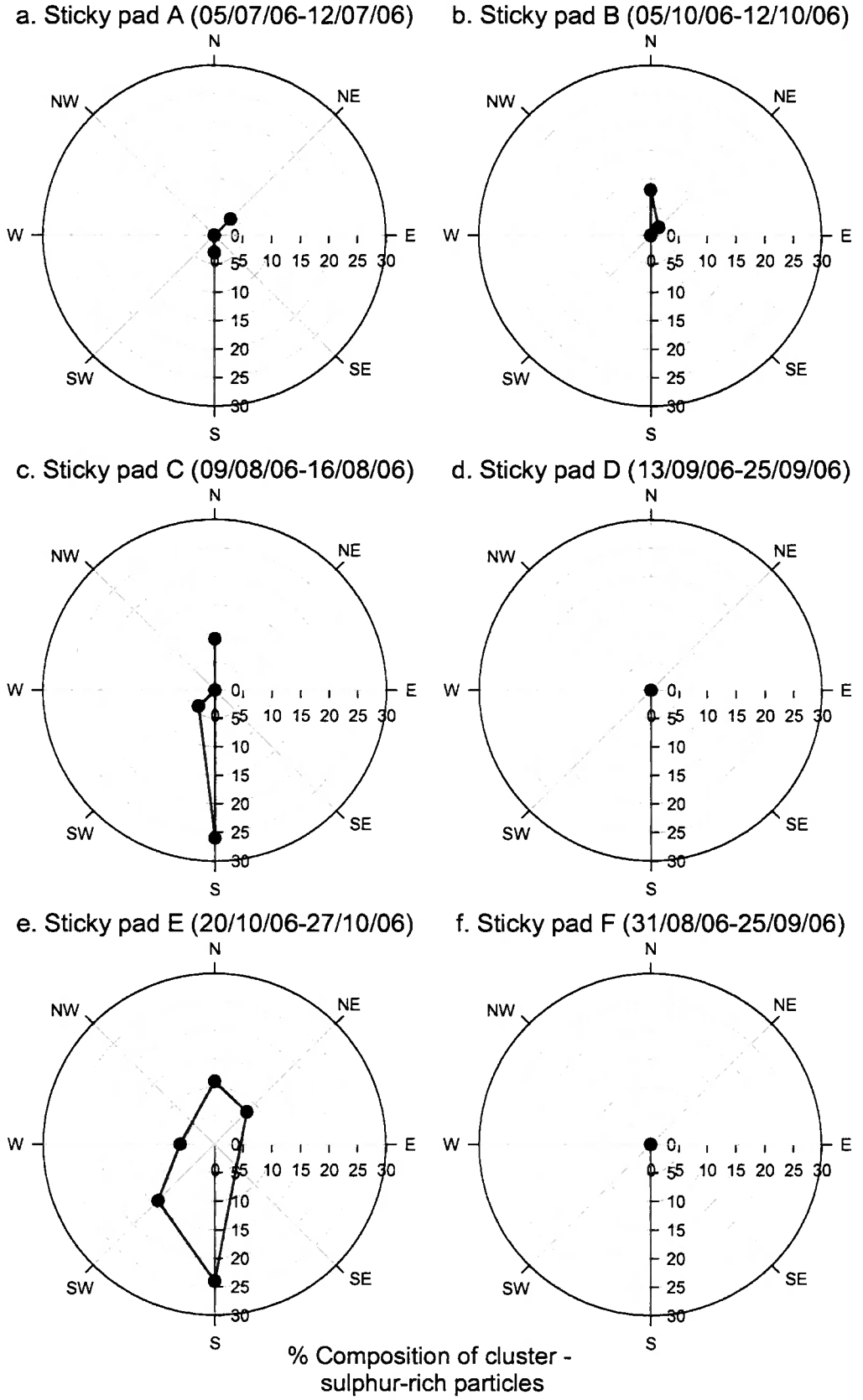

Figure 4.11 Percentage composition of the sulphur-rich particle cluster (red) for directional dust flux, using single particle analysis of SEM-EDA data, analysed using hierarchical cluster analysis. Graphs a to f show the directional flux for sticky pads A to F respectively.

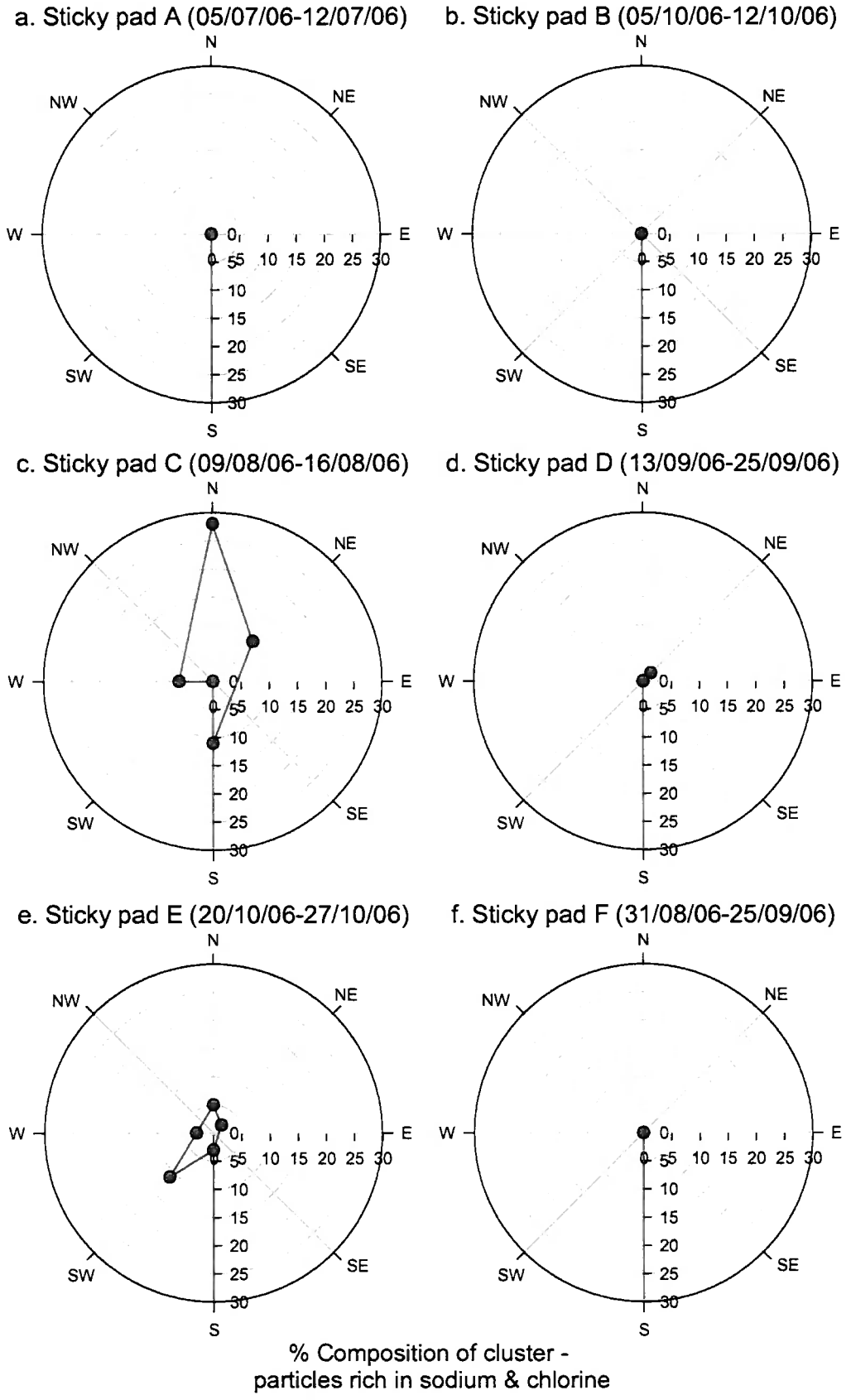

Figure 4.12 Percentage composition of the cluster rich in sodium and chlorine particles (turquoise) for directional dust flux, using single particle analysis of SEM-EDA data, analysed using hierarchical cluster analysis. Graphs a to f show the directional flux for sticky pads A to F respectively.

4.4 Discussion

4.4.1 Particle cluster definition

Hierarchical cluster analysis of the dust deposition, flux and reference samples found eight distinct particle clusters. The sample collection procedure was designed to include samples which were varied spatially and temporally, therefore it is important to consider that these particle clusters may potentially originate from different sources of emissions.

Previous studies on chemical characterisation have reported that iron-rich particles were probably a result of ferrous metallurgy processes (DeBock *et al.*, 1994; Katrinak *et al.*, 1995; Kemppainen *et al.*, 2003; Michaud *et al.*, 1993; Post & Buseck, 1984; Van Malderen *et al.*, 1996a; Xhoffer *et al.*, 1991). Whether emissions from on-site processes or fugitive emissions from iron ore stock yards, it is likely that this is the case for the cluster of particles found on and surrounding the Corus works as found in previous studies on emissions from steel works (Kemppainen *et al.*, 2003). However, the exact chemical composition of the iron ore can vary, due to its source and the on-site blending process.

Particles rich in silicon have been previously identified as sand, more specifically silicon dioxide (quartz), silicates (Katrinak *et al.*, 1995; Van Malderen *et al.*, 1996a; Xhoffer *et al.*, 1991), and as a potential result of coal combustion in power stations (Dodd *et al.*, 1991; Small *et al.*, 1981). The sources of silicon-rich particles at the Corus works could be sources of sand from the sand dunes of South Gare and Coatham Sands SSSI. However, the particles could also be from coal combustion processes on the Corus works or the surrounding industrial area.

Particles rich in calcium have been previously identified as cement dust (Katrinak *et al.*, 1995; Rybicka, 1989), marine sources of calcite, dolomite and gypsum (calcium sulphates) (Katrinak *et al.*, 1995; Xhoffer *et al.*, 1991), waste products of the desulphurisation process gypsum (Kemppainen *et al.*, 2003) and waste gases from fossil fuel power stations (Michaud *et al.*, 1993; Post & Buseck, 1984; Rybicka, 1989; Xhoffer *et al.*, 1991). At the Corus works the calcium-rich particles could have been sourced from marine processes, waste gases from the fossil fuel combustion, steel slag (calcium silicate), limestone stocks or waste products of desulphurisation.

Particles rich in aluminium and silicon have previously been found to be generated from soil dust (Katrinak *et al.*, 1995; Kemppainen *et al.*, 2003; Van Malderen

et al., 1996a; Van Malderen *et al.*, 1996b) and fly ash derived material formed during high temperature combustion (Van Malderen *et al.*, 1996b; Xhoffer *et al.*, 1991). The particles rich in both aluminium and silicon found at the Corus works could have resulted from high temperature combustion processes, waste slag (calcium silicates), or ferrosilicon and silicocalcium alloys which are materials used in the steel production process as a source of silicon. However, these particles could also result from high temperature combustion processes not only on the Corus works but from the whole Teesside industrial area.

Particles of carbon found on the Corus works were most likely from stocks of coal or coke or incomplete burning processes (Kemppainen *et al.*, 2003).

Particles rich in both sodium and chlorine found on the Corus works were most likely to be a result of sea salt particles, in agreement with earlier studies by Xhoffer *et al.* (1991) and Katrinak *et al.* (1995).

Particles rich in sulphur have been reported to be most likely a result of sulphur dioxide emissions from industrial processes, as a by-product of fossil fuel combustion (Katrinak *et al.*, 1995; Xhoffer *et al.*, 1991) although it is also a component of waste gypsum from the desulphurisation process (Kemppainen *et al.*, 2003). The sulphur-rich particles reported in the present study are likely to be associated with similar activities on the Corus works.

The particles rich in other metals found in the present study included titanium, aluminium, chromium, copper, manganese, bismuth, barium and zinc could have been the alloying elements used in steel production, or sourced from other areas beyond the Corus works. Previous work has identified metal rich particles as metal oxides resulting from foundry emissions or industrial sources (Katrinak *et al.*, 1995).

It is difficult to determine the exact source of the particle clusters due to the variety of sources, a more detailed examination of the morphology of the particle would enable differentiation between the particles; however this was not within the scope of the present study. The potential sources of some of these particle clusters has been highlighted but a more detailed examination would be required to confirm the exact sources of deposited dust and dust flux.

4.4.2 Sampling medium

The chemical composition of the foam insert and filter were determined and compared to the individual particles compositions for all samples. At this stage any particle found to have a similar chemical composition to the control sample of the filter was to be removed prior to the hierarchical cluster analysis, however, no particles were found.

4.4.3 Reference samples

The samples from the sinter bed and sinter bed track contained a large cluster of iron-rich particles, which would have been expected, as sinter is processed iron ore. The silica-rich particle cluster was relatively low and could be either sand from the SSSI or a result of on-site combustion processes. The particles rich in both aluminium and silicon could also be a by-product of combustion.

The samples taken from the ponding station contained a relatively large proportion of particles rich in aluminium and silicon; this could potentially be waste slag which is primarily calcium silicate and is discharged at this site. This could also be potentially true for the calcium-rich particles which were found at the ponding station samples. The percentage of iron-rich particles was also relatively high and confirms the expectation that the particles are a result of foundry emissions.

The sample taken the coke stock yards contained the highest amount of carbon, although only a relatively small percentage of the overall clusters. Although the spectra contain other elements, coke is a carbon based material. There are a considerable proportion of particles rich in aluminium and silicon, which could either be waste slag or a result of combustion processes. The cluster of iron-rich particles is relatively low in comparison to the other reference samples; they are probably a result of wind-blown emissions from on-site activities. The silicon-rich particles are most likely to be sand from the SSSI due to the proximity to South Gare dunes.

The sample taken from the steel slag track contains the largest proportion of particles high in aluminium and silicon, which is likely to be a result of waste slag. The iron-rich and the calcium-rich particle clusters are both relatively high, which could be wind blown from on-site combustion or foundry activities.

This process of examining reference samples from across the Corus works has enabled identification of characteristic material from a few potential on-site sources.

However, the reference sample sites are open to dust deposition from activities across the Corus works and beyond, and it is therefore difficult to identify a sample as specific to a single source of dust.

4.4.4 Dust deposition samples

The deposition pattern of iron rich particles was at its highest on or in close proximity to the Corus works, and decreases with increasing distance from the works. It is possible that the emissions of iron rich particles was a result of emissions from the Corus steel works, which is supported in work by Katrinak *et al.* (1995), Michaud *et al.* (1993), Post & Buseck (1984), Van Malderen *et al.* (1996a) and Xhoffer *et al.* (1991) which reported the most likely sources iron-rich particles were as a result of ferrous metallurgic processes.

The deposition of particles rich in aluminium and silicon was at its highest furthest away from the Corus works at Frisbees F and E. Particles rich in aluminium and silicon were also found on the Corus works, although the number of particles identified was much smaller relative to Frisbees F and E. The decline in iron-rich particle deposition may allow an increase the relative importance of particles rich in aluminium and silicon at Frisbees F and E. Therefore the actual total deposition of particles of rich in aluminium and silicon may be the same for the Frisbees monitoring sites on and surrounding the Corus works. However, due to the considerable variation in the chemical composition of the particles which were included in this cluster it is plausible that multiple sources contribute to the deposition of these particles. Determining the source or the exact contribution of the cluster to the total deposition is difficult for this cluster. However, if particles rich in aluminium and silicon are a result of high temperature combustion processes as previously found by Xhoffer *et al.* (1991) and Van Malderen *et al.* (1996b), the Corus works is one of many industrial sites in the Teesside area. This could explain the emissions of particles of a similar chemical composition, which could be sourced from multiple sites.

The calcium rich particle cluster was found to contain two subgroups, with calcium silicates and sulphates both clustered as calcium rich particles. This characteristic difference in the deposited particles indicates that the deposition is likely to generate form different sources. It is possible that the calcium silicates at Frisbees A, B, C and D are attributable to steel slag waste, it has been shown that calcium-rich particles are released from the combustion of fossil fuels (Michaud *et al.*, 1993; Post & Buseck,

1984; Rybicka, 1989; Xhoffer *et al.*, 1991) which could be attributed to multiple industrial sources of emissions in the Teesside area.

The particles rich in silicon found at Frisbees A, B, C, D and E could be a result of sand deposition from the sand dunes on the SSSI in agreement with work by Katrinak *et al.* (1995), Xhoffer *et al.* (1991) and Van Malderen *et al.* (1996a). However, the largest deposition of particle rich in silicon was at Frisbee F in September and July. It is less likely that this is deposition of sand from the SSSI sand dunes. However, silicon-rich particles have also been found to result from coal combustion processes (Dodd *et al.*, 1991; Small *et al.*, 1981), which could be attributed to multiple industrial sources of emissions in the Teesside area.

The deposition of carbon particles was very low for Frisbees B, D and F but absent at Frisbees A, C and E. However, this is a limitation of the SEM-EDA, as carbon is beyond the limits of detection. Frisbee B, which was located adjacent to the coke stock yards, had the largest deposition of carbon particles.

Particles of other metals were only found at Frisbees D and F, and were titanium-rich particles. It is difficult to attribute this particle cluster to a specific source. The particles do not occur regularly, and they were found in Frisbees located off the Corus works, hence they could be a result of industrial activities in the Teesside area.

4.4.5 Dust flux samples

The dust flux at sticky pads A, B and C is primarily iron-rich particles for all directions, with only a few exceptions. These three sticky pad monitoring sites are located on the Corus works and could potentially be subjected to the largest fluxes of iron-rich particles as a result of on-site processes. The few exceptions to this are the northern fluxes to sticky pads B and C, which are both in the direction facing away from the Corus works, and the western flux to sticky pad C where the rate of iron-rich particle flux is still relatively high. The flux of iron-rich particles to sticky pad D is relatively high, in particular for the northern and western fluxes, which are in the direction of the Corus works. At sticky pads E and F the flux of iron-rich particles is present for most directions although much lower in comparison to the sticky pads on the Corus works. The iron-rich particle flux is only absent for the northern flux at sticky pad E, which is away from the Corus works. As for the deposition to the Frisbees, the flux of iron-rich particles is likely to be a result of on-site ferrous metallurgic processes.

For the dust flux to sticky pads A, B and C the second most common particle cluster was the particles rich in aluminium and silicon. The aluminium and silicon rich particle cluster was also the most common cluster for the south-western, southern and north-eastern fluxes at sticky pad D and all directions except the southern flux for sticky pad F. The flux of particles rich in aluminium and silicon was also relatively high for the northern and north-eastern flux at sticky pad E. Since this particle cluster is dominant for many different dust flux directions to most of the sticky pads it is likely that multiple sources contribute to this particle cluster.

The most dominant particle cluster for all directions of dust flux to sticky pad E was the calcium-rich particle cluster, in particular the western, northern and north-eastern fluxes. The flux of calcium-rich particles was also relatively high for the south-eastern and northern fluxes to sticky pad A; the northern, southern and western fluxes to sticky pad B; and the north-eastern and southern fluxes to sticky pad C. The flux of calcium-rich particles was relatively low for all directions of dust flux to sticky pad D and F, except the southern flux to sticky pad F. However, it is worth considering that the particles for the southern flux to sticky pad F are mainly calcium sulphates, while the particles at the other five sticky pads were calcium silicates. This difference in chemical composition is probably attributable to two different sources. However, the particle flux for the sticky pads on the Corus works, indicate there could be an on-site source and a marine source of calcium particles.

The dust flux of silicon-rich particles is the third most dominant flux for all directions of flux to sticky pad D; and at sticky pad F it is the second most common particle cluster for the western and south-western flux, and the third most common flux for the northern flux. For sticky pads A, B, C and E the cluster of silicon-rich particles is relatively low, as the fourth most dominant cluster at sticky pad A and B, and the fifth most dominant cluster at sticky pad C and E. As both of the peaks in this cluster occur at the sticky pads which were located off the Corus works it is likely that are multiple sources for this particle cluster, including the Corus works, marine, and from activities beyond the Corus works.

The dust flux of carbon particles was the least common particle cluster, it was absent from the sticky pads at C, D, and E, for most flux directions at sticky pad A and B, with the exceptions of the northern and western flux to sticky pad A and the south-western flux to sticky pad B. The highest number of carbon particles was found at sticky pad F for the northern, north-eastern, south-western and western fluxes. The flux of

carbon particles was low since carbon based particles are beyond the limit of detection for the SEM.

The particle cluster of other metal particles is difficult to define, because by nature the cluster represents metal rich particles which did not form a cluster, but clustered together, not by similarity but because of dissimilarity to the other particle clusters. The cluster included eight different metals of which titanium was the most common metal.

The particle cluster of particles rich in sodium and chlorine was absent at sticky pad A, B and F. The largest flux of sodium and chlorine rich particles was for the northern flux to sticky pad C. The particle cluster was also present, although in low percentages for the north-eastern, southern and western fluxes to sticky pad C; and the south-western, western, northern, north-eastern and southern flux to sticky pad E. It is highly likely that this particle cluster is from marine sources as for the dust deposition samples.

The particle cluster of sulphur-rich particles was at its highest for the southern flux to sticky pad C and the southern flux to sticky pad E. The flux of sulphur-rich particles to sticky pad E was present for all flux directions, and was the third most dominant particle cluster at sticky pad E. It was also present but in very low percentages at sticky pads A, B and C, and absent at sticky pads D and F. It is possible that this particle cluster could be a result of industrial or combustion processes, but due to the directions of dust flux found here it is difficult to assign it to a single source.

4.4.6 Overview of the chemical composition analysis

Many studies have employed the use of bulk chemistry and single particle analysis to examine the chemistry of deposited dusts, spatially and temporally. The present study has examined the chemical composition of dust flux alongside dust deposition. It enables comparison between deposited and flux of material spatially across a steel works and the surrounding areas. The number of samples measured was relatively high and provides important detailed small scale information. The study provides a detailed snapshot of the chemical composition for directional dust flux, for a minimum of five flux directions to six sites, and the corresponding dust deposition for the same six sites.

The aim of the present study had been to determine the chemical characteristics across many sites, at times of 'normal' (rather than the extremities) deposition. Although over 2000 samples were analysed, on average each sample contained 45 single particle

spectra, compared to 1000 particles per sample (Choel *et al.*, 2007; Katrinak *et al.*, 1995). Katrinak *et al.* (1995) were even cautious with the interpretation of their results due to the small sample size, which exceeded 1000 particles per sample. Other work using SED-EDA have examined approximately 500 particles per sample (Xhoffer *et al.*, 1991), and 300 to 500 particles per sample (DeBock *et al.*, 1994; Osan *et al.*, 2002; Van Malderen *et al.*, 1996b; Xie *et al.*, 2005) which vastly exceed the average number of particles examined per sample in the present study. Therefore the results presented here must be interpreted cautiously. However, the present study does provide valuable information on the chemical composition of dust flux and deposition to monitoring sites on and surrounding the Corus works despite the limitations of time and resources.

The six reference samples were collected from three potential locations of fugitive dust generation on the Corus works; the sinter bed, coke stock yards and ponding station. At each site a small sample of material was taken from the stock pile and from a track side pile of dust. This guaranteed that the material analysed was directly from the potential source of material. However, wind-blown material from other sources of fugitive dust emissions could have also been in these samples. Despite this, the samples confirmed that similar clusters of particles existed in the reference samples to the deposition and flux samples.

The dust deposition and flux samples were collected from the six Frisbee and sticky pad monitoring sites on and surrounding the Corus works. The nature of the sample collection is that they can potentially collect material from all sources; they do not selectively collect information for only one wind direction. Hence the samples examined here have the potential to contain material from multiple sources, and examining 50 particles may not be sufficient to fully examine the total deposition to a single point or direction. However, the samples do provide very detailed directional information on the diversity of material which can be deposited over a wide area surrounding the Corus works.

Hierarchical cluster analysis is a method of data exploration, which clusters similar data together in this case by chemical composition. This is extremely beneficial when considering the volume of data for analysis. However, there was some discrepancy in the clustering of some particles where particles of very similar composition were clustered into different particle clusters. Despite this, the hierarchical clustering method is an extremely useful tool for data exploration.

4.4.7 Developing particle chemical composition analysis

To develop the present study, primarily it would be beneficial to increase the number of particles analysed per sample. Although previous work has examined between 300 to over 1000 particles per sample, this would be very time consuming manually. It would be beneficial to approach the analysis with a computer controlled SEM, which can be conducted in far less time compared to manual controlled analysis. Studies adopting the computer controlled analysis have been capable of examining over 500 particles per sample (Xie *et al.*, 2005) and 1000 particles per sample (Osan *et al.*, 2002). When a larger number of particles have been analysed for each sample the results can be interpreted with greater confidence, especially when examination is facilitated by computer controlled facilities. The confidence in result interpretation could be improved by analysing the filters and sticky pads on multiple areas and to examining all four weeks of dust flux within the month exposure period for deposition.

It was not possible within the constraints of the present study to examine the morphology of the particles. However, the morphology of the particles can make it easier to identify the source and the generation process for the fugitive dust emissions. The particles resulting from combustion or high temperature industrial processes, tend to be spherical in shape, whereas though naturally occurring within the crust are more angular. In particular this information could be used to determine the source of the silicon-rich and calcium-rich particles for different Frisbee monitoring sites.

It would be extremely beneficial to consider the chemical composition of the dust deposited onto the SSSI vegetation. This would enable a better understanding of the effects of the deposition on plant health. However, this was not possible within the time frame of the present study.

4.4.8 The importance of chemical composition analysis of single particles for dust deposition and flux studies

By determining the nature of the dust particles collected on the Corus works, it is possible to gauge a better understanding of the potential effects of the dust to plant health. The work presented here has developed a better understanding of the wide range of particles which could potentially be deposited onto the SSSI. The analysis of particulate matter using SEM-EDA is an important widely used tool, to determine the chemical nature of deposited dusts. The work would benefit from a more detailed examination of the

particles, in particular increasing the number of particles examined within samples. However, perhaps the most important development would be to examine the chemical composition of dust found on the flora of the SSSI. Despite this and other limitations of the study, the combination of dust deposition and multiple directional dust flux to six sites is extremely beneficial.

The method of hierarchical clustering has proven capable of classifying all of the particles which were components of the dust deposition and flux. Of the eight particle clusters identified, the potential origin or origins of these particles have been highlighted here. However, further investigation, beyond the scope of the present study, would be required to confidently determine the sources of the particle clusters.

4.5 Summary of Chapter 4 – Dust characterisation

The key outcomes of the chemical characterisation of the dust deposited to the Frisbee monitoring sites on and surrounding the Corus works were identified as the following:

A total of eight distinct clusters of particles were identified in the reference, dust deposition and flux samples. The eight particle clusters were: iron-rich particles, silicon-rich particles, calcium-rich particles, particle rich in aluminium and silicon, carbon particles, other metal particles, sulphur-rich particles and particles rich in sodium and chlorine.

The particle clusters were the same for all of the reference, deposition and flux samples, despite the samples being taken at different locations and from different exposure periods.

The most dominant particle cluster, for the dust deposition and flux to Frisbees A, B and C, on the Corus works was the iron-rich particle cluster. The most dominant particle clusters for the dust deposition and flux to Frisbee D were the particles rich in aluminium and silicon and the iron-rich particles, which contributed equally to dust deposition and flux. The most dominant particle cluster for the dust flux to Frisbee E was the calcium-rich particle, which was absent from the dust deposition. The most dominant particle in the dust deposition to Frisbee E was the particle cluster rich in aluminium and silicon. The most dominant particle cluster for the dust deposition at Frisbee F was the cluster of particles rich in aluminium and silicon.

Classifying the clusters as a single particle type may mask multiple emission sources, which produce emissions of a similar chemical composition. It is likely that the iron-rich particles are a result of processes on the Corus works. However, it is difficult to determine the exact source or sources for the other particle clusters because it has been shown that they could result from a number of processes occurring on the Corus site, from other industrial areas in Teesside or marine processes.

Chapter 5 – Review and development of a particulate emissions model

5.1 Introduction

To comply with the EU Integrated Pollution Prevention and Control (IPPC) Council Directive (96/61/EC), all installations regulated by the UK Environment Agency are required to submit an application for a permit to operate. The Corus steel works, Teesside submitted its application in August 2001. The IPPC application detailed all of the on-site activities and potential sources of pollution. By 2004 the Environment Agency had reviewed the application and produced a set of improvement conditions. These conditions are aimed at preventing pollution and where not practicable reduce pollution to acceptable levels (DEFRA, 2005). The present study was initiated by one of these improvement conditions (number 1.4.27) which stated the following;

"With regard to particulate emissions from the installation, the operator shall carry out an assessment of the effect of this emission on South Gare and Coatham Sands."

With regard to the particulate emissions, dispersion modelling was the principle method used by Corus to estimate the average daily environmental concentration of particulate matter of 10 micrometers or less (PM_{10}) (see Chapter 2 section 2.1). The primary concern of the modelling had been the potential risk to human health, in particular the residential areas of Grangetown and Redcar.

Atmospheric Dispersion Modelling System (ADMS) is an advanced Gaussian model developed by Cambridge Environmental Research Consultants (CERC) as a UK regulatory model for particle and gas dispersion studies (Carruthers *et al.*, 1994). ADMS has performed well in validation studies which have used a range of scenarios common in modelling studies using data sets from across the world (Carruthers *et al.*, 2000; Hanna *et al.*, 2001; Holmes & Morawska, 2006; Riddle *et al.*, 2004; Timmis *et al.*, 2000).

For the present study, the purpose of the modelling was to firstly develop dust emission scenarios which incorporated contemporary meteorological data. Secondly the modelling aimed to produce, expected rates of dust deposition, over the dust deposition monitoring programme which used the Frisbee dust gauges, and hence compare the real-time dust deposition data with the modelled environmental concentrations of PM_{10}.

The present chapter examines, in further detail, the initial modelling results submitted by Corus for the IPPC permit. The chapter discusses a series of scenarios developed in the current study, designed to assess the expected environmental concentration of PM_{10} on the SSSI. Finally the value of modelling will be assessed, with respect to its ability to accurately determining fugitive dust deposition.

5.2 IPPC model scenario

The most recent modelling of dust deposition to South Gare and Coatham Sands SSSI (subsequently referred to as the SSSI) was conducted by Corus and submitted for the IPPC permit application in August 2001. The estimated environmental concentration of PM_{10} was modelled using the ADMS version 3.3 (CERC, Cambridge, UK).

The primary concern of the initial modelling work was the potential health effects from particulate matter emissions on the Corus works to the surrounding residential areas including Grangetown and Redcar. The initial modelled scenarios were the 90^{th} percentile of the average daily environmental concentration and the average annual environmental concentration. Both of these parameters were related to the national air quality standards set as a Directive by the European Commission. The air quality standards set for the first stage starting in 2005 were; a maximum annual average concentration of 40 $\mu g\, m^{-3}$ PM_{10}; and a maximum daily average concentration of 50 $\mu g\, m^{-3}$ PM_{10}, which was not to be exceeded more than 35 times a year (or the 90^{th} percentile). Of the two modelled parameters, the daily average concentration was highlighted in the IPPC permit, because it was the closest to the air quality standard for human health (see Figure 5.1).

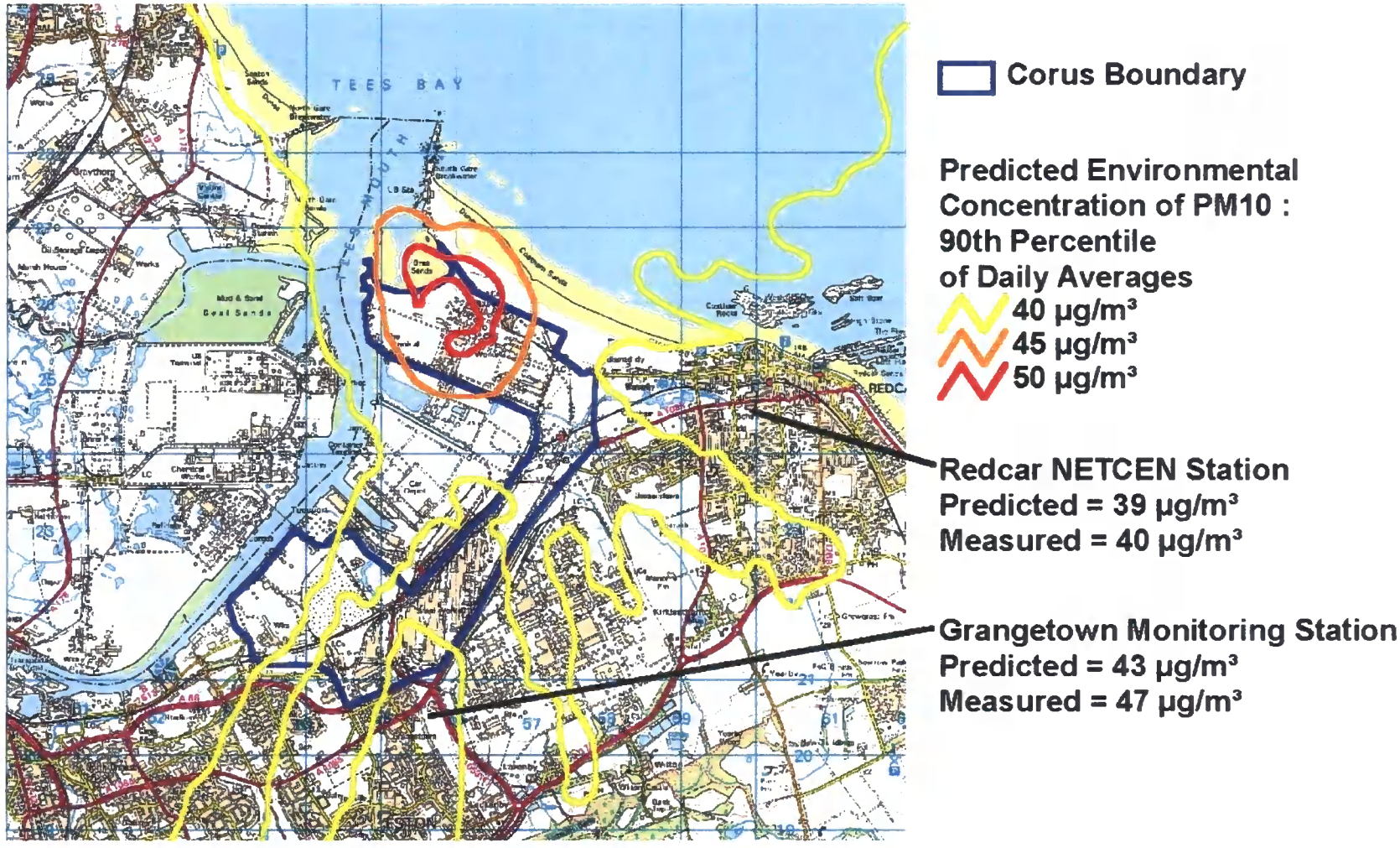

Figure 5.1 Predicted environmental concentration of PM_{10} as 90th percentiles of daily averages - Corus works & background (submitted as part of the IPPC permit application, Corus, 2001). The red line shows 50 µg/m^3, orange line shows 45 µg/m^3, yellow line shows 40 µg/m^3 and blue line shows the Corus works boundary.

Dispersion models typically use five years of meteorological data for parameterisation. The closest meteorological station to the Corus works had been located at Coulby Newham (450730, 514680 British National Grid), it was erected in September 1996, but the station was vandalised in June 1998 and not replaced. The meteorological station at Coulby Newham was only 7.5 km from the Corus works, and recorded meteorological conditions that were generally representative of those at the Corus works. Discussions between Corus, the Environment Agency and English Nature (now Natural England) resolved that the model would use historic wind speed and direction data from the Coulby Newham Meteorological station measured in 1997 and 1998. Additional meteorological data required for model parameterisation were obtained from the Boulmer Meteorological station (87 km northwest of the Corus works). Although it is preferable to parameterise dispersion models with at least 5 years of meteorological data, the 2 years of historic localised meteorological data were sufficient to consider the model outputs robust, when considering the average daily environmental concentration of PM_{10}.

The PM_{10} emissions from the stacks, and the BOS Plant roof, cast house roof of the blast furnace and the filter plant roof vents were quantified and incorporated into the model as point sources of emissions. The fugitive PM_{10} emissions from the stock yards and other activities had been estimated to be 480 tonnes per annum in a previous study by Schofield *et al.* (2001) based on the Corus works, Teesside. Sensitivity testing revealed that fugitive PM_{10} emissions modelled from either a point or area source on the Corus works had no effect on the average daily concentration of PM_{10} at the residential areas of Redcar and Grangetown. In this instance the fugitive PM_{10} emissions were modelled as a point source of emissions.

The model output in Figure 5.1 informed the present study, in particular the locations of the Frisbee gauges which were used to measure dust deposition (see Chapter 3). An aim identified by the Environment Agency and Natural England for the present study was to further develop the modelling, specifically to investigate a relationship between the modelled PM_{10} emissions with the real-time dust deposition experienced close to the Corus works. The present study aimed to identify the limitations of the parameters used in the IPPC model scenario, and to develop or improve these parameters, with a view to modelling accurate predictions of the environmental PM_{10} concentration on the SSSI. Several key parameters were identified for development included the meteorological data, the fugitive emissions from stock yards and other on-site activities including ponding.

5.3 Model selection

The Atmospheric Dispersion Modelling System (ADMS) version 3.3 (Cambridge Environmental Research Consultants (CERC), Cambridge, UK) was used to model the emissions scenario for the IPPC permit application. ADMS is an advanced Gaussian model (FORTRAN) capable of modelling the impact of existing or proposed industrial installations. The model calculates pollutant concentrations emitted continuously from point, line, volume and area sources, or discretely from point sources. The model contains many algorithms to account for effects on emission sources and dispersion, amongst which the most important for this setting include building effects, complex terrain, wet deposition, gravitational settling and dry deposition and the coastal effects of the land-sea internal boundary layer. Hence the model is ideally suited to predicting the pollutant emissions, or more specifically emissions of particulate matter from the Corus works to the surrounding areas, especially the adjacent SSSI.

As one of the most effective dispersion models available, ADMS had already been used to model emissions on the Corus works. To develop the model outcomes and produce comparable expected environmental concentrations ADMS was used in the present study.

5.4 Model parameters

5.4.1 Meteorological data

The previous model had used historic meteorological data from the stations at Coulby Newham and Boulmer. The local meteorological data collected at the Coulby Newham station from 1996 to 1998 were representative of the conditions at the Corus works. However, contemporary meteorological data from the Loftus station provided representative and contemporary conditions at the Corus works for the current model. The meteorological station at Loftus is 10.5 km southeast of the Corus works, and the closest meteorological station to the Corus works with a coastal location.

The contemporary meteorological data were supplied by the British Atmospheric Data Centre (BADC, Chilton, UK) for the Loftus meteorological station from March to December 2006. Data collected at the Loftus meteorological station on wind speed, wind

direction, relative humidity, air temperature, precipitation, cloud cover were obtained to parameterise the model.

5.4.2 Ponding station data

For each ponding event the duration, and rate or total PM_{10} emission is unknown. Therefore modelling an average PM_{10} emission from a ponding event is problematic. It was not possible to incorporate ponding into the modelled scenario. Although attempts have been made to quantify the dust generation from ponding its nature and dependence on short term meteorological conditions have made it very difficult. See Chapter 3 section 2.3.12 for a more detailed description of the ponding activity.

5.4.3 Data analysis and presentation

The scenarios were modelled in ADMS, and the model outputs were viewed and presented in ArcGIS v. 9 (Environmental Systems Research Institute (ESRI), Redlands, California, USA). The base maps were obtained from EDINA (Edinburgh University, UK). The statistical analysis was conducted using SPSS (SPSS Inc. Chicago, Illinois, USA). Data were found to be normally distributed but were tested using the Spearman rank correlation due to the small number of observations. The data are displayed using Sigma Plot v.10 (Systat Software Inc. (SSI) San Jose, California, USA).

5.5 Model scenarios

The following three modelled scenarios were parameterised with contemporary meteorological data from the Loftus meteorological station. The ten months of data, March to December 2006, used to parameterise the model, corresponded to the programme of the passive dust deposition monitoring. Although ideally five years of meteorological data is preferred for dispersion modelling, the period of ten months was sufficient to represent typical deposition conditions at the Corus works with a view to calculating the average annual deposition of PM_{10}.

5.5.1 Contemporary meteorological data model scenario

The first model scenario incorporated PM_{10} emissions from the stacks, BOS Plant roof, blast furnace cast house roof and the filter plant roof vents as point sources of emissions. Fugitive dust emissions from stockyards were not included in this scenario.

The environmental concentration of PM_{10} exceeded the average annual air quality standard in the area around the sinter plant and the blast furnace reaching 50 $\mu g\ m^3$ PM_{10}. The area of the SSSI with the highest environmental concentration of PM_{10} was the area adjacent to the blast furnace where the environmental concentration of PM_{10} was between 50 and 25 $\mu g\ m^3$ PM_{10}. The average concentration of PM_{10} on the SSSI was relatively low between 5 and 2.5 $\mu g\ m^3$ PM_{10} (see Figure 5.2). The model scenario predicted that the PM_{10} emissions from the Corus works were not at significant levels for the residential areas of Redcar.

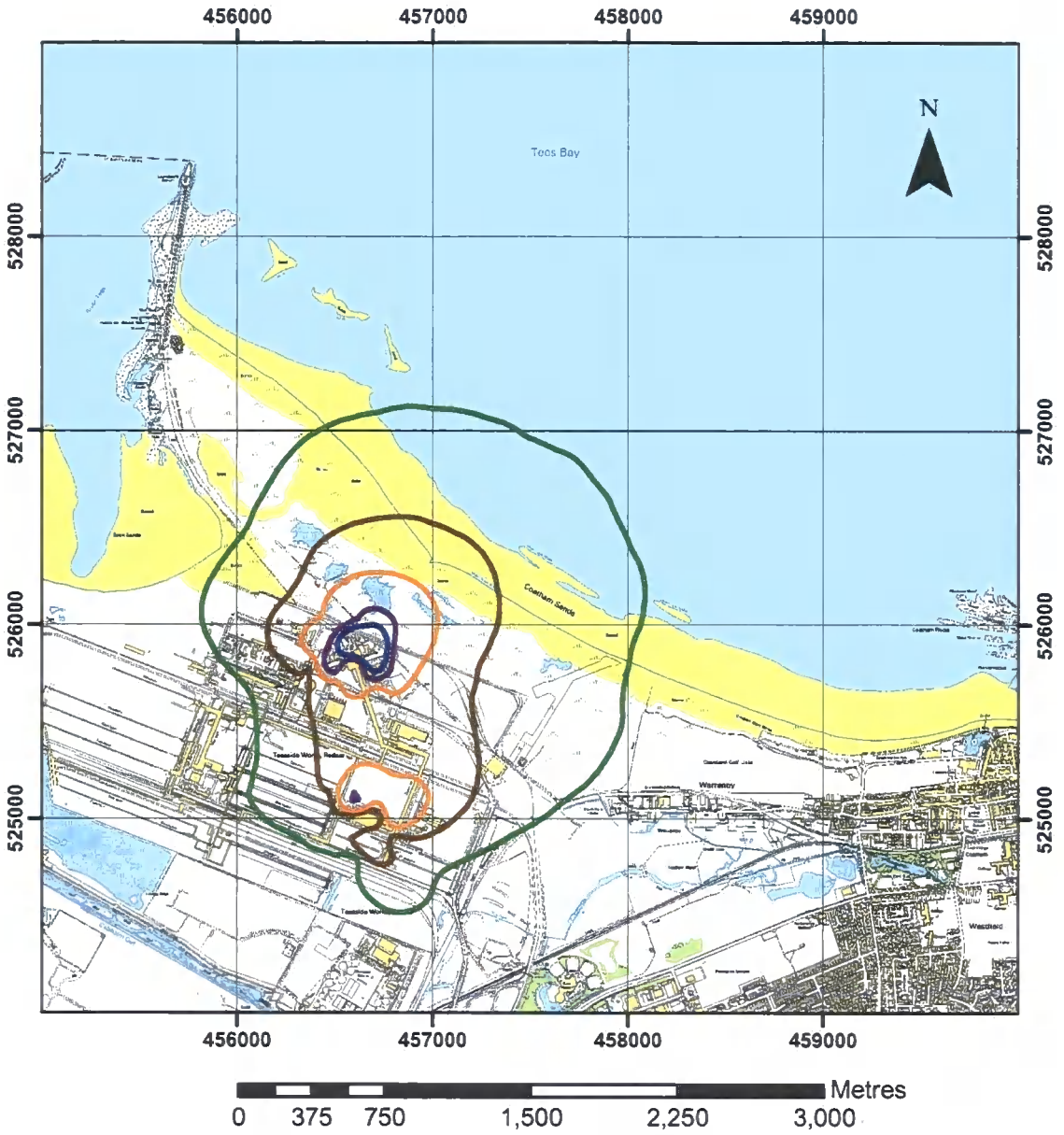

Figure 5.2 Predicted environmental concentration of PM_{10} as annual averages - Original model scenario with contemporary meteorological data. The isolines represent the environmental concentration of PM_{10} as annual averages where green line indicates 2.5 µg m^3 PM_{10}, the brown line indicates 5 µg m^3 PM_{10}, the orange line indicates 10 µg m^3 PM_{10}, the purple line indicates 25 µg m^3 PM_{10} and the blue line indicates 50 µg m^3 PM_{10}.

5.5.2 Contemporary meteorological data and stockyard emissions model scenario

In this second model scenario the PM_{10} emissions from the stacks, BOS Plant roof, blast furnace cast house roof and the filter plant roof vents were incorporated into the model as point sources of emissions, as in the first scenario. The fugitive PM_{10} emissions from stock yards were modelled from a point source (455400, 525500 British National Grid) representing the total PM_{10} emissions from the stockyards and other activities across the Corus works (estimated at 480 tonnes per annum (Schofield *et al.*, 2001) (Table 5.1)).

Table 5.1 Particulate Matter emissions from the fugitive dust source areas for the model scenario using contemporary meteorological data and stock yard emission data (see Figure 5.3 for the source area locations) (Schofield *et al.*, 2001).

Source	PM_{10} Emission	
	(tonnes/year)	% of total
Raw coal stocks	106	22
Sinter plant and pellet stocks	63	13
Coke and raw ore stocks	47	10
Blended ore stocks	40	8
Blended coal stocks	3	1
Coke ovens and blast furnace	52	11
Bunkers and coal crushing	38	8
Wharf	33	7
Stock house	29	6
Dunes	43	9
Bran sands (beach)	26	5
Total	480	100

In the second scenario the highest average annual environmental concentration of PM_{10} was found in the areas surrounding the blast furnace and the stockyards to the west of the Corus works. The previous scenario had found a peak in PM_{10} emissions at the Sinter plant, which was notably absent in this second scenario. Overall the concentration of PM_{10} on the SSSI was predicted to average 5 $\mu g\, m^3$ PM_{10} (see Figure 5.3) with a considerable area expected to receive 10 $\mu g\, m^3$ PM_{10}. The second model scenario also predicted that the PM_{10} emissions from the Corus works did not reach the closest residential areas, in Redcar, at levels greater than 2.5 $\mu g\, m^3$.

Legend: Predicted environmental concentration of PM_{10}: Annual average (µg m^3)

2.5 5 10 25 50

Co-ordinate System: British National Grid. Projection: Transverse Mercator.
Datum: OSGB 1936.

Figure 5.3 Predicted environmental concentration of PM_{10} as annual averages - Original model with contemporary meteorological data and stockyard (fugitive) emissions. The isolines represent the environmental concentration of PM_{10} as annual averages where green line indicates 2.5 µg m^3 PM_{10}, the brown line indicates 5 µg m^3 PM_{10}, the orange line indicates 10 µg m^3 PM_{10}, the purple line indicates 25 µg m^3 PM_{10} and the blue line indicates 50 µg m^3 PM_{10}.

5.5.3 Contemporary meteorological data and multiple fugitive emission sources model scenario

The PM_{10} emissions from the stacks, BOS Plant roof, blast furnace cast house roof and the filter plant roof vents were incorporated into the third model scenario as point sources of emissions as in the previous scenarios. Schofield *et al.* (2001) had estimated values for the total fugitive emissions from specific areas and activities across the Corus works (see Table 5.1). These values were modelled in the previous scenarios as a single point source of emissions (480 tonnes per annum). In this third model scenario the fugitive PM_{10} emissions from the Corus works were modelled as five area sources (see Figure 5.4). Each area represented the total PM_{10} emissions from specific stockyards and or other activities across the Corus works (see Table 5.2).

Table 5.2 Particulate Matter emissions from five source areas for the third model scenario using contemporary meteorological data and stock yard emission data (see Figure 5.4 for area locations) (Schofield *et al.*, 2001).

Source	PM_{10} emissions (tonnes/year)	Area (m^2)	Annual emission rate PM_{10} ($\mu g\ m^3$)
A - Coal stocks	106	734366	4.6
B - Coke & raw ore stock yards	50	607078	2.6
C - Blended ore stocks & Sinter plant	103	545606	6.0
D - Blast furnace & Coke ovens	81	657228	3.9
E - Beach	n/a	4810033	3.0

Source A is the total fugitive PM_{10} emissions from the raw coal stock yards. Source B is the total fugitive PM_{10} emissions from the coke and raw ore stock yards and the blended coal stock yards. Source C is the summed fugitive PM_{10} emissions from the Blended ore stocks, the Sinter plant and the pellet stocks. Source D is the summed fugitive PM_{10} emissions from the coke ovens, blast furnace and the stock house. The fugitive PM_{10} emission rate from Source E was an estimated value for sea spray, sand and other emissions from sources other than the Corus works, such as shipping or long range transport from Europe.

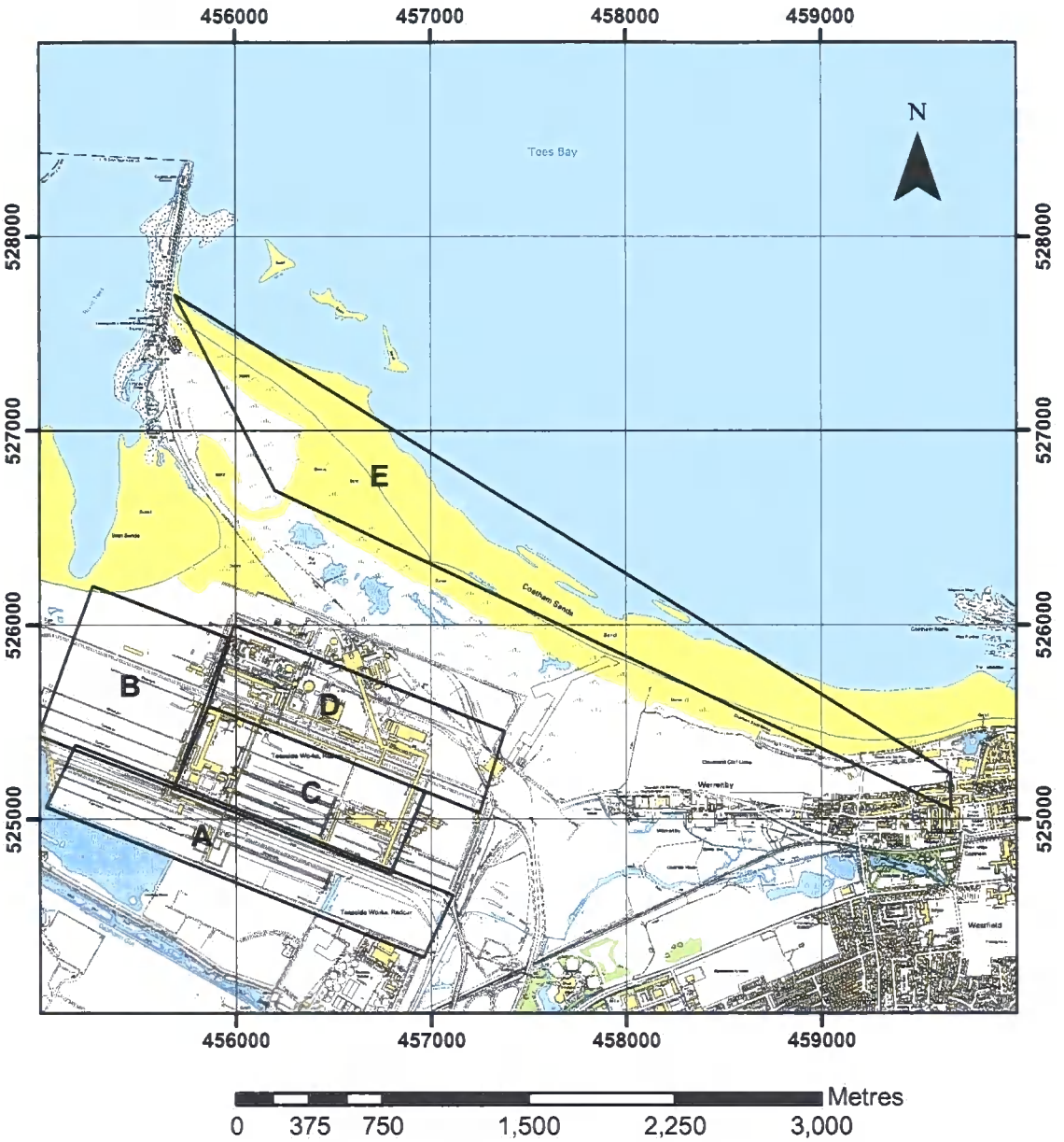

Co-ordinate System: British National Grid. Projection: Transverse Mercator.
Datum: OSGB 1936.

Figure 5.4 Source areas of fugitive dust emissions for modelling multiple stockyard (fugitive) emissions. Areas A-E represent sources of fugitive dust emissions where; A = Coal stock yards; B = Coke and raw ore stock yards; C = Blended ore stocks and Sinter plant; D = Blast furnace and Coke ovens and E = Beach.

In the third model scenario the highest average annual environmental concentration of PM_{10} was found in the areas of the blast furnace, sinter plant and blended ore stockyards at 50 $\mu g\, m^3$ PM_{10} (see Figure 5.5). The average concentration of PM_{10} across the Corus works was higher than in previous scenarios at 25 $\mu g\, m^3$ PM_{10}. The average concentration of PM_{10} on the SSSI was 25 $\mu g\, m^3$ PM_{10}, which was higher than in both of the previous scenarios. The PM_{10} emissions from the Corus works extended to the residential areas of Redcar, and into the North Sea, which in previous scenarios had been relatively unaffected by activities on the Corus works.

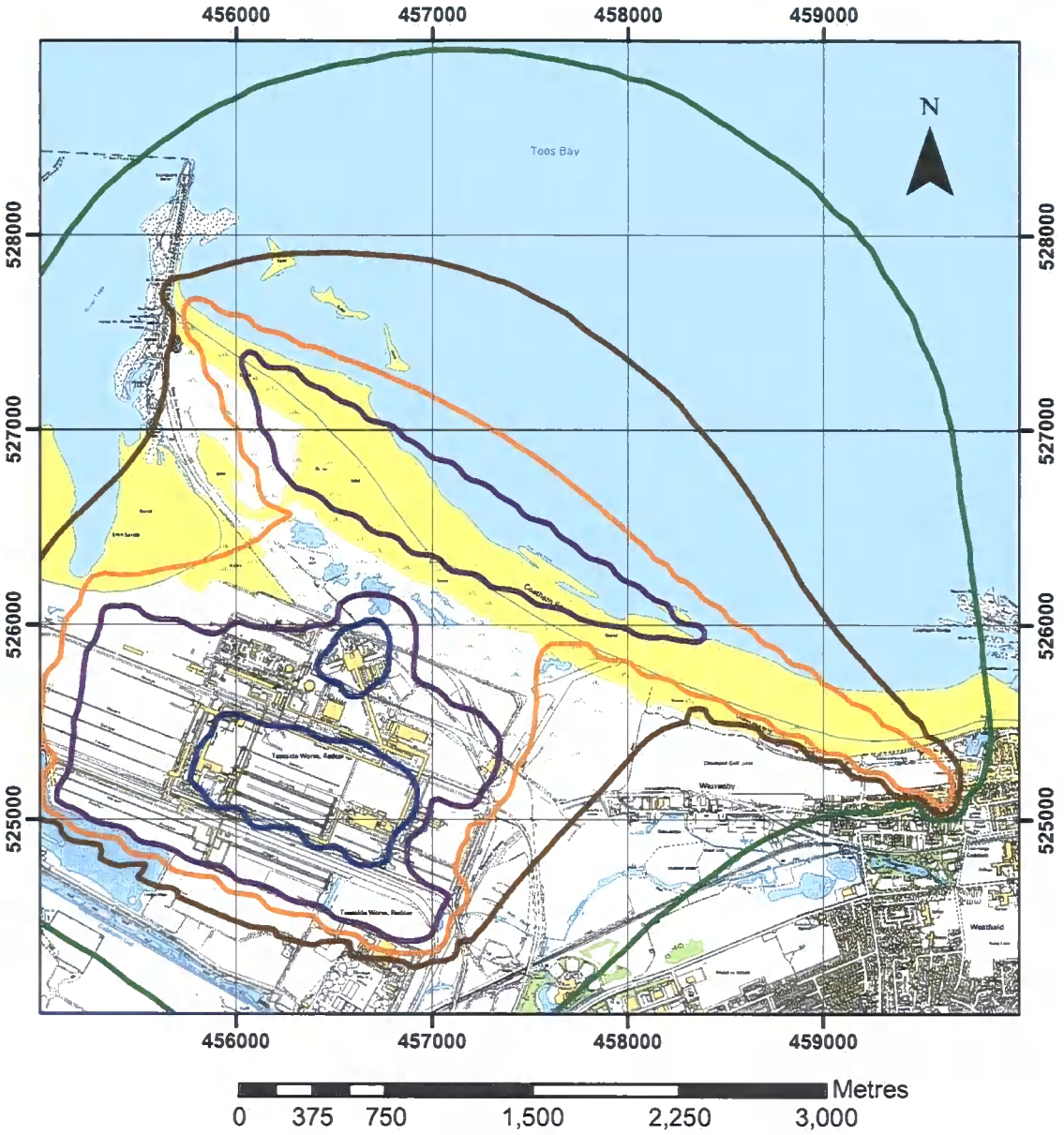

Legend: Predicted environmental concentration of PM_{10}: Annual average (µg m^3)

2.5 5 10 25 50

Co-ordinate System: British National Grid. Projection: Transverse Mercator.
Datum: OSGB 1936.

Figure 5.5 Predicted environmental concentration of PM_{10} as annual averages - New Model with contemporary meteorological data and multiple stockyard (fugitive) emission sources. The isolines represent the environmental concentration of PM_{10} as annual averages where green line indicates 2.5 µg m^3 PM_{10}, the brown line indicates 5 µg m^3 PM_{10}, the orange line indicates 10 µg m^3 PM_{10}, the purple line indicates 25 µg m^3 PM_{10} and the blue line indicates 50 µg m^3 PM_{10}.

5.5.4 Comparing measured and modelled dust deposition

As part of the third model scenario, an expected monthly output was calculated for April to December 2006 for six locations. The monthly periods and locations corresponded to the exposure periods of the Frisbee gauges exposed as part of the passive dust deposition monitoring programme. Therefore enabling a comparison between the measured dusts deposited to the Frisbees and the expected environmental concentration of PM_{10} produced by the model.

The dust deposited to the Frisbee gauges and the modelled expectations of PM_{10} concentrations broadly followed the same trends with higher concentrations at Frisbees A, B and C (see Figure 5.6 a, b & c) and lower concentrations at Frisbees D, E and F (see Figure 5.6 d, e & f).

The measured dust depositions and the modelled PM_{10} concentrations at Frisbees A, B, D and E were not correlated over the 10 month exposure period. The trends in the model's predictions of PM_{10} concentration did not follow the measured dust deposition trends, the months which experience the highest rates of deposition did not correlate with the model's expected months of highest PM_{10} concentration. The measured dust deposition and modelled PM_{10} concentration for Frisbee C were strongly positively correlated ($n = 9$, $r_s = 0.75$, $p = 0.02$) (see Appendix B Figure 1.a). The measured dust deposition and modelled PM_{10} concentration for Frisbee F were also strongly positively correlated ($n = 8$, $r_s = 0.71$, $p = 0.05$) (see Appendix B Figure 1.b). Although the measured dust deposition and the modelled PM_{10} concentrations at Frisbees C and F were positively correlated, there was variability in the data. The correlations may not be indicative of a relationship between the measured and modelled data for the Frisbees.

For each of the Frisbees the modelled concentrations of PM_{10} were calculated from a contribution from each of the five area sources in Figure 5.4. These data have not been presented in the current project because the weak correlations between the measured and modelled values indicate variability in the data. By breaking down these values further to their five contributing sources, the reliability of the data is considerably reduced.

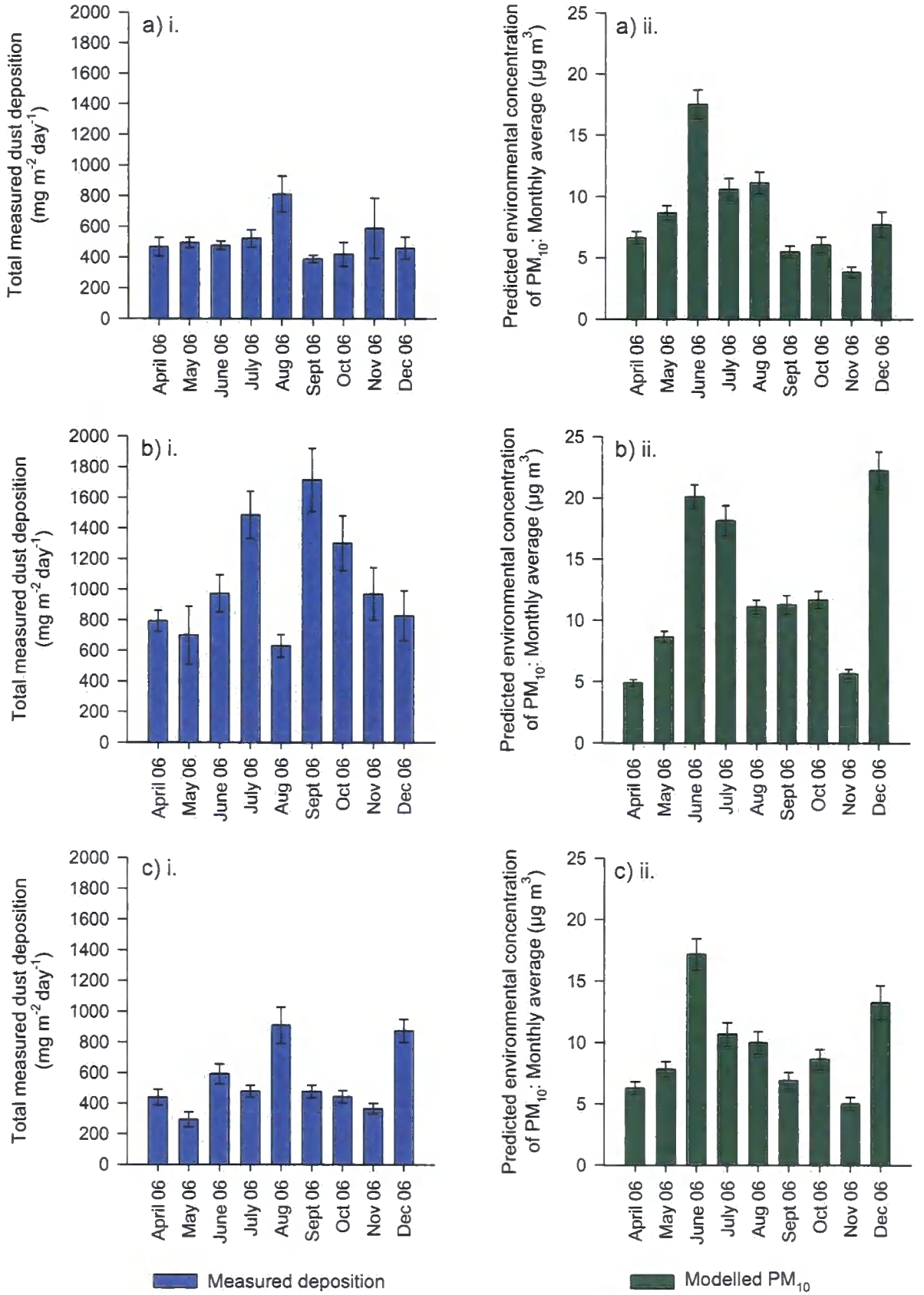

Figure 5.6 Graphs a, b & c i. (Blue) show the total measured dust deposition (mg m^{-2} day^{-1}) at Frisbees A, B & C respectively. Graphs a, b & c ii. (Green) show the predicted environmental concentration of PM_{10}: Monthly average (µg m^3) at Frisbees A, B & C respectively. Error bars show ± 1 SE, n = 5.

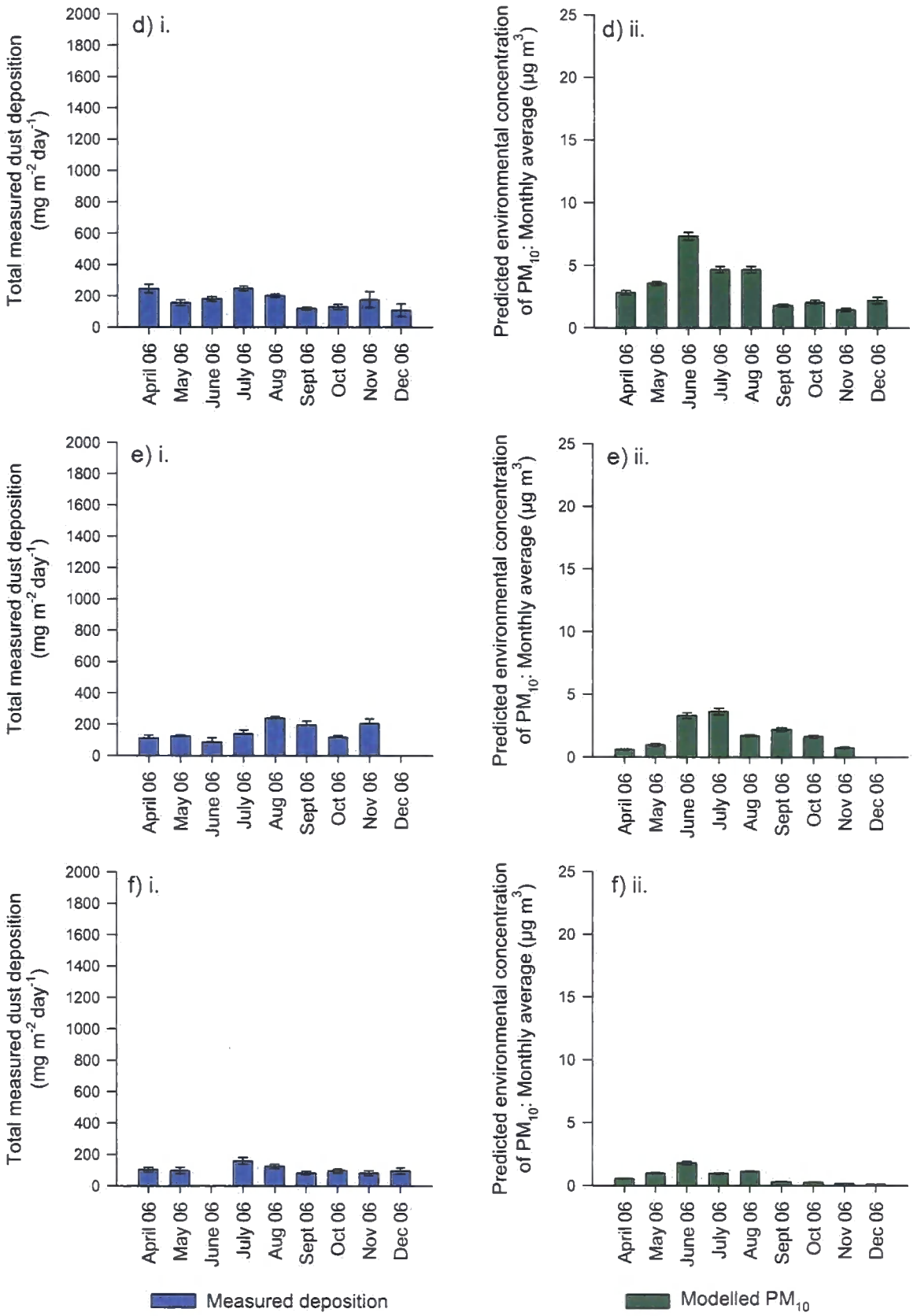

Figure 5.6 Graphs d, e & f i. (Blue) show the total measured dust deposition (mg m^{-2} day^{-1}) at Frisbees D, E & F respectively. Graphs d, e & f ii. (Green) show the predicted environmental concentration of PM_{10}: Monthly average (µg m^3) at Frisbees D, E & F respectively. Error bars show ± 1 SE, n = 5.

5.6 Discussion

5.6.1 Evaluating the model scenarios

The modelling work conducted for the IPPC permit led to the imposition of the improvement condition which initiated the present study. In turn the model outcome informed the locations of the Frisbee gauges in the passive dust monitoring programme. The model scenario had certain drawbacks, including the unrepresentative sources of PM_{10} emissions, and the historic meteorological data. The modelling was conducted with the primary concern set as the potential health effects on the residential areas of Redcar and Grangetown, it was decided the model could be developed to consider the potential effects of deposition to the SSSI. The model was run under different scenarios of PM_{10} emissions, and parameterised with contemporary meteorological data.

The first model scenario predicted environmental concentration of PM_{10} across the Corus works from the stack and roof emissions only. The main limitation of the first scenario was that it did not account for the fugitive dust emissions from stock yards or on-site activities. Fugitive dust emissions are one of the main contributors to potential deposition to the SSSI. The PM_{10} emissions from the sinter plant and blast furnace were predicted to exceed the air quality standard for the annual average concentration of PM_{10} over a small area which included the Corus works and the adjacent SSSI.

The second model scenario provided an unrealistic representation of the fugitive emissions from the stockyards. The value calculated as the total fugitive emissions for the Corus works (Schofield *et al.*, 2001) was modelled as a single point source of fugitive emissions. It exaggerated the fugitive emissions from the stockyards and unloading areas to the west of the Corus works. On the SSSI, the estimated PM_{10} concentration was higher than in the first scenario, but due to an unrealistic dust emissions scenario, it was unlikely that the PM_{10} deposition to the SSSI was representative. The air quality standard for the annual average concentration of PM_{10} was exceeded over two small areas which included the stockyards, blast furnace and the adjacent SSSI.

The third scenario provided a realistic representation of the stack, cast house roof and fugitive emissions of PM_{10}. The model predicted that two areas of the Corus works exceeded the average annual air quality standard for PM_{10} concentration; the blast furnace, and the sinter plant and blended ore stockyards. A small area of the SSSI adjacent to the blast furnace was also expect to exceed the annual average air quality standard for PM_{10} concentration, as in the previous two scenarios. The remaining area of

the Corus works was predicted to receive 25 $\mu g\, m^3$ PM_{10} as an average annual concentration of PM_{10}.

There was no measured emissions value for the Beach (Coatham Sands and South Gare SSSI), so 3.0 $\mu g\, m^2\, s^{-1}$ PM_{10} was estimated as the annual rate of PM_{10} emissions. It was designed to represent sea spray, sand particles, long distance transport of PM_{10} from Europe, shipping, and sources of PM_{10} other than Corus. However, in the third model output the dust generated from the Beach source masks any potential PM_{10} emissions generated on the Corus works and deposited onto the SSSI. It would be beneficial to run the third scenario without the beach source, because it does not represent Corus generated PM_{10}.

The predicted isolines for 25 $\mu g\, m^3$ PM_{10} on the Corus works, and 10 $\mu g\, m^3$ PM_{10} on the SSSI, directly traces the outline of the source areas. Although the majority of PM_{10} fugitive emissions are deposited close to their site of generation, viewing the concentration of PM_{10} at greater resolution, such as 60, 50, 40, 30, 20, 10, 5 and 2.5 $\mu g\, m^3$ PM_{10} may have been beneficial, yet it is possible that this is owed to the limitations of the model.

There are potential errors associated with the source areas and the rate of PM_{10} emissions. The stockyards and activities on the Corus works, areas A to F, were not calibrated with on-site GPS locations. The stockyards are subject to additions, blending (hence relocation) and removal of stocks on a daily basis, hence the volume and location of material is highly variable. However, all model scenarios contain a certain degree of error, from the accuracy in measuring the rate of PM_{10} emissions or the source size and location. The first and second model scenarios contained the least error, due to fewer sources of emissions. The cumulative error of model outputs increase when many smaller individual parameters are incorporated into the model. Therefore even though the third scenario was more representative of the sources of fugitive emissions on the Corus works than the first and second scenarios, the confidence in the model output is limited

5.6.2 Comparing modelled and measured deposition

It was not possible to directly compare the measured rates of dust deposition at the Frisbees gauges directly with the modelled expectations of the environmental concentration of PM_{10}. The model output is expressed as an annual average of PM_{10} whereas the dust deposited to the Frisbees includes all fractions of particulate matter. The processes that lead to the generation, lift-off and deposition of the PM_{10} fraction

compared with all other fractions of particulate matter are not the same and are subject to variability. In order to compare the model and deposited values in real-time, either the model must incorporate all dust fractions or the dust deposition could be measured in real-time using a continuous monitor. The present study was limited by many site factors including security, access, power, and resources, hence continuous monitoring was not feasible.

5.6.3 Issues related to data parameterisation

The meteorological data used to parameterise the model were not ideal. They contained small gaps and data resolution was poor. In particular the wind direction was given with only 10 degree resolution. There were also errors associated with the sources and their rate of PM_{10} emission. Accurate measurement of the fugitive emissions of PM_{10} from a specific activity or stockyard is both difficult and open to error. The values used for the emission rates in the model have not been validated, and their degree of accuracy is unknown. Hence there is considerable uncertainty in the model output. Nevertheless, the meteorological data and emission scenarios for the three model scenarios presented here were a better representation of the conditions on the Corus works than those used in the IPPC model, which had used unrepresentative meteorological data and PM_{10} emission scenarios. Therefore, the model outputs presented here can be interpreted with confidence.

5.6.4 Model development

Whilst outside of the scope of the present study, further development of the model scenarios would clearly be beneficial. Firstly, the third scenario run, without the Beach area source, would allow an assessment of the PM_{10} emissions from the Corus works to the concentration of PM_{10} deposited on the SSSI. The model could be further developed with the accurate measuring of other sources of fugitive emissions on and off the Corus works, and incorporation of these emissions into the model scenarios.

Ponding was incorporated into the current model and was found to have no effect on the average annual environmental concentration of PM_{10} (Haines, pers. comm.) because of its sporadic nature. It would be valuable to measure an accurate rate of PM_{10} emissions for a ponding event, incorporate it as a discrete emission, and evaluate the model output as an average daily concentration. Although the effects are possibly short-

term, acute emissions, which would seem relatively small when evaluated on an annual average scale. Yet they may play an important role in deposition of PM_{10} to the SSSI, and the potential effects on vegetation over shorter time scales.

If the model was parameterised using emission values for coarse particulate matter emissions instead of emissions of PM_{10}, a more representative scenario of fugitive dust emissions from the Corus works could be developed. This would also allow comparison between the total dust deposited to the Frisbees and the modelled expectations of coarse fugitive dust emissions. At present the model output is limited to predicting the PM_{10} fraction of particulate matter. By modelling emissions from the Corus works which included all fractions of particulate matter, the model would produce a more representative output which could be interpreted with confidence.

5.6.5 Overall value of modelling and its contribution to deposition studies

Overall, the modelling has proved very beneficial because at the very least it led to the present study; it then informed the passive dust monitoring programme for the present study and finally it has been developed using several dust generation scenarios. Although a considerable degree of uncertainty has to be taken into account with any modelling work, it is an important tool for examining the potential impacts from PM_{10} emissions. The model would benefit from reliable emissions rates for all fractions of particulate matter, in particular from the stockyards, and the inclusion of dust generating activities such as heavy vehicles on roads, and tracks and the ponding of molten iron. The model outputs should also be produced for daily and annual average environmental concentrations. The most beneficial though, would be the inclusion of all dust fractions, allowing comparison of measured real-time deposition with the modelled expectations.

Modelling is limited and it cannot accurately reproduce the actual daily deposition on-site. The model produces an output which is representative of the input, therefore, any error or inaccuracies in the input meteorological or emission data will be replicated in the model output. In the model the dispersion behaviour of the pollutants is dependant upon the state of the atmosphere, of these, both are approximations and their limitations must be considered (Hall *et al.*, 2002). The limitations are partly a result of variability in the meteorological data and the state of the atmosphere (Hall *et al.*, 2002). Since the emission data for the Corus works are at best an informed estimate, and the meteorological conditions cannot be the exact conditions, it would not be possible to

produce a model which accurately predicts the deposition to all areas under all circumstances. These difficulties are commonly accepted as unavoidable in practical models (Hall *et al.*, 2002).

5.7 Summary of Chapter 5 – Review and development of a particulate emissions model

The key outcomes of the review and development of modelling the particulate emissions from the Corus works were identified as the following:

The initial modelling conducted by Corus was part of the IPPC permit application submitted in 2001. The model output indicated areas of the SSSI which exceeded the maximum daily average concentration of PM_{10} for human health, but the impact of these levels on ecological systems was unknown. The model was parameterised using historic meteorological data and unrepresentative emission scenarios.

The present study developed a further three model scenarios, with contemporary meteorological data and more representative fugitive dust emission sources. Although valuable, the model outputs contain uncertainty, and have several limiting components. The model outputs are not directly comparable with the measured dust deposition data, but the model expects the concentration of PM_{10} to be higher on the Corus works than in the surrounding area. The trends in PM_{10} environmental concentration at individual monitoring sites did not correlate to the trends found in dust deposition measured at the Frisbees on the Corus works or surrounding areas.

The model could benefit from further development. Key areas identified include; removing the beach source area; adding emissions from paved and unpaved roads; adding emissions from ponding events; calibrating the source area with GPS locations; improving knowledge of stock movement; improved meteorological data resolution; reduced error and uncertainty of the measured values; greater resolution of particulate matter on the model outputs; modelling generation and deposition of all fractions of particulate matter; and model scenarios to produce average daily and annual environmental concentrations for all fractions of particulate matter.

Modelling can not produce actual values of deposition to the SSSI, but it can be improved. Investing time and resources into measuring and monitoring the actual particulate matter deposition would be of greater value. However, there are many limiting factors on this site which make continuous monitoring difficult.

Chapter 6 - Ecological impacts of dust deposition on the SSSI

6.1 Introduction

Determining the effects of the potential particulate matter emissions from the Corus works to the flora on South Gare and Coatham Sands SSSI is a key aim of the present study. The Integrated Pollution Prevention and Control (IPPC) permit application submitted to the Environment Agency in 2001 outlined the effects of the particulate emissions on the SSSI as one of the improvement conditions (see Chapter 2 section 1.2). The present chapter will present the potential effects of dust deposition on the flora of the SSSI with the use of on-site field measurements. The chapter will initially present the sites chosen on the sands dunes of the SSSI and Seaton Carew for conducting these field measurements. Next the deposition of dust to the vegetation growing on the Gare SSSI will be presented, followed by the iron concentration of the soil on the SSSI, and finally the potential effects of dust deposition on gas exchange measurements to plants growing on the SSSI.

6.2 Site selection

Seaton Carew was selected to determine the levels of background iron in the dune systems. It is close to South Gare and Coatham Sands SSSI, but not adjacent to the Corus works. Sample locations were taken using a GeoTX (Trimble GmbH, Germany) Global Positioning System (GPS) device (See Chapter 3 section 2.3.9). Six soil samples were taken from sampling points on Coatham Sands SSSI and Seaton Carew, on one of the following transects:

The South Gare transect was located on Coatham Sands and South Gare SSSI, close to the South Gare breakwater (see Table 6.1 and Figure 6.1). From the fixed dunes sampling point the transect headed in a northerly direction to the embryo dunes sampling point for a distance of 680 m. The fixed dune sampling point was 260 m distance from the Corus works boundary and the embryo dune sampling point was 270 m from the high tide line. The South Gare transect was 2000 m from the Coatham Sands transect and 789 m in a north-easterly direction from the Corus blast furnace.

The Coatham Sands transect was located on Coatham Sands and South Gare SSSI. The transect headed in a easterly direction from the fixed to the embryo dune

sampling point for 360 m, the fixed dune sampling point was 82 m from the Corus works boundary and the embryo dune sampling point was 85 m from the high tide line. The Coatham Sands transect was 840 m in an easterly direction from the Corus blast furnace.

The Seaton Carew transect was located on the northern shores of the river Tees estuary, on Seaton Dunes and Common SSSI. The transect heads in the northerly direction from the fixed dunes to embryo dunes for around 120 m, and the embryo dunes are 100 m from the high tide. The Seaton Carew transect is 2710 m in a north-westerly direction from the South Gare transect, 4650 m from the Coatham Sands transect and 3800 m from the Corus works blast furnace.

Table 6.1 Sample point GPS co-ordinates in British National Grid for South Gare and Coatham Sands SSSI and Seaton Dunes and Common SSSI.

Transect	Location	GPS co-ordinates (British National Grid)
Seaton Carew	Embryo Dunes	453819, 528437
	Fixed Dunes	453847, 528318
Coatham Sands	Embryo Dunes	457788, 525816
	Dune Midpoint	457619, 525750
	Fixed Dunes	457449, 525700
South Gare	Embryo Dunes	455943, 527095
	Dune Midpoint	456013, 526869
	Fixed Dunes	456111, 526433

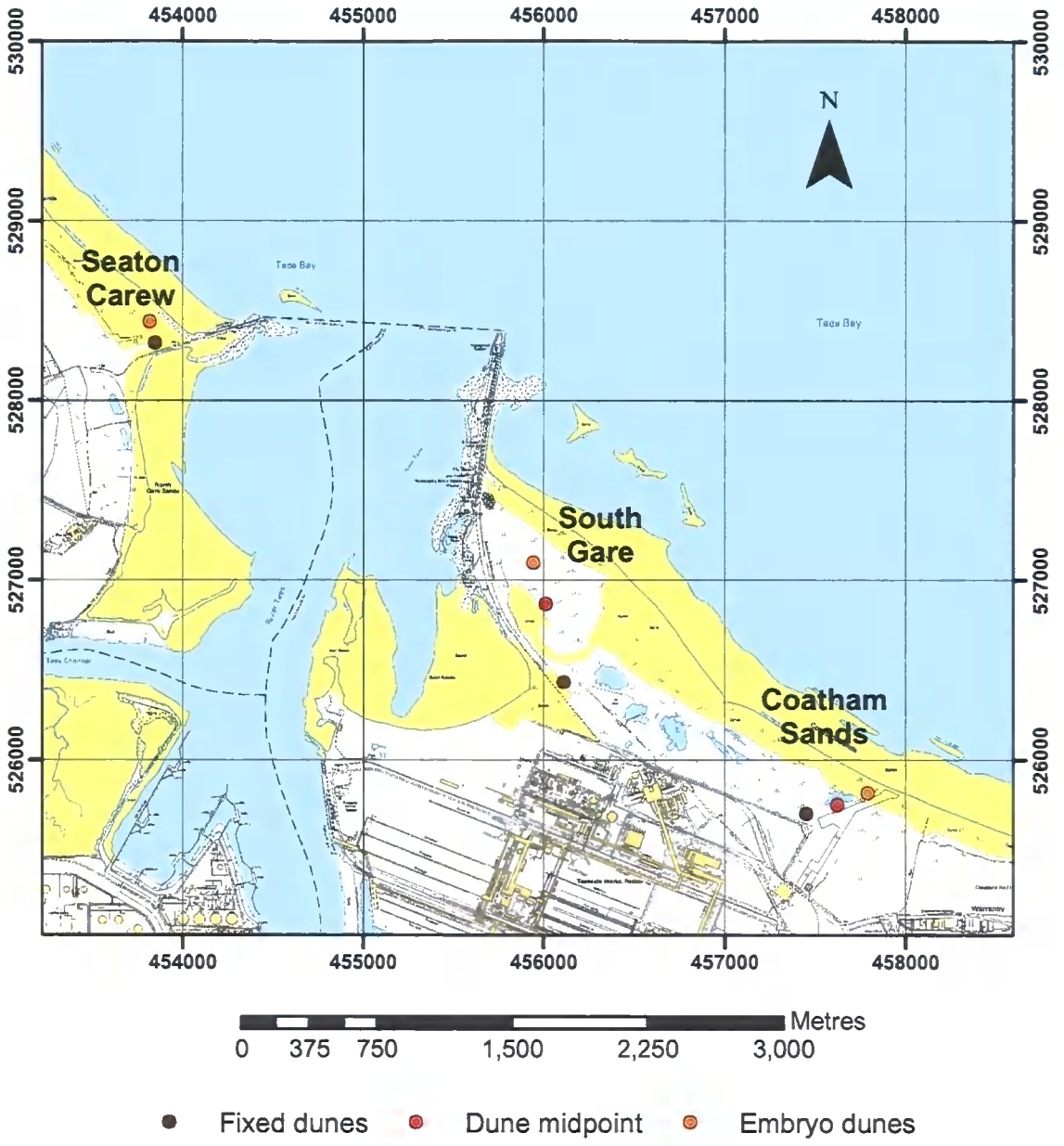

Co-ordinate System: British National Grid. Projection: Transverse Mercator.
Datum: OSGB 1936.

Figure 6.1 Map of the three transects and the sampling points. Brown circles show fixed dunes, red circles show dune midpoint and orange circles show embryo dunes.

6.3 Assessing dust deposition to plants with artificial leaves

6.3.1 Introduction to dust deposition to plants

Chapter 3 presented the dust deposition and flux to six monitoring sites on and surrounding the Corus works, however, it was not possible to locate one of these monitoring sites on the SSSI. Therefore the first section of the present chapter aims to quantify the dust deposition to the flora on South Gare and Coatham Sands SSSI, using artificial leaves.

The deposition of dust to the surfaces of leaves has been shown to occlude stomata and increase leaf temperature (Hirano *et al.*, 1995), reduce photosynthetically active radiation and plant growth (Naidoo & Chirkoot, 2004; Sharifi *et al.*, 1997) (see section 5 for more details). Therefore quantifying the dust deposited to individual leaves over a range of spatial and temporal exposures, will determine the extent of dust loading to the leaves of the plants on the SSSI.

6.3.2 Methods

It was not feasible to expose a Frisbee dust deposit gauge on the SSSI. To determine the deposition of dust to the SSSI an inconspicuous, cheap, easily retrievable and replaceable gauge was required. It was decided that the white fablon sticky pads would be cut into the shape of leaves. These artificial leaves were then erected perpendicular to the ground in a rosette arrangement to record dust deposition. On each rosette four leaves were exposed in the cardinal compass points and a fifth leaf was left unexposed on the rosette (see Figure 6.2). To minimise disturbance to the area surrounding the location of the artificial leaves, a GPS was used to record the location.

The artificial leaves were exposed at six points on the SSSI; the fixed dunes, the dune midpoint and the embryo dunes, along the Coatham Sands and South Gare transects (see Figure 6.1). The artificial leaves were exposed from 24th May to the 31st May 2007 for periods of one, two, four or six days. The leaves were carefully replaced onto the backing paper and returned for analysis.

The artificial leaves were analysed using the sticky pad reader (see Chapter 3 section 2.3 and 2.4) (I R Hanby, Newark, UK). Six readings were taken on each artificial leaf, and then averaged for each location to calculate an average percentage Effective Area Coverage (% EAC day^{-1}) for the six sample sites.

Figure 6.2 Artificial leaves exposed on the South Gare transect at the midpoint sample point.

6.3.2.1 Data analysis

Data for leaf dust deposition were determined as being normally distributed. To normalise the distribution of these data a reflect and square root, and a square root transformation was conducted (Kolmogorov-Smirnov) ($n = 24$, $KS = 0.160$, $p > 0.10$). These data were then analysed using a three-way nested ANOVA.

6.3.3 Results

There was no significant difference between the two transects on the SSSI ($f = 0$, $p < 0.99$), however there was a significant difference of dune location nested within the transect location ($f = 4.95$, $p < 0.01$). Post-hoc testing revealed the level of dust deposition at the fixed dunes was significantly higher than the level of dust deposition to the embryo and midpoint dunes for both transects (see Figure 6.3) (see appendix C Table 1). However, the level of dust deposition was not significantly different between the embryo and midpoint dunes.

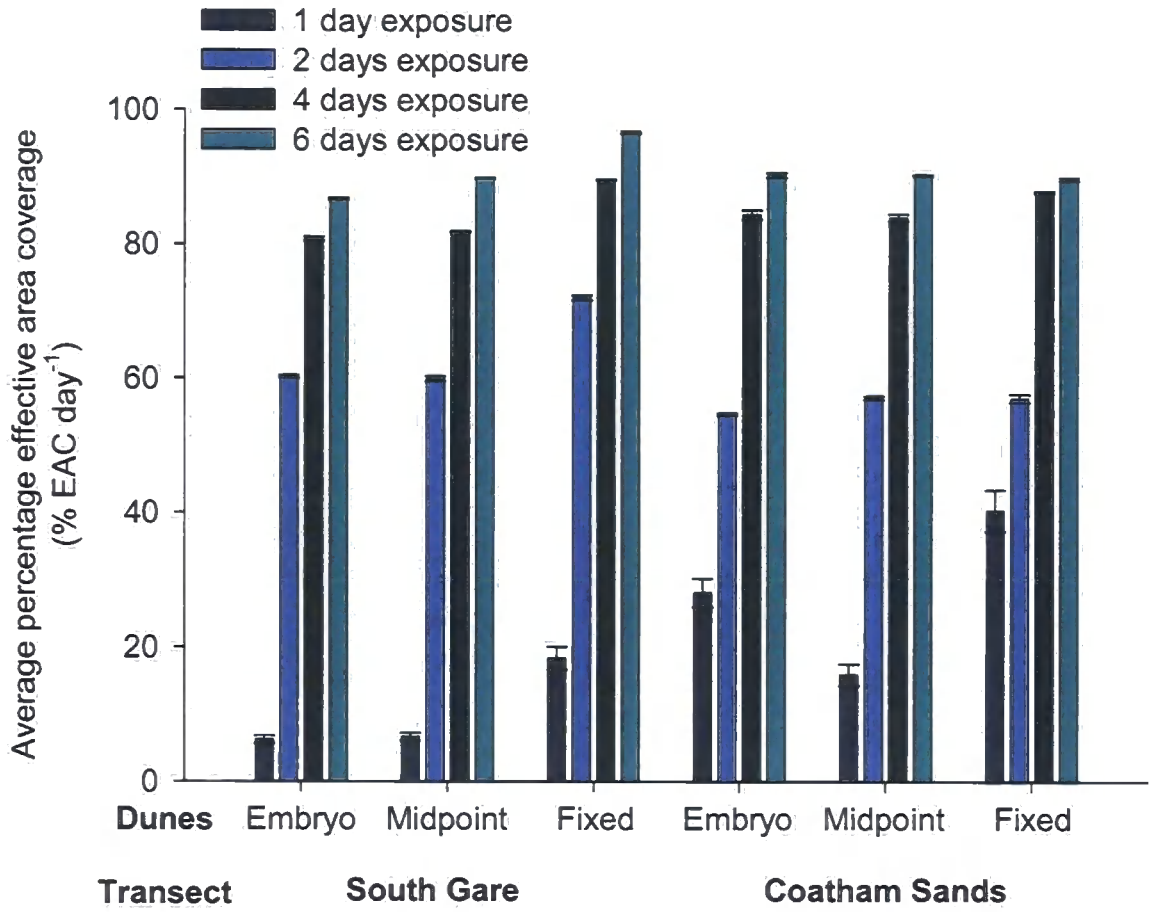

Figure 6.3 Average percentage Effective Area Coverage (% EAC day^{-1}) for artificial leaves exposed at the embryo dunes, dune midpoints and fixed dunes on the South Gare and Coatham Sands transects. Error bars show ±1 SE (n=4, 5, 6).

The dust deposition to the artificial leaves increased significantly with each incrementing exposure period ($f = 186.20$, $p < 0.001$). Post-hoc testing revealed that the dust deposited to the artificial leaves exposed for one day was significantly lower than the dust deposited to the leaves exposed for two, four and six days (see appendix C Table 2). The dust deposited to the artificial leaves exposed for two days was significantly lower than the dust deposited to the leaves exposed for four and six days. The dust deposited to the artificial leaves exposed for four days was significantly less than the dust deposited to the leaves exposed for six days.

6.3.4 Discussion

The South Gare and Coatham Sands transects were both located downwind of the prevailing direction from the Corus works. The dust deposition to the two transects was not significantly different, although after the artificial leaves were exposed for one day the dust deposited at the Coatham sands transect was higher at the embryo, midpoint and fixed dunes.

The dust deposition was significantly higher at sites closest to the Corus works, and was significantly increased by increasing exposure time, in relation to sites located further away from the Corus works. Therefore the potential for the effects of dust deposition to the plants on the SSSI is at its highest closest to the Corus works, and increases over time across the SSSI. There was no significant difference in the dust deposited to the midpoint and embryo dunes, but the total dust deposited was still relatively high with respect to the fixed dunes.

Although real-time or passive monitoring would have provided a more accurate representation of the dust deposited to the SSSI, this was not feasible due to the site constraints. The dust deposition study using the white fablon sticky pads was an effective approach to determine the relative deposition of dust to the SSSI. It would be beneficial to conduct a similar investigation on Seaton Carew sand dunes in parallel to this study. However, this was not possible within the time constraints of the present study.

One problem with the fablon sticky pads concerns the capacity of the pads to collect total deposition. Once a particle had been deposited onto the sticky pad, it is not possible for another particle to be deposited in that location. Therefore, the sticky pads reach a maximum capacity for collecting dust and cannot continually collect material like the Frisbee deposit gauge or a real-time monitor. From the artificial leaves exposed at the SSSI, the maximum capacity for dust collection is reached after 6 days. However a further investigation would be required to confirm exposure length required to reach the maximum capacity. Despite this the artificial leaves were an effective tool for determining the dust deposition to sites on the SSSI.

6.4 Soil iron concentration

6.4.1 Introduction to soil iron concentration

The first section of this chapter has shown that dust is deposited to the SSSI, and the present section will identify one of the potential effects of dust deposition to the SSSI. It is accepted that much of the dust deposited to a site, will settle on vegetation and the soil, but will eventually reach the soil by through-fall, and therefore determining the concentration of heavy metals in the soil was an important step.

A previous study on the contamination of the soil around an iron and steel works in Algeria found increased heavy metal incidence in the soil surrounding the works, after conducting an aqua regia digestion and analysis using Atomic Absorption Spectrometry (ASS) (Kadem *et al.*, 2004). It is commonly accepted that indirect effects of deposition to the soil can change the soil chemistry by altering nutrient cycling and inhibiting plant nutrient uptake (Grantz *et al.*, 2003), which in turns affects the vegetation. The chemical characterisation of deposited dusts in chapter four had shown the main constituent of deposited dusts to be iron-rich particles. Therefore, the section that follows presents the iron concentration of the soils on the SSSI and Seaton Carew monitoring sites.

6.4.2 Methods of soil analysis

6.4.2.1 Sample collection

The soil sample collection procedure was limited to the fixed and embryo dunes for each of the three transects; South Gare, Coatham Sands and Seaton Carew. For each sampling point, six surface soil samples were taken systematically to account for any spatial variation. A further six control (blank) samples were added to the samples for analysis. The six control samples were to ensure the iron concentration of the samples was not affected by the digestion process.

6.4.2.2 Digestion method

The method used is the US Environmental Protection Agency method 3050B, Acid digestion for sediments, sludges and soils (Environmental Protection Agency, 1996). The

technique is designed to dissolve almost all 'environmentally available' elements but it is not a total digestion technique. All chemical reagents conformed to the trace analysis grade, with appropriate health and safety precautions.

The soil samples were dried at 80 °C in an oven overnight. They were thoroughly mixed, sieved, weighed (*ca.* 1 g dry weight) to the nearest 0.01 g and transferred to a beaker for digestion.

Initially each soil sample received 10 ml of conc. HNO_3 to reagent water (1:1). The samples were thoroughly mixed, covered with a watch glass and heated to 80 °C ± 5 °C and allowed to reflux for 10 - 15 minutes without boiling. The samples were allowed to cool. A further 5 ml conc. HNO_3 was added; the beakers were covered with watch glasses and refluxed for 30 minutes. This step (addition of 5 ml conc. HNO_3 and 30 minutes reflux) was repeated until brown fumes ceased (brown fumes indicate oxidation of the sample by HNO_3) indicating complete reaction with HNO_3. The samples were heated, without boiling, at 80 °C and allowed to evaporate to 5 ml (maintaining a covering of solution in the bottom of the beaker at all times).

The samples were allowed to cool, and 2 ml of reagent (distilled) water and 3 ml of 30 % H_2O_2 were added. The beakers were covered with watch glasses and returned to the heat source to initiate the peroxide reaction. The samples were heated until effervescence subsided, and the samples were allowed to cool. Losses due to excessive effervescence did not occur.

The samples received 30 % H_2O_2 in 1 ml aliquots followed by warming until the effervescence subsided or until the sample appearance was unchanged. No more than 10 ml 30 % H_2O_2 was added. The acid-peroxide digestate was then heated to 80 °C, without boiling, reduced to a final volume of 5 ml and allowed to cool.

The samples then received 10 ml conc. HCl and were covered with watch glasses. The samples were again heated to 80 °C, refluxed for 15 minutes and allowed to cool.

Cooled samples were filtered through Whatman No. 452 filter papers into 100 ml volumetric flasks and made to volume.

6.4.2.3 Atomic absorption spectrophotometry

The samples were analysed using an Atomic Absorption Spectrophotometer (AAS) (SpectraAA 220 Fast Sequential (FS), Varian Inc., Palo Alto, California, USA, Wavelength = 372.0 nm. and Slip Width = 0.2 nm.) and correlated against a range of standard reference samples.

The reference samples were prepared using the stock AA standard (SCP Science, 1000 mg Fe/l in 4 % HNO_3) which was diluted to make 10, 20, 50 and 100 mg Fe/l standards. A calibration blank sample was also prepared to 50 mg Fe/l, using the stock AA standard. These reference and calibration blank samples were matched to contain the same concentration of HCl and HNO_3 which were used in the soil samples.

The soil samples were diluted using deionised water, HCl and HNO_3 to give the acid concentrations equal to the original (undiluted) samples, by either a factor of 10 (1 ml in 10 ml) or 20 (0.5 ml in 10 ml) to get a signal within the calibration range. Values were measured on the AAS in ml of iron (mg Fe/l) per litre of sample and then converted into mg iron per g soil (mg Fe g^{-1}).

6.4.3 Data analysis

Data were tested for normality (Kolmogorov-Smirnov) and found to be non-normal despite data transformation ($n = 36$, $KS = 0.186$, $p < 0.01$), therefore these data were analysed using the nonparametric Friedman test.

6.4.4 Results

The iron concentration of the soil at the fixed dunes for the Coatham Sands and South Gare transects were 98.3 and 72.9 mg Fe g^{-1} soil respectively (see Figure 6.4). The iron concentration of the soil at the embryo dunes for the Coatham Sands and South Gare transects were 16.9 and 48.9 mg Fe g^{-1} soil respectively. The iron concentration of the soil on the Seaton Carew transect for the fixed and embryo dune sites were 4.6 and 5.6 mg Fe g^{-1} soil respectively.

The iron concentration of the soil on the South Gare, Coatham Sands and Seaton Carew transects were significantly different ($n = 12$, $df = 2$, $\chi^2 = 18.7$, $p < 0.005$) with the highest soil iron concentration measured at the South Gare transect, followed by the Coatham Sands transect and the lowest at the Seaton Carew transect.

The iron concentration of the soil at the fixed and embryo dune sites were significantly different ($n = 18$, $df = 1$, $\chi^2 = 18.0$, $p < 0.005$) with the highest soil iron concentration measured at the fixed dune sites and the lowest at the embryo dune sites, the only exception to this was the Seaton Carew transect.

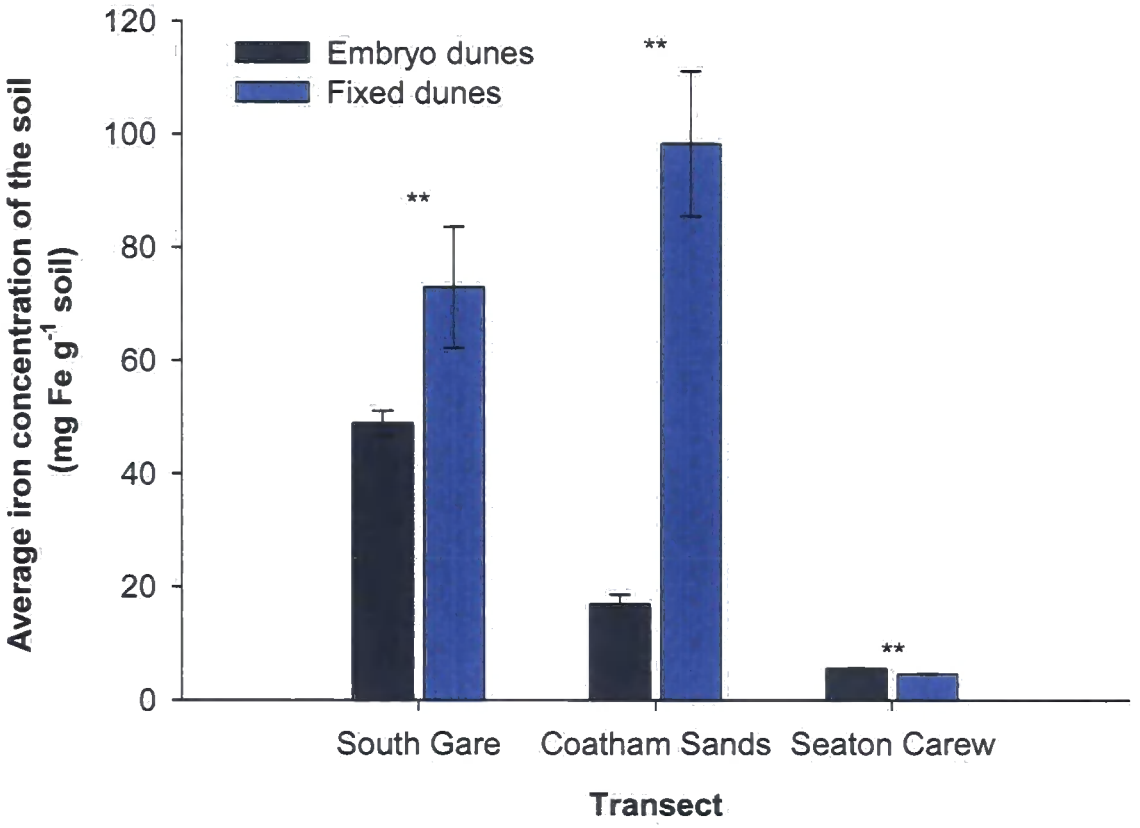

Figure 6.4 Average iron concentration of the soil samples (mg Fe g^{-1} soil) taken from the fixed and embryo dune sampling sites on three transects. Error bars show ±1 S.E. (significant at < 0.005).**

6.4.5 Discussion

The iron concentration of the soil on the SSSI was found to be significantly higher than the iron concentration of the soil on Seaton Carew. The iron concentrations of the soil at the fixed dune sites on the Coatham Sands and the South Gare transect were over 21 and 15 times higher than those at Seaton Carew transect. Whereas the iron concentration of the soil at the embryo dune sites on the Coatham Sands and South Gare transect were over 3 and 8 times higher than those on the Seaton Carew transect. Previous studies have shown heavy metal pollution to decrease the rate of decomposition in soils (Fritze, 1991; Martin & Coughtrey, 1981) and cause changes in the mycorrhizal communities (Cairney & Meharg, 1999; Chappelka *et al.*, 1991). The effect of dust deposition to flora is often difficult to determine as deposition effects can be either the effect of deposition to the leaf surface or deposition to the soil (Smith & Staskawicz, 1977), these effects can be difficult to partition (Grantz *et al.*, 2003). Therefore the increased iron concentration of the soils on the SSSI may influence the rate of deposition or mycorrhizal communities, further investigation with litter bags would be required to determine the rate of decomposition on the SSSI in relation to similar ecosystems.

The iron concentration of the soil on the SSSI was also significantly higher at the fixed dune sites on both transects, which were the closest monitoring sites to the Corus works, which could potentially affect the flora and fauna living on the SSSI. Therefore the potential effects of iron enriched soils may be more prominent at the fixed dune sites. However, the higher iron concentration at the fixed dune sites may be due to poor drainage. The soil receives iron as a result of particulate deposition and through-fall of particulates deposited to vegetation washed down to the soil. Although it has been shown that the total daily deposition is lower at the embryo dunes than the fixed dunes, it might be that the soils at the embryo dunes are more freely draining and could explain the lower iron concentration of the soils. Less freely draining soils at the fixed dune sites could explain the accumulation of iron content over 15 times higher than to the soils at Seaton Carew. This would require further investigation, which was beyond the scope of the present study. An investigation into the spatial variation of soil iron concentration across the sand dunes would be a valuable investigation.

6.5 Gas exchange measurements

6.5.1 Gas exchange in disturbed environments

Chapter 3 presented the total dust deposition and flux to six monitoring sites on and surrounding the Corus works, Teesside, and the first section of this chapter has investigated the spatial and temporal patterning in dust deposition across the SSSI. The next section of the present chapter investigates the potential effects of dust deposition to the gas exchange of the flora on the SSSI.

The deposition of dust to the surfaces of leaves has been shown in previous studies to reduce plant health (Bignal *et al.*, 2007; Paling *et al.*, 2001) through effects on leaf gas exchange (Ernst, 1982). Dust deposits have been shown to occlude stomata (Ricks & Williams, 1974) and increase leaf temperature by absorbing excessive radiation (Hirano *et al.*, 1995), shade the leaf (Thompson *et al.*, 1984), and reduce photosynthetically active radiation to the leaf surface and hence reduce plant growth (Naidoo & Chirkoot, 2004; Sharifi *et al.*, 1997) which could potentially increase the rate of photosynthesis and transpiration, inducing water stress.

In this section gas exchange measurements of leaves from four sites are compared between untreated and cleaned leaves in September 2007 to assess the influence that dust deposition may have on carbon gain, transpiration and water-use efficiency.

6.5.2 Methods for measuring gas exchange

To determine the potential effects of dust deposition to the flora of the SSSI, two plants were chosen for conducting gas exchange measurements which represented the typical flora of the sand dunes. It was important both species were native to English maritime sand dunes, so *Leymus arenarius* (Lyme Grass) and *Plantago lanceolata* (Ribwort Plantain) were selected. The prevailing inclement weather conditions prevented measurements of *Plantago* at all four sites, and was only measured at the Coatham Sands, fixed dune site.

The leaves of *Leymus* are characteristically flat, inrolled and blue-grey in appearance, between 8-20 mm wide and up to 35 cm long, easily identified by its short blunt ligule. *Plantago* grows from basal rosettes, the leaves are long and narrow, between 4 to 8 cm which taper to a pointed tip. For the purposes of this investigation leaf

size was used as an approximation of leaf age, and similar sized leaves were chosen for conducting measurements of gas exchange.

The fieldwork was limited to four sites for gas exchange measurements due to the prevailing inclement weather in the summer of 2007. These sites were the fixed and embryo dunes on the Coatham Sands and South Gare transects (see Figure 6.1). At each of the four sites on the SSSI gas exchange measurements were taken on ten separate plants. Five leaves were untreated, while the upper and lower surfaces of another five leaves were cleaned gently using a distilled water wash and concomitant gentle stroking of the leaf surface with a soft-bristled paintbrush. After cleaning, the surface water upon the leaf was allowed to evaporate to full dryness (a period of 30 to 60 minutes).

All measurements were taken between 1100 and 1500 h on the 5th, 6th and 7th September 2007. All days were dry, warm and sunny with patchy high-level cloud. Gas exchange was measured using an Infra Red Gas Analyser (IRGA; (LCA-4, ADC BioScientific Ltd, Great Amwell, UK) at an air flow rate of 376 μmol s^{-1}. A section of leaf was enclosed within the leaf chamber (area 6 cm^2) for measuring gas exchange.

To examine the potential impact of dust deposition to the leaf surface on leaf carbon acquisition, saturating light was provided by a bright white light source at 1000 μmol $m^{-2}s^{-1}$ (LCA-4, ADC BioScientific Ltd, Great Amwell, UK). For each measurement; net photosynthesis per unit leaf area A_n (μmol $m^{-2}s^{-1}$) and transpiration rate E (mol $m^{-2}s^{-1}$) were recorded. Instantaneous water-use efficiency (W) was calculated as the rate of photosynthesis divided by the rate of transpiration (A_n/E) (μmol CO_2 $mmol^{-1}H_2O$). After all gas exchange measurements were made, the material enclosed within the chamber was clipped and returned to the laboratory to calculate leaf area. It was not possible to record the leaf temperature; hence the stomatal conductance could not be calculated.

6.5.3 Data analysis

Data were analysed using SPSS statistical software (SPSS Inc. Chicago, Illinois, USA) on the photosynthetic rate, transpiration rate, and instantaneous water-use efficiency. The data for *Leymus* leaves were tested for normality (Kolmogorov-Smirnov), and were found to be normally distributed ($KS \geq 0.44$, $n = 8$, $p < 0.05$). The data were analysed using three-way nested ANOVAs without replicates. The same data for the *Plantago* were tested for normality (Kolmogorov-Smirnov), and were found to be non-normally distributed, despite transformation, probably attributable to the small sample size. The

non-parametric test (Kruskal-Wallis) was used to test the leaves of *Plantago*. The results were presented using Sigma Plot v.10 (Systat Software Inc. San Jose, California, USA).

6.5.4 Results

The rates of photosynthesis at all sites were significantly higher for the cleaned leaves ($f = 15.94$, $p = 0.028$) compared to the untreated leaves (see Figure 6.5). The biggest difference in the *Leymus* leaves was measured at the embryo dune site, on the Coatham Sands transect, where the photosynthetic rate of the cleaned leaves compared to the untreated leaves increased by 68 % from 9.4 to 15.7 µmol m^{-2} s^{-1}. The *Leymus* leaves at the fixed dune site on the Coatham Sands transect saw a 23.8 % increase in photosynthetic efficiency from 12 to 14.9 µmol m^{-2} s^{-1}.

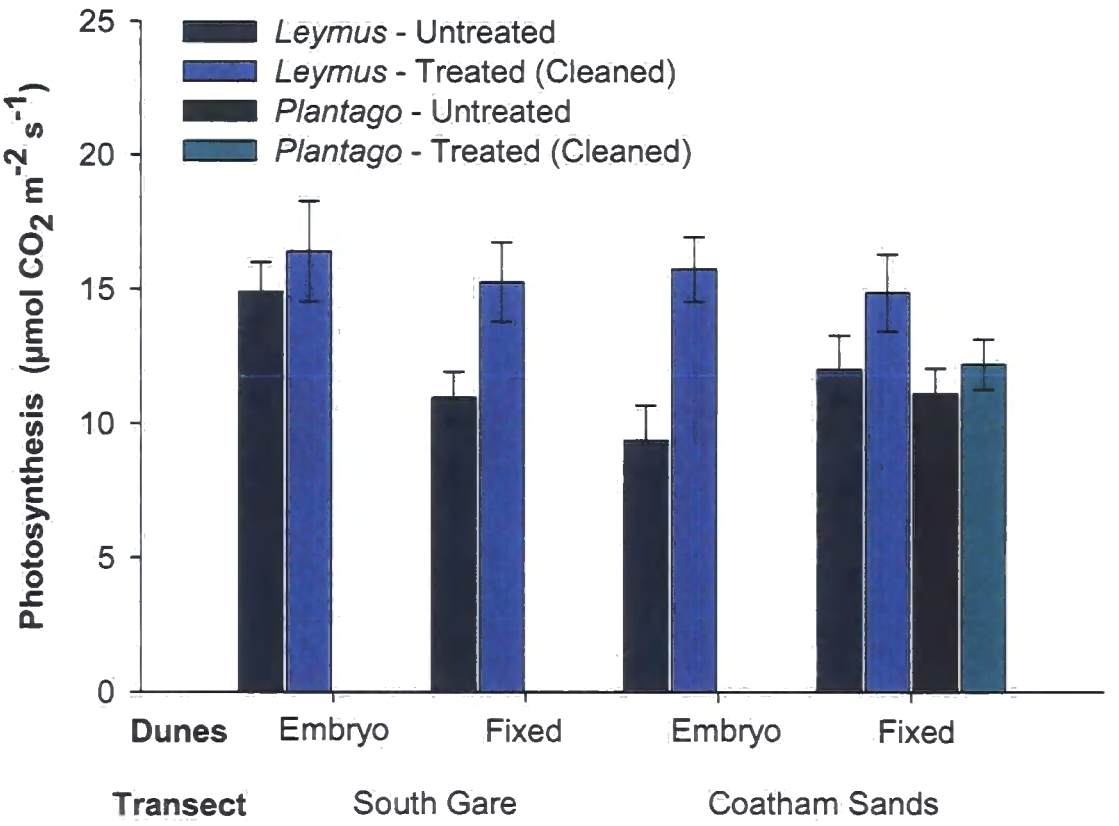

Figure 6.5 Average rate of photosynthesis (µmol m^{-2} s^{-1}) at the fixed and embryo dune sites on the South Gare and Coatham Sands transects on the SSSI for *Leymus* and *Plantago* species. Error bars show ± 1 SE. (n=6).

The rate of photosynthesis on the South Gare transect increased significantly by 39.2 % from 11 to 15.3 µmol m^{-2} s^{-1} at the fixed dune site and by 10.1 % from 14.9 to 16.4 µmol m^{-2} s^{-1} at the embryo dunes for *Leymus*. The smallest difference was

that of the *Plantago* which saw only a 10 % increase in photosynthetic rate from 11.1 to 12.2 μmol m^{-2} s^{-1}. The rate of photosynthesis was not effected by transect ($f = 2.15$, $p > 0.05$) or dune location within transect ($f = 2.03$, $p > 0.05$).

The rates of transpiration at all sites were not significantly different for the cleaned compared to the untreated leaves ($f = 1.11$, $p > 0.05$). There was a significant effect of dune location within transect ($f = 10.13$, $p < 0.05$) and no effect of transect ($f = 0.03$, $p > 0.05$) (see Figure 6.6).

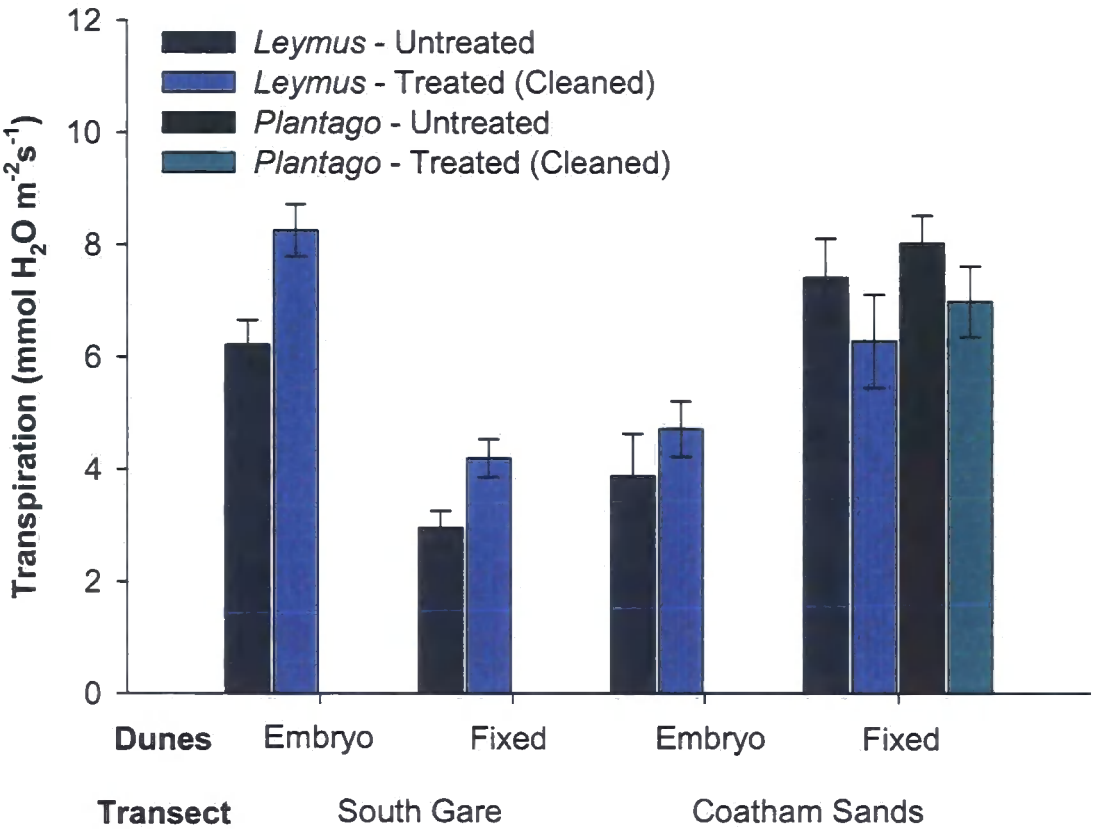

Figure 6.6 Rate of transpiration at four sites on the SSSI for *Leymus* and *Plantago* leaves. Error bars show ± 1 SE. (n = 6).

The transpiration rate of the untreated and cleaned *Leymus* leaves at the embryo dunes on the South Gare transect was 6.2 and 8.3 mmol m^{-2} s^{-1} respectively, while the transpiration rate at the fixed dunes for the untreated and cleaned *Leymus* leaves was 3 and 4.2 mmol m^{-2} s^{-1} respectively. The transpiration rate of the untreated and cleaned *Leymus* leaves on the Coatham Sands transect at the embryo dunes was 3.9 and 4.7 mmol m^{-2} s^{-1} respectively, while at the fixed dunes the untreated and cleaned *Leymus* leaves was 7.4 and 6.3 mmol m^{-2} s^{-1} respectively. The transpiration rate of the

untreated and cleaned *Plantago* leaves at the fixed dune site on the Coatham Sands transect was 8.1 and 7 mmol m^{-2} s^{-1} respectively.

The effect of cleaning leaves was found not to have a significant effect on the water-use efficiency ($f = 0.56$, $p > 0.05$) (see Figure 6.7). There was no significant effect of transect on the water-use efficiency of the leaves ($f = 0.50$, $p > 0.05$), although the effect of dune location within transect was approaching significance ($f = 7.68$, $p = 0.066$).

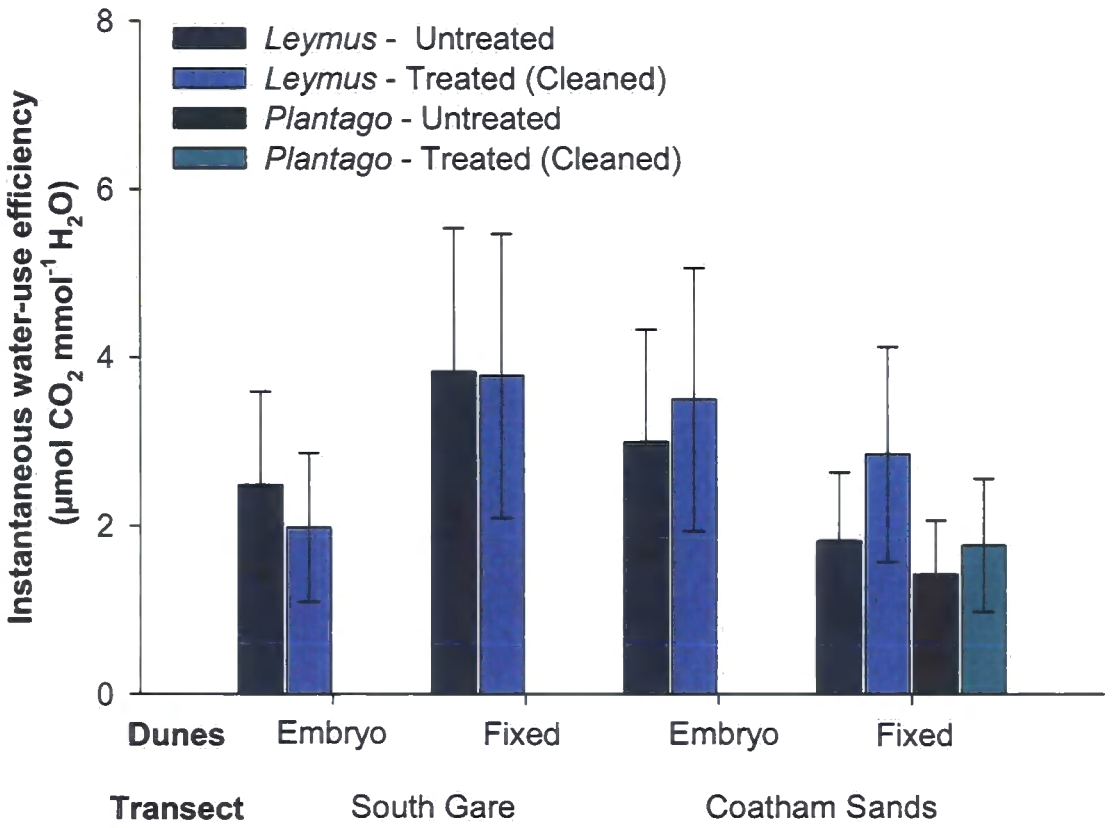

Figure 6.7 Water-use efficiency at four sites on the SSSI for *Leymus* and *Plantago* leaves. Error bars show ± 1 SE. (n = 6).

The water-use efficiency of the untreated and cleaned *Leymus* leaves on the Coatham Sands transect was 1.8 and 2.9 µmol CO_2 $mmol^{-1}$ H_2O respectively for the fixed dune site, and 3 and 3.5 µmol CO_2 $mmol^{-1}$ H_2O respectively for the embryo dune site. While the water use efficiency of the *Plantago* leaves at the fixed dune site on the Coatham Sands transect was 1.4 and 1.8 µmol CO_2 $mmol^{-1}$ H_2O for the untreated and cleaned leaves, respectively. The water-use efficiency of the untreated and cleaned *Leymus* leaves on the South Gare transect was 3.83 and 3.78 µmol CO_2 $mmol^{-1}$ H_2O

respectively for the fixed dune site, and 2.5 and 2 μmol CO_2 $mmol^{-1}$ H_2O respectively at the embryo dune site.

6.5.5 Discussion

The rate of photosynthesis for the cleaned leaves of *Leymus* and *Plantago* significantly increased at all sites. Removing the accumulated dust on the upper and lower surfaces of the *Leymus* leaves increased the plants ability to fix carbon by 68 % at the embryo dune site and by 24 % at the fixed dune site on the Coatham Sands transect. Cleaning increased the plants ability to fix carbon by 10 % at the embryo dune site and by 39 % fixed dune site on the South Gare transect. The smallest effect of cleaning on photosynthetic efficiency was measured for *Plantago* leaves at the fixed dune site, on the Coatham Sands transect, where the plants ability to fix carbon was increased by 10 % compared to the untreated leaves. Dust deposition therefore has the potential to affect the growth and function of *Leymus* and *Plantago* species across the SSSI, although to a lesser degree for the *Plantago* species. Cleaned leaves of *Leymus* had similar rates of photosynthesis, irrespective of location. Therefore, the effect of foliar surface cleaning was able to restore the rate of photosynthesis to the same rate of carbon fixation for all locations.

Within each transect the rate of dust deposition at the fixed dune sites were found to be significantly higher than at the embryo dune sites. The relatively small increase in photosynthetic efficiency at the fixed dune site on the Coatham Sands transect compared to that on the South Gare transect, could potentially be attributed to the high deposition of dust deposition having an effect on the plants other than shading. Therefore, it could be attributed particulate matter blocking the stomata, which has the potential to reduce the water-use efficiency, and the water-use efficiency of the *Leymus* leaves was very low at the fixed dune site on the Coatham Sands transect. The lower rate of photosynthesis measured on the untreated or dusted leaves is in agreement with the available literature (Gale & Easton, 1979; Sharifi *et al.*, 1997; Thompson *et al.*, 1984).

The cleaning of the leaves did not have a significant effect on the transpiration rates of either species at all four sites. The rate of transpiration was highly variable, and possibly attributable to small scale variation in water availability or soil moisture for each plant.

The cleaning of the leaves did not have a significant effect on the water-use efficiency for both species at all four species. It could be that dust deposition has no effect on the water-use efficiency of *Leymus* and *Plantago* leaves, but this is unlikely due to the variation in measured water-use efficiency. Repeated measures of the same plant

would be beneficial in determining the effect of cleaning on the water-use efficiency of the leaves.

The investigations conducted into the effects of dust deposition on gas exchange would benefit from repeated measures of the same plants, greater spatial and temporal resolution and a higher sample size. The present study provides a valuable examination of the effects of dust deposition on photosynthesis. However, development and further analysis of this analysis would provide valuable information on the specific effects.

6.6 Summary of Chapter 6 – Ecological impacts of dust deposition on the SSSI

The key outcomes of the ecological investigation into the effects of particulate emission from the Corus works were identified as the following:

Dust deposition

To determine the deposition of dust to the SSSI, a study was undertaken using leaf shaped sticky pads on six monitoring sites on the SSSI in May 2007.

The deposition of dust to the SSSI was considerably higher at the fixed dune monitoring sites than at the midpoint and embryo dune monitoring sites. There was no significant difference in the dust deposition to the embryo and midpoint dune sites.

The dust deposited to the sites increased within longer exposure periods, with significantly more dust after 6, 4, and 2 days with respect to 4, 2 and 1 day exposure periods.

Soil iron concentration

The soil iron concentration was significantly higher on the SSSI compared to Seaton Carew, between 3 to 21 times higher on the SSSI.

The soil iron concentration is significantly higher at the fixed dune monitoring sites than at the embryo dune monitoring sites.

The increased iron concentration of the soils on the SSSI may be affecting the soil chemistry, rate of decomposition and mycorrhizal communities.

Gas exchange

To determine the affects of dust deposition to the flora of the SSSI gas exchange measurements were conducted on the leaves of *Leymus arenarius* and *Plantago lanceolata*, during September 2007.

The cleaning of the upper and lower surface of the leaves caused a significant increase in the photosynthetic efficiency the leaves of *Leymus* and *Plantago*, relative to untreated leaves.

The cleaning of the upper and lower surface of the leaves did not cause a significant affect on the rate of transpiration and water-use efficiency on the leaves of *Leymus* and *Plantago*, relative to untreated leaves.

Chapter 7 – Discussion

7.1 Introduction

The principle aim of the present study was to investigate the fugitive dust emissions from the Corus works, Teesside on the Coatham Sands and South Gare Site of Special Scientific Interest (SSSI). In the current chapter the results presented and discussed in Chapters 3, 4, 5 and 6 will be discussed in relation to the broad research questions of this study. The three research questions identified for this study were firstly to examine the fugitive particle deposition from the Corus works, secondly to examine the relevance of model scenarios of the environmental concentrations of particulate matter with the actual deposition to the SSSI and thirdly to examine the ecological effects of particle matter deposition to the SSSI.

7.1.1 Quantifying and characterising the spatial distribution of dust deposition and flux on the Corus works and South Gare and Coatham Sands SSSI

The passive dust monitoring gauges found that the deposition and flux of dust to monitoring sites located on the Corus works was significantly higher than the deposition and flux to monitoring sites located beyond the Corus works (Chapter 3). It is commonly accepted that emissions from steel works are deposited near to the site of generation and result in high levels of pollution (Mukherjee & Nuorteva, 1994; Pilegaard, 1979; Turkan *et al.*, 1995; Vestergaard *et al.*, 1986). Further to this it has been shown that for various steel works the emissions were found to decline with increasing distance away from the works. This decline in pollution with increasing distance from the steel works has also been shown on a steel works in Finland, where the epiphytic lichen *Hypogymnia physodes* was used to illustrate a decline in iron-rich particles at 10 km from a steel works (Mukherjee & Nuorteva, 1994). A similar study investigating the emissions from a steel works in Turkey found a decline using the bark of Pine *Pinus brutia* and using the moss *Hypnum cupressiforme* up to 2.5 km away from a steel works (Turkan *et al.*, 1995).

The highest percentages of iron-rich particles were found in the samples of dust flux and deposition taken from the three Frisbees located on the Corus works. This was in agreement with a previous study by Kemppainen *et al.* (2003) who found that the iron-rich particles emitted from a steel works in Finland, decreased in concentration with

increasing distance from the works using the bark of Scots Pine *Pinus sylvestris* (Kemppainen *et al.*, 2003). Of the three Frisbees located on the Corus works, the highest deposition and flux of dust was recorded at Frisbee B. Frisbee B was located to the north-west of the Corus works adjacent to the coke stock yards and 550 m to the north-west from the blast furnace. The dust deposited at Frisbee B was dominated by clusters of iron-rich particles (Chapter 4). The dust deposition and fluxes for each of the Frisbees were found to correlate to a function of the wind speed when the prevailing wind direction was from the direction of the Corus works. This has also been found in previous studies using Frisbee dust deposition gauges at Drax power station, in North Yorkshire (Vallack & Chadwick, 1993; Vallack, 2004).

Sources of iron-rich particles have been identified as potential emissions from metallurgic industries (DeBock *et al.*, 1994; Katrinak *et al.*, 1995; Kemppainen *et al.*, 2003; Michaud *et al.*, 1993; Post & Buseck, 1984; Van Malderen *et al.*, 1996a; Xhoffer *et al.*, 1991) and it is mostly likely that these particles identified in the present study are a result of emissions from the Corus works due to a high correlation in chemical composition with the reference samples. Emissions of iron-rich particles from the Corus works would also explain the peaks of iron-rich particle clusters for the directional dust fluxes, in the direction of the Corus works, to Frisbee A, B, C and D. Though it is possible the iron-rich particles could result from emissions other than the Corus works, it is unlikely due to the high correlation with the reference samples taken from the Corus works.

The dust deposition to Frisbee C was not related to a function of the wind speed from any direction. However, the southern and south-western fluxes of dust were related to a function of the respective wind speed and direction. The relationship between increasing dust deposition and iron discharged at the ponding station was approaching significance. The chemical characteristics of the reference samples taken from the ponding station and the ponding station track were not of similar chemical composition to that of the dust deposition and flux to Frisbee C. The deposition and flux samples contained a higher percentage of the iron-rich particles, with respect to the reference samples which had contained a higher proportion of particles rich in aluminium and silicon.

The dominant particle clusters for the flux and deposited dusts to the Frisbees located beyond the Corus works were not dominated by iron-rich particles (Chapter 4). The dust flux to Frisbee E was dominated by calcium rich-particles in the direction of the river Tees and the North Sea, along with the northern flux to Frisbee B, and the north-

eastern flux to Frisbee C. Previous studies have identified calcium-rich particles as marine sources of calcite, dolomite and gypsum (Katrinak *et al.*, 1995; Xhoffer *et al.*, 1991), and it is highly likley that these dust deposits and fluxes are also from marine processes. However, it is also possible that they could result from the waste gases produced from fossil fuel combustion at power stations (Michaud *et al.*, 1993; Post & Buseck, 1984; Rybicka, 1989; Xhoffer *et al.*, 1991) or fugitive emissions from waste gypsum, a by-product of the desulphurisation process. Therefore, these emissions could be from the power station located approximately 4 km to the north-west of the Corus works, the North Sea located to the north-east of the Corus works or from fugitive emissions of gypsum on the Corus works. Higher resolution reference sampling would be required to determine the exact origin of these particles. The northern flux to Frisbee C was dominated by particles rich in sodium and chlorine, which were representative of marine particles, as found by Choel *et al.*, (2007).

The deposition of dust to Frisbee F was found to be related to a function of the westerly wind component, which corresponded to the peak in dust flux to Frisbee F (Chapter 3). The lowest dust deposition and flux for all of the six Frisbees was recorded at Frisbee F, where the dominate particles were rich in aluminium and silicon. The dust fluxes to Frisbee D away from the Corus works were also dominated by particles rich in aluminium and silicon. Particles rich in aluminium and silicon have been previously associated with soil particles (Katrinak *et al.*, 1995; Van Malderen *et al.*, 1996a; Van Malderen *et al.*, 1996b) and fly-ash derived from high temperature combustion processes (Van Malderen *et al.*, 1996b; Xhoffer *et al.*, 1991). As these fluxes are in the direction away from the works they probably do not originate from the Corus works but other industrial activities in the lower Teesside valley area, for example the installations located on the Wilton site.

The Scanning Electron Microscopy with Energy Dispersive X-ray analysis (SEM-EDX) of particulate matter was an effective tool in the present study to determine the chemical composition of the dusts which contributed to the depositions for each Frisbee (Chapter 4). It is known that single particle analysis methods like SEM-EDX yield far more information on the chemical composition of deposited dusts than bulk analysis methods (Yue *et al.*, 2006). Previous dust deposition studies conducted using Frisbee deposition gauges have used a light microscope to determine dust chemistry and hence potential sources (Vallack & Chadwick, 1992; Vallack & Chadwick, 1993) and have yielded limited results in comparison to the present study.

Single particle analysis using SEM-EDX have been used effectively in a range of studies on particulate matter. However, previous studies have examined over 500 (Xhoffer *et al.*, 1991), 1000 (Choel *et al.*, 2007; Katrinak *et al.*, 1995) particles per sample using Computer Controlled Scanning Electron Microscopy (CCSEM). The number of particles analysed in the present study was limited by the manual approach used for the SEM-EDX, as fewer than 50 particles were analysed per sample. An automated approach would have enabled a greater number of particle spectra to be analysed both within samples and also to increase the total number of samples analysed. Overall this would have improved the reliability of the results by providing increased confidence in the clustering, and greater spatial and temporal analysis to account for variations in meteorological conditions and dust generation.

7.1.2 Assessing the relevance of particulate matter model scenarios with measurements of particulate matter for South Gare and Coatham Sands SSSI

The second aim outlined for the present study was to assess the relevance of a modelled scenario, to the actual environmental concentration of PM_{10} on the Corus works and surrounding areas. The passive dust deposition monitoring study determined the temporal dust deposition to six specific locations. This encompassed the passive monitoring study of environmental particulate matter, presented in chapter 3 and an assessment of the IPPC permit application model, which underwent several stages of development using different model parameters, presented in Chapter 5.

The final model scenario compared six months of dust deposition data collected from Frisbee deposit gauges, to the modelled expectations of the environmental concentration of PM_{10} for the period from April to December 2006. However, the model scenario only accounted for the environmental concentration of the PM_{10} fraction (particulate matter between 2.5 and 10 micrometres), whereas the Frisbee gauges caught the total particulate matter deposited, irrespective of size fraction. The constraints on the dust deposition study made continuous monitoring unfeasible and the model parameterisation data were limited to the PM_{10} fraction for the present study. Therefore, the model scenario is limited at quantitatively predicting the actual deposition of particulate matter, but the model scenarios are a valuable qualitative tool for determining the spatial variation in deposition.

The broad trends in the model scenario follow those of the dust deposited to the Frisbees (Chapter 5). The model scenario expected that the total dust deposited to the Frisbees located on the Corus works was higher than the total dust deposited to the Frisbees located beyond the Corus works. There was also a strong positive correlation between the total dust deposited and the expected concentration of PM_{10} to Frisbee C and F, but there was variability in the correlation curves. However, there was no quantitative correlation between the dust deposited and the expected modelled concentration of PM_{10} for Frisbee A, B, D and E.

Many of the studies examining emissions of particulates from industrial sites have concentrated on the effective location and size of stock piles (Badr & Harion, 2005; Badr & Harion, 2007; Xuan & Robins, 1994) and the use of windbreaks (Borges & Viegas, 1988) in particular porous fences (Lee & Kim, 1999; Lee *et al.*, 2002; Stunder & Arya, 1988) for the effective management of fugitive emissions from stockpiles. Studies focussed on the validation of the Atmospheric Dispersion Modelling System (ADMS) have used a range of parameterisation data from sites with differing meteorological conditions to show ADMS as an effective dispersion model (Carruthers *et al.*, 1994; Carruthers *et al.*, 1997; Carruthers *et al.*, 2000; Hall *et al.*, 2002; Hanna *et al.*, 2001; Holmes & Morawska, 2006; Riddle *et al.*, 2004; Timmis *et al.*, 2000). However, relatively few studies have focussed on quantifying the specific emissions from specific industrial sites. This work is primarily undertaken by installations and does not enter the published literature. It would be difficult to compare the emissions between industrial sites, as the location, meteorological conditions, potential areas at risk from emissions, and the proximity to residential areas are extremely variable. Studies of the particulate emissions from some works have focussed on the potential threat to human health (Polizzi *et al.*, 2007) and characterisation (Moreno *et al.*, 2004) but there are relatively few papers which focus on the effects of particulate matter deposition on vegetation. Although the area of research has been identified as an important area, our present knowledge is relatively limited.

For the present study, ADMS has produced a representative scenario of the environmental concentration of PM_{10} for the SSSI. A model which included all fractions of particulate matter would have been comparable with the dust deposited to the Frisbee dust gauges. However, the model would still have contained uncertainties due to the approximations of meteorology, atmospheric stability and hence the pollutant dispersion (Hall *et al.*, 2002), but these limitations are known to be unavoidable in modelling. Therefore the most effective and informative study would be provided by real-time

monitoring across the Corus works and SSSI, which measured all size fractions of particulate matter. However, certain site limitations must be over-come before this is a feasible option. As in the paper produced by Vrins (1996) the measurements of dust emissions for sampling representative coarse dusts requires high time and particle size resolution in combination with gravimetric analysis (Vrins, 1996).

There was a strong positive correlation between the measured and modelled PM_{10} concentrations for Frisbee C and F (Chapter 5). The dust deposited at Frisbee C was found to be approaching significance when regressed with the total iron discharged at the ponding station. However, the model did not incorporate potential emissions from the iron discharged at the ponding site. The dust deposition at Frisbee F was correlated to westerly winds, which is in the direction of the Corus works but also other industrial areas with potential emissions. Even though there was a correlation between the deposited and modelled particulate matter, it may be coincidental as the modelled predictions are only a qualitative indication of the actual deposition.

Passive techniques were the best available technique for measuring dust deposition as they were an efficient use of resources, and provided a good estimation of chronic dust deposition. The passive dust deposition gauges and sticky pads were used effectively in the present study to determine the average weekly dust flux and monthly deposition. Although real-time monitoring would have yielded considerably more information, in particular surrounding acute periods of deposition, it was not feasible within the present study.

7.1.3 Assessing the potential impact of particulate matter emissions on the flora of South Gare and Coatham Sands SSSI

The third aim outlined for the present study was to assess the potential effects of particulate matter emissions from the Corus works to South Gare and Coatham Sands SSSI. This was addressed with a study of dust deposition on the SSSI, an investigation into the iron concentration of the soil on the SSSI in relation to a similar ecosystem and an assessment of the impacts of dust deposition on the gas exchange of the flora on the SSSI.

The impacts of dust deposition to the SSSI are difficult to assess because there is no environmental standard for particulate emissions to ecosystems or vegetation. Also due to the variation in the chemical nature of particulate matter, natural spatial variation

in dust deposition and differing sensitivity of flora, it is difficult to assess the impact of particulate emissions to the SSSI.

To determine the effects of particulate emissions to the soil, samples were taken from two transects on the SSSI and a transect on Seaton Carew another sand dune ecosystem, approximately 3.5 km away. The soil samples were digested and analysed using Atomic Absorption Spectrometry (AAS). The soil iron concentration on the SSSI was found to be between 3 and 21 times higher than on the sand dunes at Seaton Carew. Dust deposition has been shown to alter the soil chemistry, soil pH, microbial communities and reduce the rate of decomposition in the current literature (Cairney & Meharg, 1999; Chappelka *et al.*, 1991; Farmer, 1993; Grantz *et al.*, 2003; Martin & Coughtrey, 1981; Petavratzi *et al.*, 2005). All of these effects have an indirect effect on the flora of the SSSI, but are difficult to distinguish (Smith & Staskawicz, 1977). The digestion and AAS have shown that the iron concentration of the soil on the SSSI is considerably higher than a similar ecosystem less than 4 km away. It would be beneficial to conduct more samples on the SSSI, in addition to more samples from similar sand dune ecosystems in the North-East of England. Previous studies on the effects of particulate emissions from steel works have shown that the soil microbial communities are significantly affected by emissions from the works (Baath *et al.*, 1992; Fritze, 1991). Even though iron-rich particles are accepted as a typical emission from iron and steel works, a study by Kadem *et al.* (2004) on an iron and steel plant in Algeria, conducted heavy metal analysis of aqua-regia digested samples analysed by AAS. They found high levels of contamination were found for lead, nickel and zinc, but iron was excluded from the heavy metal analyses (Kadem *et al.*, 2004). Kadem *et al.* (2004) suggests that the heavy metal contamination of the soil is attributable to the particulates that are deposited to soils, and also particulates brought to the soil by through-fall of the vegetation, which brings the particulates deposited to the vegetation into the soil.

The dust deposition study on the SSSI was conducted using sticky pads placed horizontally amongst the vegetation and analysed with a sticky pad reader (Chapter 6). The results indicated that the total deposition increased significantly with longer exposure periods, and with reduced distance to the Corus works. The chemical characterisation of the particulate matter deposited to the SSSI was beyond the scope of the present study. However, due to the high deposition and flux of iron-rich particles to Frisbee B and C (Chapter 3 and Chapter 4) and the dust deposited to the SSSI was most likely dominated by iron-rich particles.

The gas exchange study revealed that the photosynthetic rate was considerably reduced on the dusted leaves of *Leymus arenarius* and *Plantago lanceolata,* at all four sites on the SSSI, in comparison to the cleaned leaves. However, there was no clear effect of dust deposition on the transpiration rate or water-use efficiency. The decline in photosynthesis and the lack of response in the transpiration rate, and water-use efficiency indicates that the effects of dust deposition are most likely an effect of leaf shading, and not stomatal blocking. However, the variation in measurements of transpiration and water-use efficiency suggests the deposition may affect plants differently.

One study based on the mangrove *Avicennia marina* found reduced photosynthesis and reduced plant health due to coal dust, but the dust were not found to occlude the stomata (Naidoo & Chirkoot, 2004). Another study on the mangrove *Avicennia marina* found reduced plant health within 50 m of the emissions and only one of 3000 stomata analysed blocked by iron-ore dust (Paling *et al.*, 2001). Therefore, the reduction in photosynthesis was attributed in both cases to leaf shading which induced higher leaf temperatures (Naidoo & Chirkoot, 2004; Paling *et al.*, 2001), also the particles were too large to enter the stomata.

Increasing the dust deposited to the sites on the SSSI was found to correlate with a decrease in the photosynthetic rate of untreated or dusty leaves. Although, there was no effect of location on the rate of photosynthesis in the treated or cleaned leaves. Therefore, irrespective of the total loading of particulates all the plants were able to recover to the same extent.

The gas exchange measurements were an extremely useful tool for assessing the effect of dust deposition on the flora of the SSSI. In addition to this the artificial leaves and iron concentration analyses were also extremely useful tool for determining the potential effects of dust deposition to the flora of the SSSI. Although, individually all these techniques could be developed into more comprehensive field investigations, they provide an initial evaluation of the particulate emissions to the SSSI.

7.1.4 Future work

Continued passive sampling around the Corus works would be extremely beneficial for examining the temporal fluctuations in particulate matter deposition. However, as previously discussed, real-time sampling would provide the most useful information on the short-term spatial and temporal variability in the environmental concentrations of particulate matter on the Corus works and SSSI.

The chemical characterisation of particulate matter has proven extremely useful for determining the possible sources of particulates. Development of this method to incorporate a larger number of particles per sample and also the particulate matter deposited on sticky pads on the SSSI would provide a valuable addition to the present study. However, the analysis of more samples covering a greater temporal scale would be beneficial, especially to determine the variation in particle clusters for weekly flux and monthly deposition to validate the present findings. This method could also include chemical analysis of particulate matter from foliar washing. Foliar washing is one of the best methods available for determining the dry deposition of particulate matter to vegetation. The washing experiments in the present study were not able to incorporate analysis of deposited material but the determination by weight and characterisation would be an important step in determining the specific effects of particulate matter to the leaf surface (Grantz *et al.*, 2003).

As discussed earlier there are many model parameters which could be developed to make the model scenario more representative of the emissions or the site. However, modelling is inherently limited and further model development is unlikely to provide a more realistic quantitative scenario of the emissions of particulate matter. Therefore, it would be more beneficial to invest in a comprehensive real-time monitoring scheme.

Development of the ecological assessments would provide information to validate the findings of the present study. An expansion of the gas exchange investigations to include a greater spatial resolution by examining more sites would be advantageous; however, the number of reading taken per plant and plants per site should also be increased to improve confidence and reliability in the measurements. Using more plants would also be favourable in determining the overall effect of dust deposition. The analysis of the iron concentration of the soil would benefit from greater spatial resolution, but in addition to soil pH, loss-on-ignition, AAS of other essential and non-essential elements of the soil but also provide more information of the soil conditions. Finally a spatial assessment of visual leaf injury i.e. necrotic spots, in combination with chemical analyses of plant material for heavy metals, to infer the overall plant health would be of value, especially if compared to leaf injury on Seaton Carew sand dunes.

It would be interesting to extend the research to examine faunal responses to deposited dusts, as the SSSI is valued for its diverse bird life and invertebrate fauna. A study in Kenting National Park (Hsu *et al.*, 2005), Taiwan found relatively high concentrations of essential and non-essential elements in the soil and plants. However, the accumulation was far higher amongst earthworms, snails, crabs, bats, invertebrates,

amphibians and reptiles (Hsu *et al.*, 2005). This highlights a potential risk to the fauna of the SSSI, which has not been considered in the present study.

7.2 Thesis summary

Overall the research evaluated in the present thesis is of considerable importance. Few studies on dust deposition and flux have been published in the recent literature, even though it has been highlighted as an important area of research, especially considering the potential impact to flora and fauna. The null hypotheses of the present study were as follows:

1. There is no deposition of particulate matter to South Gare and Coatham Sands SSSI.
2. There is no flux of particulate matter to South Gare and Coatham Sands SSSI.
3. The deposition and flux of particulate matter is not affected by meteorological conditions including wind speed, wind direction and rainfall.
4. There is no deposition or flux of particulate matter emissions from the Corus works to South Gare and Coatham Sands SSSI.
5. The model scenario is not relevant for predicting particulate matter deposition onto South Gare and Coatham Sands SSSI.
6. There is no impact of particulate matter emissions on the flora of South Gare and Coatham Sands SSSI.

The first two hypotheses have been proven false, as there is considerable dust deposition and flux to the monitoring sites adjacent to the SSSI. The third hypothesis on meteorological conditions has been proven false for a function of wind, as peaks in dust deposition and flux were found correlate to specific peaks in wind speed and direction. However, rainfall was found to not affect the total dust deposition at the six monitoring sites. The fourth hypothesis has been proven false as the deposition and flux of particles to the monitoring sites located adjacent to the SSSI were dominated by particles most likely to have originated from activities on the Corus works. The fifth hypothesis has been proven true to an extent as all model scenarios of particulate matter are uncertain and contain inaccuracies. However, the modelled scenarios and measurements are not representative of the same fractions of particulate matter. Although modelling is beneficial, real-time monitoring across the Corus works and the SSSI would accurately determine the emissions of particulate matter. The sixth hypothesis has been proven false as plants growing at monitoring sites with increased dust deposition had the lowest rates of photosynthesis, and hence less carbon gain for

plant growth and development. The iron concentration of the soil on the SSSI was very high and could potentially cause indirect effects on the plants through altered soil chemistry, in addition to the direct effects of leaf shading on the foliar surface.

References

Adams, S.J. (1997) Dust deposition and measurement: A modified approach. *Environmental Technology*, **18** (3), 345-350.

Anderson, K.R., Avol, E.L., Edwards, S.A., Shamoo, D.A., Peng, R.C., Linn, W.S., & Hackney, J.D. (1992) Controlled Exposures of Volunteers to Respirable Carbon and Sulfuric-Acid Aerosols. *Journal of the Air & Waste Management Association*, **42** (6), 770-776.

AQEG (2005). Particulate Matter in the UK: Summary. DEFRA, London.

Aunan, K. (1996) Exposure-response functions for health effects of air pollutants based on epidemiological findings. *Risk Analysis*, **16** (5), 693-709.

Baath, E., Frostegard, A., & Fritze, H. (1992) Soil Bacterial Biomass, Activity, Phospholipid Fatty-Acid Pattern, and Ph Tolerance in an Area Polluted with Alkaline Dust Deposition. *Applied and Environmental Microbiology*, **58** (12), 4026-4031.

Badr, T. & Harion, J.L. (2005) Numerical modelling of flow over stockpiles: Implications on dust emissions. *Atmospheric Environment*, **39** (30), 5576-5584.

Badr, T. & Harion, J.L. (2007) Effect of aggregate storage piles configuration on dust emissions. *Atmospheric Environment*, **41** (2), 360-368.

Beaman, A.L. & Kingsbury, R.W.S.M. (1981) Assessment of Nuisance from deposited particulates using a simple and inexpensive measuring system. *Clean Air*, **11** (2), 77-81.

Beaman, A.L. & Kingsbury, R.W.S.M. (1984) Recent developments in the method of using sticky pads for the measurement of particulate nuisance. *Clean Air*, **14** (2), 74-81.

Bignal, K.L., Ashmore, M.R., Headley, A.D., Stewart, K., & Weigert, K. (2007) Ecological impacts of air pollution from road transport on local vegetation. *Applied Geochemistry*, **22** (6), 1265-1271.

Borges, A.R. & Viegas, D.X. (1988) Shelter Effect on a Row of Coal Piles to Prevent Wind Erosion. *Journal of Wind Engineering and Industrial Aerodynamics*, **29** (1-3), 145-154.

Bourrier, P. & Desmonts, T. (2007) Monitoring dust collection in the environment of an integrated steel plant: Source identification. *Revue De Metallurgie-Cahiers D Informations Techniques*, **104** (6), 287-295.

Brandt, C.J. & Rhoades, R.W. (1972) Effects of limestone dust accumulation on lateral growth of forest trees. *Environmental Pollution*, **3**, 213-7.

Brandt, C.J. & Rhoades, R.W. (1973) Effects of limestone dust accumulation on lateral growth of forest trees. *Environmental Pollution*, **4**, 207-13.

Braun, S. & Flückiger, W. (1987). Does exhaust from motorway tunnels affect the surrouding vegetation. In *Air Pollution and Ecosystems* (eds P. Mathy & D. Reidel), pp. 665-670. Reidel Publishing Company, Dordrecht, Holland.

Brooks, K. & Schwar, M.J.R. (1987) Dust Deposition and the Soiling of Glossy Surfaces. *Environmental Pollution*, **43** (2), 129-141.

Cairney, J.W.G. & Meharg, A.A. (1999) Influences of anthropogenic pollution on mycorrhizal fungal communities. *Environmental Pollution*, **106** (2), 169-182.

Carruthers, D.J., Edmunds, H.A., Bennett, M., Woods, P.T., Milton, M.J.T., Robinson, R., Underwood, B.Y., Franklin, C.J., & Timmis, R. (1997) Validation of the ADMS dispersion model and assessment of its performance relative to R-91 and ISC using archived LIDAR data. *International Journal of Environment and Pollution*, **8** (3-6), 264-278.

Carruthers, D.J., Edmunds, H.A., Lester, A.E., McHugh, C.A., & Singles, R.J. (2000) Use and validation of ADMS-Urban in contrasting urban and industrial locations. *International Journal of Environment and Pollution*, **14** (1-6), 364-374.

Carruthers, D.J., Holroy, D.R.J., Hunt, J.C.R., Weng, W.S., Robins, A.G., Apsley, D.D., Thomson, D.J., & Smith, F.B. (1994) Uk-Adms - a New Approach to Modeling Dispersion in the Earths Atmospheric Boundary-Layer. *Journal of Wind Engineering and Industrial Aerodynamics*, **52** (1-3), 139-153.

Chappelka, A.H., Kush, J.S., Runion, G.B., Meier, S., & Kelley, W.D. (1991) Effects of Soil-Applied Lead on Seedling Growth and Ectomycorrhizal Colonization of Loblolly-Pine. *Environmental Pollution*, **72** (4), 307-316.

Chillrud, S.N., Epstein, D., Ross, J.M., Sax, S.N., Pederson, D., Spengler, J.D., & Kinney, P.L. (2004) Elevated airborne exposures of teenagers to manganese, chromium, and iron from steel dust and New York City's subway system. *Environmental Science & Technology*, **38** (3), 732-737.

Choel, M., Deboudt, K., Flament, P., Aimoz, L., & Meriaux, X. (2007) Single-particle analysis of atmospheric aerosols at Cape Gris-Nez, English Channel: Influence of steel works on iron apportionment. *Atmospheric Environment*, **41** (13), 2820-2830.

Clapham, A.R., Tutin, T.G., & Warburg, E.F. (1981) *Excursion Flora of the British Isles*, Third edn. Cambridge University Press, Cambridge.

Corus (2005). Assessment of the Impact of Emissions on the Environment - Corus Teeside.

Czaja, A.T. (1961) Zementstaubwirkungen auf pflanzen: Die entstehung der zementkrusten. *Qual Plant et Mat Veg*, **8**, 201-38.

Datson, H. & Birch, W.J. (2007) The development of a novel method for directional dust monitoring. *Environmental Monitoring and Assessment*, **124** (1-3), 301-308.

DeBock, L.A., VanMalderen, H., & VanGrieken, R.E. (1994) Individual Aerosol-Particle Composition Variations in Air Masses Crossing the North-Sea. *Environmental Science & Technology*, **28** (8), 1513-1520.

DEFRA (2005). Integrated pollution prevention and control: A practical guide Edition 4, London.

DEFRA (2007). Air quality strategy for England, Scotland, Wales and Northern Ireland. Volume 1.

Dixit, A.B. (1988) Effects of Particulate Pollutants on Plants at Ultrstructural and Cellular Levels. *Annals of Botany*, **62**, 643 - 651.

Dockery, D.W. & Pope, C.A. (1994) Acute Respiratory Effects of Particulate Air-Pollution. *Annual Review of Public Health*, **15**, 107-132.

Dockery, D.W., Pope, C.A., Xu, X.P., Spengler, J.D., Ware, J.H., Fay, M.E., Ferris, B.G., & Speizer, F.E. (1993) An Association between Air-Pollution and Mortality in 6 United-States Cities. *New England Journal of Medicine*, **329** (24), 1753-1759.

Dodd, J.A., Ondov, J.M., Tuncel, G., Dzubay, T.G., & Stevens, R.K. (1991) Multimodal size spectra of submicrometer particles bearing various elements in rural air. *Environmental Science & Technology*, **25** (5), 890-903.

Eller, B.M. (1977) Road dust induced increase of leaf temperature. *Environmental Pollution*, **13**, 145-50.

Energy and the Environment Programme (1999). Studies into the origins and composition of airborne particulate matter around the UK: Project summary 040.

Environment Agency (2004). Monitoring of particulate matter in ambient air around waste facilities, Rep. No. 1 844 322610. Environment Agency, Bristol.

Environmental Protection Agency (1996). Method 3050B Acid digestion of sediment, sludges and soils. Revison 2.

EPAQS (1995). Particles, Expert Panel on Air Quality Standards, HMSO, London.

Ernst, W.H.O. (1982). Monitoring of particulate pollutants. In *Monitoring of air pollution by plants: Methods and problems* (eds L. Steubing & H.-J. Jager). Dr W Junk Publishers, The Hague.

Eveling, D.W. (1969) Effects of spraying plants with suspensions of inert dusts. . *Annals of applied biology*, **64** (1), 139-51.

Farmer, A.M. (1993) The Effects of Dust on Vegetation - a Review. *Environmental Pollution*, **79** (1), 63-75.

Farnfield, R.A. & Birch, W.J. (1997) Environmental dust monitoring using computer scanned images obtained from sticky pad poly directional dust gauges. *Clean Air and Environmental Protection*, **3** (27), 73-76

Fowler, D. (1980) Removal of sulphur and nitrogen compounds from the atmosphere in rain and by dry deposition. APges 22-32 *in* D. Drablos and A. Tolan, editors. Ecological effects of acid precipitation. SNSF (Acid Precipitation - Effects on Forests and Fish) Project, Oslo, Norway.

Fowler, D., Duyzer, J.H., & Baldocchi, D.D. (1991) Inputs of Trace Gases, Particles and Cloud Droplets to Terrestrial Surfaces. *Proceedings of the Royal Society of Edinburgh Section B-Biological Sciences*, **97**, 35-59.

Fritze, H. (1991) Forest Soil Microbial Response to Emissions from an Iron and Steel Works. *Soil Biology & Biochemistry*, **23** (2), 151-155.

Gale, J. & Easton, J. (1979) The effect of limestone dust on vegetation in an area with a Mediterranean climate. *Environmental Pollution*, **19**, 89-101.

Gilbert, O.L. (1976) An alkaline dust effect on epiphytic lichens. *Lichenol*, **8**, 173-8.

Goldbeck, L.J. & Marti, A.D. (1996) Dust control at conveyor transfer points: containment supression and collection. *Bulk soilds handling*, **16** (3), 367-372.

Grantz, D.A., Garner, J.H.B., & Johnson, D.W. (2003) Ecological effects of particulate matter. *Environment International*, **29** (2-3), 213-239.

Gupta, A.K., Gupta, S.K., & Patil, R.S. (2005) Environmental management plan for port and harbour projects. *Clean Technologies and Environmental Policy*, **7** (2), 133-141.

Hall, D.J., Spanton, A.M., Bennett, M., Dunkerley, F., Griffiths, R.F., Fisher, B.E.A., & Timmis, R.J. (2002) Evaluation of new generation atmospheric dispersion models. *International Journal of Environment and Pollution*, **18** (1), 22-32.

Hall, D.J., Upton, S.L., & Marsland, G.W. (1993). Improvements in Dust Gauge Design. In *Measurements of Airborne Pollutants* (ed S. Couling), pp. 171-217. Butterworth-Heinemann Ltd, Oxford.

Hanby, I. (2007a) Calibration and use of the sticky pad reader. http://www.hanby.co.uk/CAL%20&%20USE%20SPR.htm.

Hanby, I. (2007b) Operating principle of the reader. http://www.hanby.co.uk/Sticky%20Pad%20Reader.htm.

Hanna, S.R., Egan, B.A., & Purdum, J. (2001) Evaluation of the ADMS, AERMOD, and ISC3 dispersion models with the OPTEX, Duke Forest, Kincaid, Indianapolis and Lovett field datasets. *International Journal of Environment and Pollution*, **16** (1-6), 301-314.

Hirano, T., Kiyota, M., & Aiga, I. (1995) Physical effects of dust on leaf physiology of cucumber and kidney bean plants. *Environmental Pollution*, **89** (3), 255-261.

Holmes, N.S. & Morawska, L. (2006) A review of dispersion modelling and its application to the dispersion of particles: An overview of different dispersion models available. *Atmospheric Environment*, **40** (30), 5902-5928.

Hsu, M.J., Selvaraj, K., & Agoramoorthy, G. (2005) Taiwan's industrial heavy metal pollution threatens terrestrial biota. *Environmental Pollution*, **In Press, Corrected Proof**.

Hutchison, G.R., Brown, D.M., Hibbs, L.R., Heal, M.R., Donaldson, K., Maynard, R.L., Monaghan, M., Nicholl, A., & Stone, V. (2005) The effect of refurbishing a UK

steel plant on PM10 metal composition and ability to induce inflammation. *Respiratory Research*, **6**.

Jambers, W., De Bock, L., & Van Grieken, R. (1995) Recent advances in the analysis of individual environmental particles: A review. *Analyst*, **120**, 681-692.

Kadem, D.E.D., Rached, O., Krika, A., & Gheribi-Aoulmi, Z. (2004) Statistical analysis of vegetation incidence on contamination of soils by heavy metals (Pb, Ni and Zn) in the vicinity of an iron steel industrial plant in Algeria. *Environmetrics*, **15** (5), 447-462.

Katrinak, K.A., Anderson, J.R., & Buseck, P.R. (1995) Individual Particle Types in the Aerosol of Phoenix, Arizona. *Environmental Science & Technology*, **29** (2), 321-329.

Kemppainen, S., Tervahattu, H., & Kikuchi, R. (2003) Distribution of airborne particles from multi-emission source. *Environmental Monitoring and Assessment*, **85** (1), 99-113.

Lee, S.J. & Kim, H.B. (1999) Laboratory measurements of velocity and turbulence field behind porous fences. *Journal of Wind Engineering and Industrial Aerodynamics*, **80** (3), 311-326.

Lee, S.J., Park, K.C., & Park, C.W. (2002) Wind tunnel observations about the shelter effect of porous fences on the sand particle movements. *Atmospheric Environment*, **36** (9), 1453-1463.

Lindberg, S.E. & McLaughlin, S.B. (1986) *Air pollution interactions with vegetation: research needs in data acquisition and interpretation. In: Legge, A.H., Krupa, S.V., editors. Air pollutants and their effects on the terrestrial ecosystem. (Nriagu, J.O., ed. Advances in environmental science and technology: vol 18).* Wiley, New York.

Lorenzo, R., Kaegi, R., Gehrig, R., & Grobety, B. (2006) Particle emissions of a railway line determined by detailed single particle analysis. *Atmospheric Environment*, **40** (40), 7831-7841.

Lovett, G.M. (1994) Atmospheric Deposition of Nutrients and Pollutants in North America: An Ecological Perspective. *Ecological Applications*, **4** (4), 629-650.

Lovett, G.M. & Kinsman, J.D. (1990) Atmospheric pollutant deposition to high-elevation ecosystems. *Atmospheric Environment*, **24A**, 2767-2786.

Lovett, G.M. & Lindberg, S.E. (1984) Dry deposition and canopy exchange in a mixed oak forest as determined by analysis of throughfall. *Journal of Applied Ecology*, **21**, 1013-27.

Martin, M.H. & Coughtrey, P.J. (1981). Impacts of metals on ecosystem function and productivity. In *Effect of heavy metal polluition on plants* (ed N.W. Lepp), Vol. 2: Metals in the environment. Polluting Monitoring series., pp. 119-158. Applied Science Publishers, Barking (UK).

Michaud, D., Baril, M., & Perrault, G. (1993) Characterization of Airborne Dust from Cast-Iron Foundries by Physicochemical Methods and Multivariate Statistical-Analyses. *Journal of the Air & Waste Management Association*, **43** (5), 729-735.

Moreno, T., Jones, J.P., & Richards, R.J. (2004) Characterisation of aerosol particulate matter from urban and industrial environments: examples from Cardiff and Port Talbot, South Wales, UK. *Science of The Total Environment*, **334-35**, 337-346.

Mukherjee, A.B. & Nuorteva, P. (1994) Toxic Metals in Forest Biota around the Steel Works of Rautaruukki-Oy, Raahe, Finland. *Science of The Total Environment*, **151** (3), 191-204.

Naidoo, G. & Chirkoot, D. (2004) The effects of coal dust on photosynthetic performance of the mangrove, Avicennia marina in Richards Bay, South Africa. *Environmental Pollution*, **127**, 359-366.

Namiesnik, J., Zabiegala, B., Kot-Wasik, A., Partyka, M., & Wasik, A. (2005) Passive sampling and/or extraction techniques in environmental analysis: a review. *Analytical and Bioanalytical Chemistry*, **381** (2), 279-301.

Neuman, C., Lancaster, N., & Nickling, W. (1997) Relations between dune morphology, air flow, and sediment flux over reversing dunes, Silver Peak, NV, USA. *Sedimentology*, **44**, 1103-1113.

Osan, J., Alfoldy, B., Torok, S., & Van Grieken, R. (2002) Characterisation of wood combustion particles using electron probe microanalysis. *Atmospheric Environment*, **36** (13), 2207-2214.

Pagotto, C., Remy, N., Legret, M., & Le Cloirec, P. (2001) Heavy metal pollution of road dust and roadside soil near a major rural highway. *Environmental Technology*, **22** (3), 307-319.

Paling, E.I., Humphries, G., McCardle, I., & Thomson, G. (2001) The effects of iron ore dust on mangroves in Western Australia: Lack of evidence for stomatal damage. *Wetlands Ecology and Management*, **9** (5), 363 - 370.

Paoletti, L., De Berardis, B., Arrizza, L., Passacantando, M., Inglessis, M., & Mosca, M. (2003) Seasonal effects on the physico-chemical characteristics of PM2.1 in Rome: a study by SEM and XPS. *Atmospheric Environment*, **37** (35), 4869-4879.

Paoletti, L., Diociaiuti, M., De Berardis, B., Santucci, S., Lozzi, L., & Picozzi, P. (1999) Characterisation of aerosol individual particles in a controlled underground area. *Atmospheric Environment*, **33** (22), 3603-3611.

Parsons, B. & Salter, L. (2000). Report on particulate matter monitoring in Truro using the Osiris particulate monitor, Cornwall.

Petavratzi, E., Kingman, S., & Lowndes, I. (2005) Particulates from mining operations: A review of sources, effects and regulations. *Minerals Engineering*, **18** (12), 1183-1199.

Pilegaard, K. (1979) Heavy-Metals in Bulk Precipitation and Transplanted Hypogymnia-Physodes and Dicranoweisia-Cirrata in the Vicinity of a Danish Steelworks. *Water Air and Soil Pollution*, **11** (1), 77-91.

Polizzi, S., Ferrara, M., Bugiani, M., Barbero, D., & Baccolo, T. (2007) Aluminium and iron air pollution near an iron casting and aluminium foundry in Turin district (Italy). *Journal of Inorganic Biochemistry*, **101** (9), 1339-1343.

Post, J.E. & Buseck, P.R. (1984) Characterization of Individual Particles in the Phoenix Urban Aerosol Using Electron-Beam Instruments. *Environmental Science & Technology*, **18** (1), 35-42.

QUARG (1996). Airborne particulate matter in the United Kingdom, Third report of the Quality of Urban Air Review Group, QUARG Birmingham.

Ricks, G.R. & Williams, R.J. (1974) Effects of Atmospheric Pollution on Deciduous Woodland .2. Effects of Particulate Matter Upon Stomatal Diffusion Resistance in Leaves of Quercus-Petrea (Mattuschka) Leibl. *Environmental Pollution*, **6** (2), 87-109.

Riddle, A., Carruthers, D., Sharpe, A., McHugh, C., & Stocker, J. (2004) Comparisons between FLUENT and ADMS for atmospheric dispersion modelling. *Atmospheric Environment*, **38** (7), 1029-1038.

Rybicka, E.H. (1989) Metals and Their Chemical and Mineralogical Forms in Industrial Pollutants of the Atmosphere. *Environmental Technology Letters*, **10** (10), 921-928.

Schofield, N., Haines, A.N., & Vrins, E. (2001) The quantification of windblown dust emissions from an integrated steelworks site. *Revue De Metallurgie-Cahiers D Informations Techniques*, **98** (6), 607-612.

Schwar, M.J.R. (1994) A dust meter for measuring dust deposition and soiling of glossy surfaces *Clean Air*, **24** (4), 164-9.

Schwar, M.J.R. (1998) Nuisance dust deposition and soiling rate measurements. *Environmental Technology*, **19** (2), 223-229.

Sharifi, M.R., Gibson, A.C., & Rundel, P.W. (1997) Surface dust impacts on gas exchange in Mojave Desert shrubs. *Journal of Applied Ecology*, **34** (4), 837 - 846.

Sigal, L.L. & Suter, G.W. (1987) Evaluation of methods for determining adverse impacts of air pollution on terrestrial ecosystems. *Environmental Management (Historical Archive)*, **11** (5), 675-694.

Small, M., Germani, M.S., Small, A.M., Zoller, W.H., & Moyers, J.L. (1981) Airborne plume study of emissions from the processing of copper ores in southeastern Arizona. *Environmental Science & Technology*, **15** (3), 293-299.

Smith, W.H. & Staskawicz, B.J. (1977) Removal of atmospheric particles by leaves and twigs of urban trees: Some preliminary observations and assessment of research needs. *Environmental Management*, **1** (4), 317-330.

Stace, C. (1997) *New flora of the British Isles* Cambridge University Press, Cambridge.

Stunder, B.J.B. & Arya, S.P.S. (1988) Windbreak Effectiveness for Storage Pile Fugitive Dust Control - a Wind-Tunnel Study. *Japca-the International Journal of Air Pollution Control and Hazardous Waste Management*, **38** (2), 135-143.

Swanson, E.S., Thomson, W.W., & Mudd, J.B. (1973) The effect of ozone on the leaf cell membranes. *Canadian Journal of Botany*, **51**, 983-8.

Talley, T., Holyoak, M., & Piechnik, D. (2006) The Effects of Dust on the Federally Threatened Valley Elderberry Longhorn Beetle. *Environmental Management*, **37** (5), 647-658.

Thompson, J.R., Mueller, P.W., Fluckiger, W., & Rutter, A.J. (1984) The effects of dust on photosynthesis and its significance for roadside plants. *Environmental Pollution Series A*, **34**, 171-90.

Thomson, W.W., Dugger, W.M., & Palmer, R.L. (1966) Effects of ozone on the fine structure of the palisade parenchyma cells of the bean leaves. *Canadian Journal of Botany*, **44**, 1677-82.

Timmis, R., Wilkinson, S., Carruthers, D.J., & McHugh, C.A. (2000) Recent studies to validate and compare atmospheric dispersion models for regulatory purposes in the UK. *International Journal of Environment and Pollution*, **14** (1-6), 431-442.

Trombulak, S.C. & Frissell, C.A. (2000) Review of ecological effects of roads on terrestrial and aquatic communities. *Conservation Biology*, **14**, 18-30.

Turkan, I., Henden, E., Celik, U., & Kivilcim, S. (1995) Comparison of Moss and Bark Samples as Biomonitors of Heavy-Metals in a Highly Industrialized Area in Izmir, Turkey. *Science of The Total Environment*, **166** (1-3), 61-67.

Vallack, H.W. (1995a) A Field-Evaluation of Frisbee-Type Dust Deposit Gauges. *Atmospheric Environment*, **29** (12), 1465-1469.

Vallack, H.W. (1995b) Protocol for using the dry Frisbee (with foam insert) dust deposit gauge, pp. 2. Stockholm Environment Institute - York (SEI-Y).

Vallack, H.W. (2004) *Monitoring Dust Deposition in the vicinity of Drax Power Station, North Yorkshire from January to December 2003* Stockholm Environment Institute at York, University of York.

Vallack, H.W. & Chadwick, M.J. (1992) A Field Comparison of Dust Deposit Gauge Performance at 2 Sites in Yorkshire, 1987-1989. *Atmospheric Environment Part a-General Topics*, **26** (8), 1445-1451.

Vallack, H.W. & Chadwick, M.J. (1993) Monitoring Airborne Dust in a High-Density Coal-Fired Power-Station Region in North Yorkshire. *Environmental Pollution*, **80** (2), 177-183.

Vallack, H.W. & Shillito, D.E. (1998) Suggested guidelines for deposited ambient dust. *Atmospheric Environment*, **32** (16), 2737-2744.

Van Malderen, H., vanGrieken, R., Bufetov, N.V., & Koutzenogii, K.P. (1996a) Chemical characterization of individual aerosol particles in central Siberia. *Environmental Science & Technology*, **30** (1), 312-321.

Van Malderen, H., VanGrieken, R., Khodzher, T., Obolkin, V., & Potemkin, V. (1996b) Composition of individual aerosol particles above Lake Baikal, Siberia. *Atmospheric Environment*, **30** (9), 1453-1465.

Vestergaard, N.K., Stephansen, U., Rasmussen, L., & Pilegaard, K. (1986) Airborne Heavy-Metal Pollution in the Environment of a Danish Steel Plant. *Water Air and Soil Pollution*, **27** (3-4), 363-377.

Vrins, E. (1996) Sampling requirements for estimating fugitive dust emissions. *Journal of Aerosol Science*, **27** (1), 71-72.

Walker, I. & Nickling, W. (2003) Simulation and measurement of surface shear stress over isolated and closely spaced transverse dunes in a wind tunnel. *Earth Surface Processes and Landforms*, **28**, 1111-1124.

Winner, W.E. (1994) Mechanistic Analysis of Plant-Responses to Air-Pollution. *Ecological Applications*, **4** (4), 651-661.

Wise, R.R., McWilliam, J.R.S., & Naylor, A.W. (1983) A comparable study of low temperature induced ultrastructural alterations of three species with differing chilling sensitivies. *Plant Cell and Environment*, **6**, 525-35.

Woolven, S.C. & Radley, G.P. (1988). Contract surveys no.80, National Sand Dune Vegetation Survey, Site Report No. 38, Tees Bay Dunes, Cleveland. Nature Conservancy Council.

Xhoffer, C., Bernard, P., Vangrieken, R., & Vanderauwera, L. (1991) Chemical Characterization and Source Apportionment of Individual Aerosol-Particles over the North-Sea and the English-Channel Using Multivariate Techniques. *Environmental Science & Technology*, **25** (8), 1470-1478.

Xie, R.K., Seip, H.M., Leinum, J.R., Winje, T., & Xiao, J.S. (2005) Chemical characterization of individual particles (PM10) from ambient air in Guiyang City, China. *Science of The Total Environment*, **343** (1-3), 261-272.

Xuan, J. & Robins, A. (1994) The Effects of Turbulence and Complex Terrain on Dust Emissions and Depositions from Coal Stockpiles. *Atmospheric Environment*, **28** (11), 1951-1960.

Yue, W., Li, X., Liu, J., Li, Y., Yu, X., Deng, B., Wan, T., Zhang, G., Huang, Y., He, W., Hua, W., Shao, L., Li, W., & Yang, S. (2006) Characterization of PM2.5 in the ambient air of Shanghai city by analyzing individual particles. *Science of The Total Environment*, **368** (2-3), 916-925.

Appendices

Appendix A (Chapter 3)

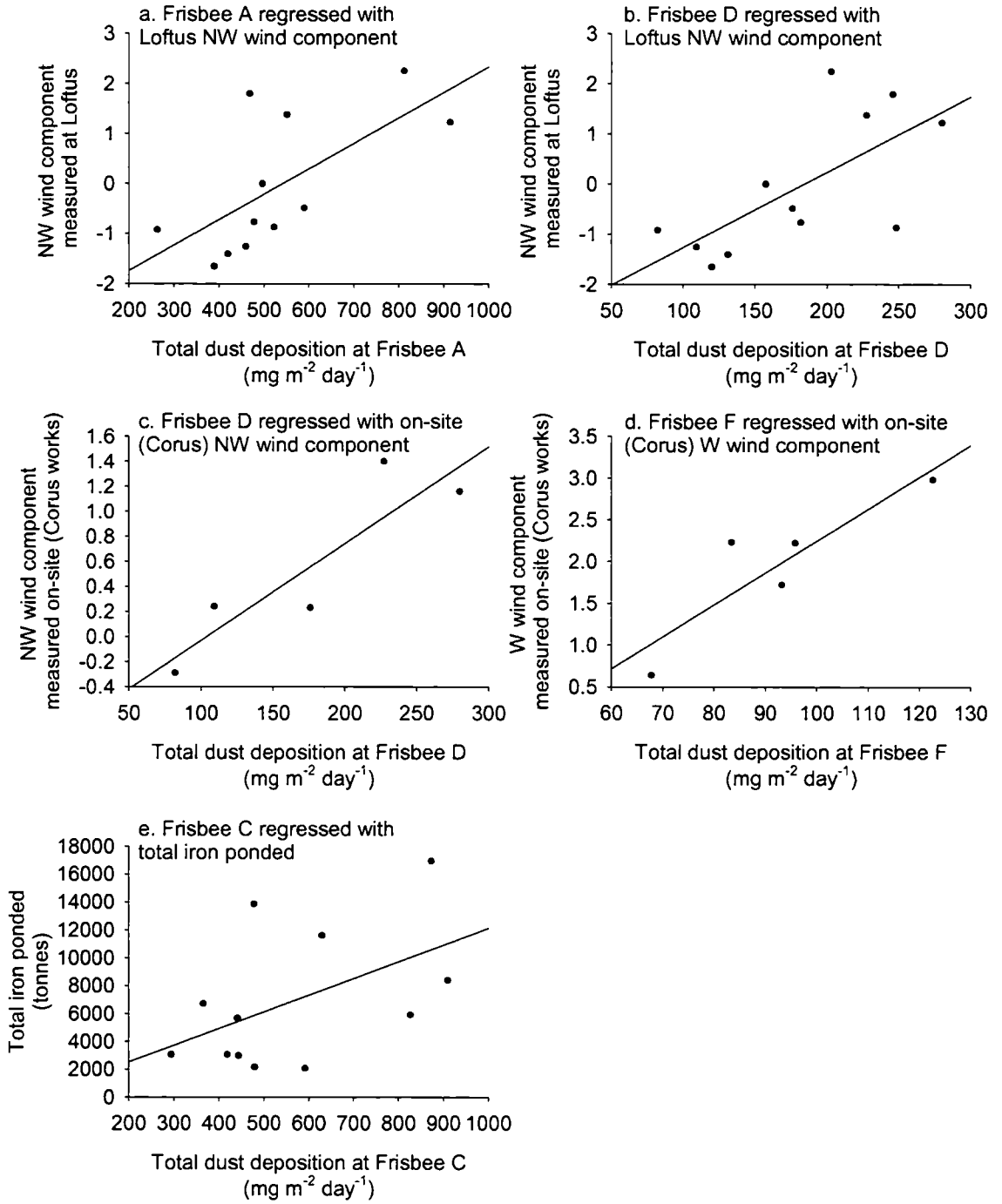

Appendix A Figure 1 – Regression curves for dust deposition.
Graph a. Total dust deposited at Frisbee A regressed with the NW wind component measured at Loftus.
Graph b. Total dust deposited at Frisbee D regressed with the NW wind component measured at Loftus.
Graph c. Total dust deposited at Frisbee D regressed with the NW wind component measured at Corus.
Graph d. Total dust deposited at Frisbee F regressed with the W wind component measured at Corus.
Graph e. Total dust deposited at Frisbee C regressed with the total iron ponded (tonnes).

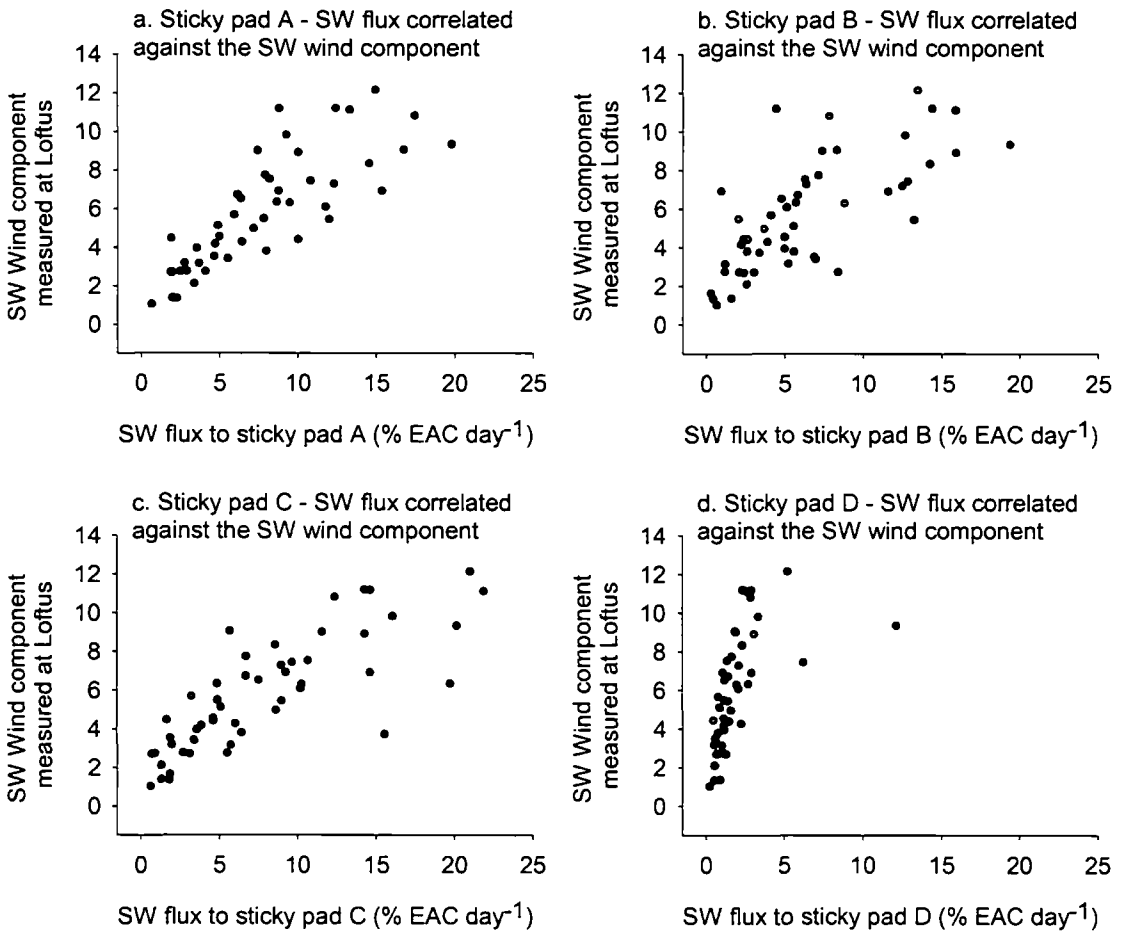

Appendix A Figure 2 – Correlating dust flux and wind components measured at Loftus.
Graph a. SW dust flux to sticky pad A correlated with the SW wind component measured at Loftus.
Graph b. SW dust flux to sticky pad B correlated with the SW wind component measured at Loftus.
Graph c. SW dust flux to sticky pad C correlated with the SW wind component measured at Loftus.
Graph d. SW dust flux to sticky pad D correlated with the SW wind component measured at Loftus.

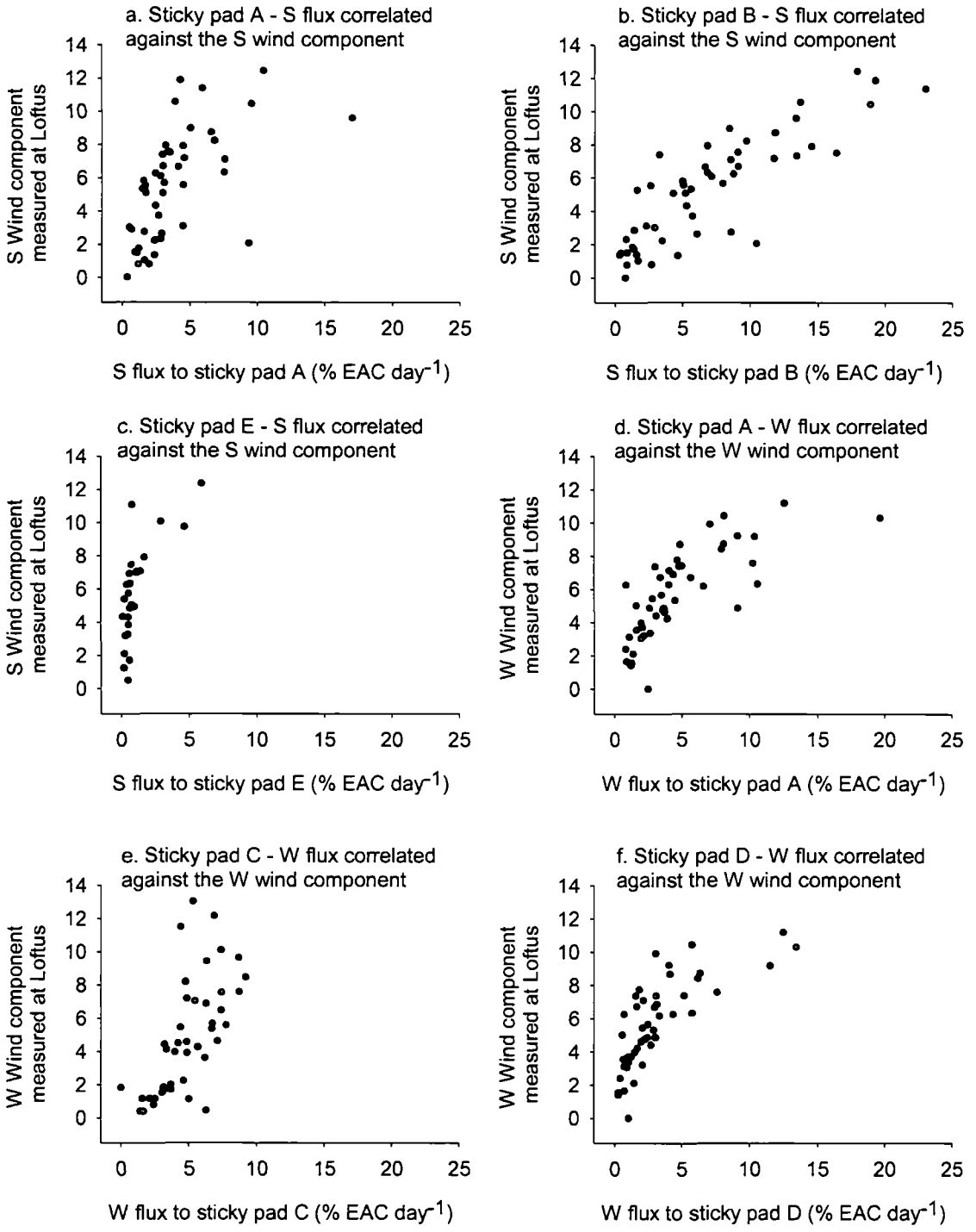

Appendix A Figure 3 – Correlating dust flux and wind components measured at Loftus.
Graph a. S dust flux to sticky pad A correlated with the S wind component measured at Loftus.
Graph b. S dust flux to sticky pad B correlated with the S wind component measured at Loftus.
Graph c. S dust flux to sticky pad E correlated with the S wind component measured at Loftus.
Graph d. W dust flux to sticky pad A correlated with the W wind component measured at Loftus.
Graph e. W dust flux to sticky pad C correlated with the W wind component measured at Loftus.
Graph f. W dust flux to sticky pad D correlated with the W wind component measured at Loftus.

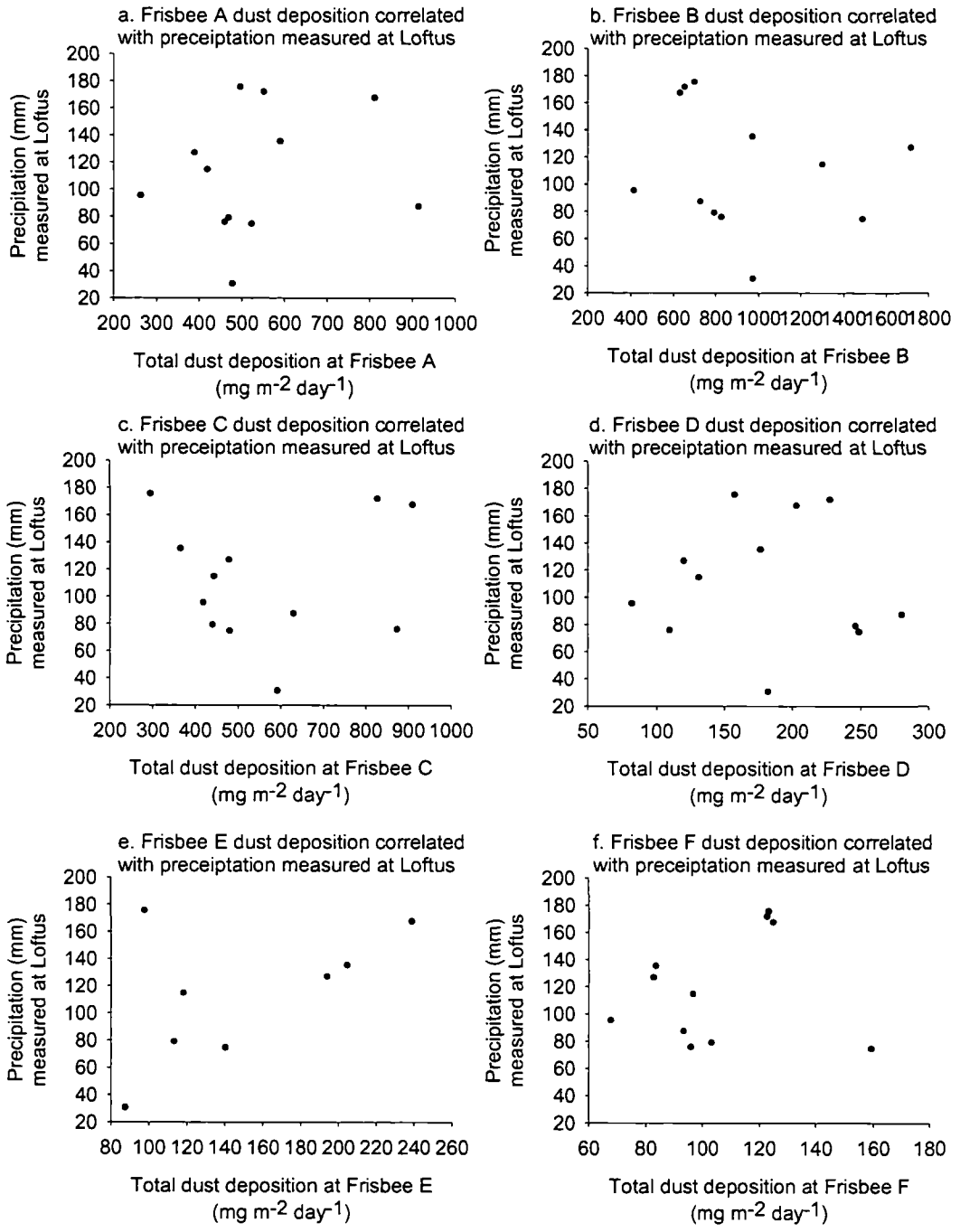

Appendix A Figure 4 – Correlating the total dust deposition (mg m^{-2} day^{-1}) and precipitation (mm) measured at Loftus. Note the difference in scale on the Total dust deposition (x) axis.
Graph a. Total dust deposition to Frisbee A correlated with the precipitation measured at Loftus.
Graph b. Total dust deposition to Frisbee B correlated with the precipitation measured at Loftus.
Graph c. Total dust deposition to Frisbee C correlated with the precipitation measured at Loftus.
Graph d. Total dust deposition to Frisbee D correlated with the precipitation measured at Loftus.
Graph e. Total dust deposition to Frisbee E correlated with the precipitation measured at Loftus.
Graph f. Total dust deposition to Frisbee F correlated with the precipitation measured at Loftus.

Appendix B (Chapter 5)

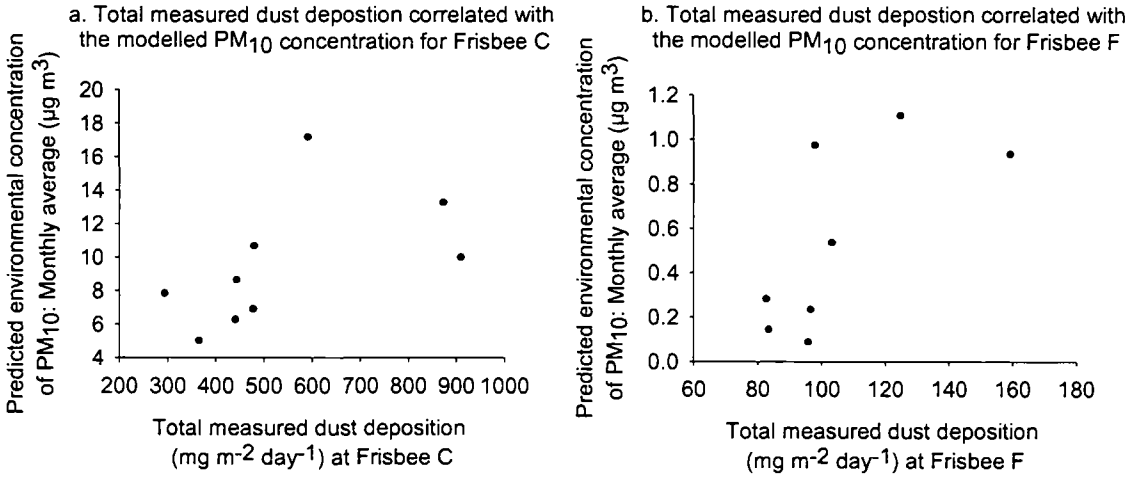

Appendix B Figure 1 – Correlating total dust deposition and modelled predicted environmental concentrations of PM_{10}: Monthly averages (µg m^3). Graph a. Frisbee C. Graph b. Frisbee F.

Appendix C (Chapter 6)

Appendix C Table 1. Post-hoc testing of the artificial leaves - dune location effect in a three way nested ANOVA on dust deposition.

Dependent Variable: SQRTreflectsqrt (LSD)						
(I) dunes	(J) dunes	Mean Difference (I-J)	Std. Error	Sig.	95% Confidence Interval	
					Lower Bound	Upper Bound
Embryo	Midpoint	.0056	.04767	.910	-.1111	.1222
	Fixed	.1673(*)	.04767	.013	.0506	.2839
Midpoint	Embryo	-.0056	.04767	.910	-.1222	.1111
	Fixed	.1617(*)	.04767	.015	.0450	.2783
Fixed	Embryo	-.1673(*)	.04767	.013	-.2839	-.0506
	Midpoint	-.1617(*)	.04767	.015	-.2783	-.0450
Based on observed means. * The mean difference is significant at the .05 level.						

Appendix C Table 2. Post-hoc testing of the artificial leaves - exposure length effect in a three way nested ANOVA on dust deposition.

Dependent Variable: % EAC of artificial leaves (Transformation:SQRTreflectsqrt) (LSD)						
(I) exposure	(J) exposure	Mean Difference (I-J)	Std. Error	Sig.	95% Confidence Interval	
					Lower Bound	Upper Bound
1 day	2 days	.4772(*)	.05505	.000	.3425	.6119
	4 days	.9981(*)	.05505	.000	.8634	1.1328
	6 days	1.2204(*)	.05505	.000	1.0857	1.3550
2 days	1 day	-.4772(*)	.05505	.000	-.6119	-.3425
	4 days	.5209(*)	.05505	.000	.3862	.6556
	6 days	.7432(*)	.05505	.000	.6085	.8779
4 days	1 day	-.9981(*)	.05505	.000	-1.1328	-.8634
	2 days	-.5209(*)	.05505	.000	-.6556	-.3862
	6 days	.2222(*)	.05505	.007	.0875	.3569
6 days	1 day	-1.2204(*)	.05505	.000	-1.3550	-1.0857
	2 days	-.7432(*)	.05505	.000	-.8779	-.6085
	4 days	-.2222(*)	.05505	.007	-.3569	-.0875
Based on observed means. * The mean difference is significant at the .05 level.						